UNIVERSITY OF CALIFORNIA
SANTA CRUZ

How does Y*ersinia* coordinate iron/oxygen sensing with virulence regulation?

A dissertation submitted in partial satisfaction
of the requirements for the degree of

DOCTOR OF PHILOSOPHY

in

MICROBIOLOGY AND ENVIRONMENTAL TOXICOLOGY

By

Diana K. Hooker Romero

September 2019

The Dissertation of Diana K. Hooker Romero is approved:

_____
Victoria Auerbuch Stone, chair

_____
Fitnat Yildiz, Ph.D.

_____
Patricia J Kiley, Ph.D.

_____

Quentin Williams
Acting Vice Provost and Dean of Graduate Studies

Table of contents

List of figures/tables

Chapter 3.

Abstract

Diana Hooker Romero

How does *Yersinia* coordinate iron/oxygen sensing with virulence regulation?

Iron is an essential element for most bacterial pathogens, including *Yersinia*. During infection, the mammalian immune system sequesters iron from invading pathogens; yet in response to this "nutritional immunity", many pathogenic bacteria are able to colonize host tissue despite the decrease in iron availability. Additionally, when these pathogens travel from the outside environment into a mammalian host, they also encounter varying levels of oxygen depending on the tissue, or inflammation state. The aim of this dissertation is to improve our understanding of how bacterial pathogens couple iron and oxygen sending with virulence regulation. Specifically, I used the bacterial pathogen *Yersinia pseudotuberculosis* to determine how the type III secretion system (T3SS) is controlled in response to iron and oxygen. The T3SS is a bacterial injectisome apparatus used by human pathogenic *Yersinia spp*., to manipulate host defenses. Some of our recent studies suggest that *Yersinia pseudotuberculosis* uses the transcriptional regulator IscR to control the T3SS through direct regulation of the T3SS master regulator LcrF. IscR is a transcriptional regulator that binds different DNA sequence motifs, depending on its [2Fe-2S] cluster-coordinating (holo-) or clusterless (apo-) form. Iron availability and oxygen tension have been shown to affect *E. coli* IscR [2Fe-2S] cluster integrity, therefore impacting expression of IscR target genes[4]. Collectively, these data suggest that *Y. pseudotuberculosis* may use IscR to sense changes in oxygen tension and iron bioavailability to control critical virulence genes. However, it is not yet known whether changes in iron and oxygen availability alter expression or function of the T3SS or other virulence factors in *Yersinia*. Understanding how iron impacts microbial virulence can contribute to better guidelines for patient care in the context of anemia, iron supplementation, iron overload and inflammation.

The main goal of this dissertation is to determine the role of IscR on the regulation of the T3SS master regulator LcrF. The first part of my dissertation sought to study *in vitro* how both iron and oxygen availability affect the expression of *iscR, lcrF* and T3SS. We demonstrated that the presence of oxygen drives expression of *iscR* and this in turn upregulates *lcrF* expression and T3SS activity. Additionally, we showed that under anaerobic conditions, *iscR* expression is upregulated when iron is depleted, activating *lcrF* expression and, thus, T3SS expression. The second part of this dissertation was to determine if IscR control on T3SS is important for virulence in the mouse model of infection. To test this, we performed a bread feeding model of infection, which mimics oral intake of contaminated food. Our results suggest that regulation of the T3SS in response to iron and oxygen through IscR is critical for virulence.

Dedication and Acknowledgements

I dedicate this PhD to my mother, who made so many sacrifices so that I could be in this country getting the education she always wanted for me- Thank you for always being by my side and for being a role model for me and my daughter.

I would like to thank my family and friends. Your love and support have given me the strength to work hard and never give up, even during the hardest moments of my graduate career. I love you and I am so glad you are in my life. Also, I would like to thank my lab mates for all of their help and support. I could have not been able to do this without you! I will always cherish our fun times together, and the cool things I learned from you.

I would like to thank my advisor Vicki Auerbuch Stone for being a great advisor and helping me become a better person. Thanks for providing me great advise and for always having something positive to say.

I dedicate this to my daughter Mia to show you that you can dream big and achieve anything, as long as you work hard. I love you!

The text of this dissertation includes a reprint of the following previously multi-author published material: Chapter 2, titled "Mouse Models of Yersiniosis" was published by Springer protocols in June, 2019. For this chapter I am responsible for all of the figures and for writing and editing the manuscript with the help of Vicki Auerbuch Stone. For Chapter 3, titled "Iron availability and oxygen tension regulate the *Yersinia* Ysc type III secretion system through IscR to enable disseminated infection I am responsible for figures 1A, 2-6, and also performed some of the infections for figure 8 with Leah Schwiesow.

Chapter 1.

Coregulation of host-adapted iron uptake mechanisms and the type three secretion system in *Yersinia pseudotuberculosis*

By Diana Hooker-Romero and Victoria Auerbuch

Introduction

Infectious diseases are one of the main causes of mortality in the world [1]. To cause disease in mammals, bacteria need to overcome numerous environmental factors such as temperature, pH, availability of nutrients, and immune response [2]. One remarkable feature of the mammalian host environment and its effects on bacterial growth relates to the availability of iron (Fe). The majority of bacterial pathogens require Fe for growth. During infection, the host immune system withholds Fe from invading pathogens; but despite this protection system, pathogenic bacteria manage to replicate and colonize host tissue to establish infection [3-5]. In the case of enteric bacterial pathogens, the use of a wide range of iron transport and sensing systems provides them with an advantage to survive the changing iron concentrations they encounter when traveling within the human gut as well as to other organs [6]. For example, a variety of high affinity Fe uptake systems have been shown to be essential for infection by pathogenic *Yersinia* [7].

The type III secretion system (T3SS) is a bacterial injectisome apparatus used by over two dozen human pathogens, including human pathogenic *Yersinia* species, to manipulate host defenses [8]. These pathogens only utilize their T3SS when in contact with a host cell; therefore, it is not surprising that T3SSs are typically under the control of regulators that sense a variety of different environmental cues such as oxygen tension, temperature, and iron [9-11]. In the case of *Yersinia pseudotuberculosis,* a recent study demonstrated that the iron-dependent transcriptional regulator, IscR, directly controls expression of the Ysc T3SS [12]. Despite this, iron was not known to regulate the *Yersinia* T3SS. However, I describe in chapter 3 that both iron and oxygen control the *Yersinia* Ysc T3SS. To provide context for this finding, in this chapter I will compare and contrast the different iron sensing/transport systems in *Yersinia* and discuss how iron affects virulence gene expression in pathogenic *Yersinia*. Understanding the link between host-specific metabolism and virulence factors, such as iron

uptake and the T3SS, will allow us to develop better therapeutic tools to target enteric pathogens.

Human pathogenic *Yersinia*

The family *Enterobacteriaceae* contains the biggest, most diverse assortment of medically important Gram-negative bacilli. These organisms are ubiquitous, found in soil, water, vegetation, and as part of normal intestinal flora in most animals, including humans [6, 13]. The genus *Yersinia* is an example of intensively studied *Enterobacteriaceae*. Out of the 17 recognized *Yersinia* species, only three are known to cause disease in humans: *Yersinia enterocolitica, Yersinia pseudotuberculosis, and Yersinia pestis* [14, 15]. These human pathogens are zoonotic, and can grow under facultative anaerobic conditions, within temperatures that range between 4°C to 42°C [16]. *Y. pestis* causes pneumonic and bubonic plague, which can be lethal if not treated within the first several days of infection. In fact, bubonic plague is regarded as one of the most fatal diseases in human history. [17]. The plague is contracted when *Y. pestis* enters the human body by inhalation of contaminated aerosols, or via fleabite, during which the bacteria is regurgitated into the dermis. Many flea species can serve as plague vectors, with the most common species being *Xenopsylla chopis,* associated with the oriental rat [18]. Once it is in the body, *Y. pestis* migrates to draining lymph nodes where it activates immune responses by polymorphonuclear neutrophils (PMNs), which in turn causes the characteristic inflammation and hemorrhage of the lymph nodes observed in plague patients [19].

Y. enterocolitica and *Y. pseudotuberculosis* are extracellular enteropathogens that are contracted through ingestion of contaminated food or water [20, 21]. Enteric yersiniosis has an infection rate of 0.33% in the U.S., however, these values are considered underestimated because many cases are not reported due to the lack of testing and difficulty of detection of the

pathogen. The majority of the yersiniosis cases in the U.S. are caused by *Y. enterocolitica.* Conversely, in Europe *Y. enterocolitica* is the third most common enteric infection [22].

After ingestion, *Y. enterocolitica* colonize the gut lumen and from there they can access the Peyer's patches (PP). Studies using the mouse model of infection demonstrated that *Y. enterocolitica* is not only able to invade and colonize the PP, but it can also disseminate to the liver and spleen directly from the gut lumen [23-25]. Yersiniosis caused by *Y. enterocolitica* is characterized by bloody diarrhea, acute gastroenteritis, pseudo-appendicitis, and fever [21]. Several studies have shown that yersiniosis cause by *Y. enterocolitica* is more common in children [22]. *Y. pseudotuberculosis* infections are less common but affect adults more often than children. Most of the outbreaks caused by *Y. pseudotuberculosis* have been reported in Finland, Switzerland, Japan, and Russia. An increased number of cases has also been observed in France [26]

Y. pseudotuberculosis also causes abdominal pain and diarrhea. Experiments performing infections in mice have shown that *Y. pseudotuberculosis* colonize the PP and lymph nodes, and that they can disseminate to distant lymphatic organs such as liver, spleen and lungs, and in rare occasions it can cause septicemia [27]. In another study using the mouse model of yersiniosis, *Y. pseudotuberculosis* was shown to colonize the spleen and liver from a replicating pool of bacteria in the intestine [28].

Previous studies comparing the DNA and RNA sequences between *Y. pestis* and *Y. pseudotuberculosis* have demonstrated that their genomes have 97% nucleotide sequence identity for most of the chromosomal genes; additionally, their 16S rRNA sequences are identical [29, 30]. Based on information from the first plague epidemic, and the molecular clock hypothesis, which uses the sequence variation at synonymous sites to calculate when the last common ancestor existed, Achtman et al estimated that *Y. pestis* evolved from *Y. pseudotuberculosis* within the last 1,500 to 20,000 years [31]. In addition, *Y. pestis* contains two extra plasmids, pPCP1 and pMT1, which have been shown to be involved in capsule formation, tissue invasion, and infection of the flea vector [32]. It has been suggested that

acquisition of these virulence plasmids as well as mutation and inactivation of certain virulence genes in *Y. pestis* facilitated the high pathogenicity associated with black death epidemics [31, 32].

Another characteristic that pathogenic *Yersinia* have in common is the presence of a 70 kb virulence plasmid, named pYV in *Y. enterocolitica* and *Y. pseudotuberculosis,* and pCD1 in *Y. pestis.* This plasmid has been shown to be essential for causing disease, and it encodes the T3SS structural genes, effector proteins (Yops, for *Yersinia* outer proteins), and genes involved in the regulation of T3SS function and expression [33]. Expression of most of the pYV-encoded virulence genes is tightly regulated by temperature. At mammalian body temperature, these virulence genes are induced [34]. Temperature regulation of virulence genes is only one example of the numerous factors that the pathogenic *Yersinia* species use to fine tune and coordinate expression of virulence factors only when inside the host and in contact with host cells. Consequently, understanding how the genetic difference between the three species affects their pathogenicity and virulence may provide us with new tools to prevent future epidemics.

Yersinia **virulence factors**

Adhesins

Despite the difference in pathology, the three *Yersinia* pathogens have various features in common, such as tropism for lymphoid tissues, using various adhesion and internalization factors, as well as the use of the Ysc T3SS to survive against immune responses. Following ingestion, *Yersinia* enteropathogens travel through the gastrointestinal tract until they arrive at the ileum, where they use the outer membrane protein invasin to bind to the β1-integrins on the apical surface of M cells in the small intestine of the host epithelial cells, where they cross the epithelial barrier and invade Payer's patches. [35, 36]. Studies on expression of the *inv* gene have shown that invasin is highly expressed prior to ingestion, when

food is stored at low temperature [37]. Intragastric infection of mice with a *Y. pseudotuberculosis* mutant strain lacking *inv* gene resulted in a reduced number of bacteria in the PPs during the early phase of the infection; however, its virulence was not reduced in comparison to the wild type strain after several days post-inoculation. [35, 37]. In the case of *Y. pestis,* the *inv* gene is not expressed because it contains an IS200 element, consistent with the irrelevance of crossing the gut barrier to the life cycle of *Y. pestis* [38].

Another protein that is important during the early stages of infection is Ail (attachment-invasion locus). This outer membrane protein is present in all three pathogenic *Yersinia* species. It is only expressed at 37°C, under low oxygen conditions [39]. Ail has also been shown to be important for *Yersinia* Yop secretion, since it binds to laminin and fibronectin on target cells during *Y. pseudotuberculosis* infection, enabling the close association between pathogen and host cell that is important for type III secretion [40]. In addition, Ail recruits complement regulatory factors to enable evasion of the complement [41]

The *Yersinia* adhesin A protein, YadA is an adhesin protein that is encoded by the pYV 70 kb virulence plasmid, and has been shown to play a role in bacterial adherence to different extracellular matrix components of eukaryotic cells, specifically to β-integrins found on epithelial cells [42]. YadA is a trimeric protein found in the outer membrane of *Y. enterocolitica* and *Y. pseudotuberculosis,* and has been shown to mediate protection against the complement Molecular Attack Complex (MAC), and certain antimicrobial peptides synthesized by PMNs [43]. YadA also mediates the close bacterial-host cell contact necessary for the T3SS to deliver Yop proteins into target host cells [44]. It is important to note that the *yadA* gene is not functional in *Y. pestis* due to deletion of a single nucleotide that caused a frame shift mutation [45]. However, it has been recently discovered that *Y. pestis* contains two chromosomal genes, *yadB* and *yadC,* which are similar to *yadA* [46]. YadA is not essential for virulence in *Y. pseudotuberculosis,* but it is for *Y. enterocolitica* following the intraperitoneal route of infection [23, 47].

Y. pestis also produces the pH6 antigen, which is an acidic, anti-phagocytic putative adhesin composed of PsaA protein subunits [32]. This protein is expressed at 37°C, in acidic conditions. Different studies have shown that *Y. pestis* producing pH6 antigen can escape from phagolysosomes in macrophages and, when in blood, can agglutinate erythrocytes and even interact with low density lipoproteins in plasma, protecting the bacteria from immune recognition [48]. *Y. pseudotuberculosis* and *Y. enterocolitica* also express the pH6 antigen, called Myf, mucoid *Yersinia* factor [49]. In *Y. pseudotuberculosis*, but not in *Y. enterocolitica,* MyfA also plays a role in hemagglutination [50].

The Ysc type III secretion system

As previously mentioned, the pYV/CD1 plasmid also encodes a series of effector proteins called *Yersinia* outer proteins (Yops), as well as structural and regulatory genes of the Ysc type III secretion system (T3SS). The Ysc T3SS serves to deliver cytotoxic effectors into eukaryotic target cells [51]. It is important to note that although the T3SS was first described in *Yersinia,* this conserved virulence factor is found in many other human pathogens such as enteropathogenic *Escherichia coli* (EPEC), enterohemorrhagic *E. coli* (EHEC)*, Salmonella sp., Pseudomonas* aeruginosa, *Shigella flexneri,* and *Chlamydia sp.* [33]. The Ysc T3SS is required for virulence in the three pathogenic *Yersinia* species. The Yop proteins dampen the phagocytic immune response by targeting the actin cytoskeleton, suppressing cytokine production, inhibiting phagocyte oxidative burst, or impacting the survival of phagocytic cells [7].

The T3SS is a molecular syringe that is composed of a basal body, a needle structure, and a translocon complex. The basal body spans the cell envelope (the inner and outer membranes and the peptidoglycan layer within the periplasm), and is composed of an outer membrane ring, formed by YscC with the help of the pilotin YscW, and an inner membrane ring formed by YscD and YscJ. The basal body also includes the export apparatus (YscRSTUV), the ATPase complex (YscNKL), and the C ring, made up of the protein YscQ., which direct the

assembly of the sorting complex that allows for recognition and processing of substrates [52]. Studies suggest that YscI forms an inner rod that allows firm connection between the basal body and the needle [53]. The needle is composed of a polymer of YscF subunits, which are secreted through the YscI rod, and polymerize outward from the basal body outside of the bacterial cell [54]. The secreted YscP protein is thought to function as a molecular ruler to determine the proper length of the needle [55], which reflects the distance between the host cell and the pathogen during intimate contact mediated by the adhesins [56]. Mutants that cannot synthesize YscF are unable to secrete Yops [57]. At the distal side of the needle, a pentamer of LcrV forms the tip of the needle (Mueller et al, 2005). Upon secretion, the hydrophobic proteins YopB and YopD interact with LcrV, forming the pore complex on the host cell membrane. This pore has yet to be visualized, nor is it well-characterized [58]. In addition to its role in translocon formation, YopD is also an important component of the T3SS regulatory network, as its central region is required for proper translocation of the Yops into target cells, [59]. Furthermore, a recent study demonstrated that YopD also plays a role in a positive feedback loop that regulates *lcrF* mRNA stability. During active type III secretion, YopD is secreted, leading to modulation of CsrA and RNaseE/ PNPase activity, which in turn increases stabilization of *lcrF* mRNA and enhanced LcrF translation [60]. The pYV/pCD1 plasmid also encodes chaperone proteins that aid in the proper translocation of certain Yops into eukaryotic cells [33]. Different studies have also demonstrated that the needle undergoes a conformational change, caused by either cell contact or calcium depletion, which triggers the actual secretion of seven effector proteins, YopJETMOHK, into the host cytosol. Once inside the host cell, these effector proteins target different cell processes [61].

Inhibition of phagocytosis by macrophages and neutrophils is mediated by the effector proteins YopEHOT [62]. YopH is a protein tyrosine phosphatase, whose activity antagonizes numerous signaling pathways that are associated with phagocytosis of bacteria by host cells. Experiments with *Y. pseudotuberculosis* have shown that YopH can block Ca^{2+} signaling in neutrophils, which is important in degranulation [63]. Moreover, YopE, T and O are toxins that

target RhoGTPases, which regulate different cellular functions [64], For example, YopE deactivates RhoGTPases, disrupting the host actin cytoskeleton [63]. Studies have also shown that YopE possesses a robust GTPase activity that allows it to dampen ROS production, [65]. In *Y. pestis,* a mutant lacking *yopE* had ~10,000 fold decreased virulence in comparison to the parental strain [66]. Similar studies show that in *Y. pseudotuberculosis*, YopE is necessary for systemic spread after oral infection [62]. However, *Y. enterocolitica* lacking *yopE* was able to spread systematically in mice after oral infection [67]. Characterization of YopT demonstrated that it can act as a cysteine protease and cleave RhoA, RhoG, Rac, and Cdc42, disturbing actin structures such as stress fibers and phagocytic cups [68]. YopH is a protein tyrosine phosphatase that antagonizes a number of signaling pathways involved in phagocytosis, such as counteracting oxidative burst in macrophages and neutrophils, and inhibiting integrin-mediated phagocytosis [63]. YopJ/P inhibits NF-κB and MAPK signaling, which prevents the expression of pro-inflammatory cytokines and pro-survival molecules, resulting in cell death in macrophages [69]. Interestingly, this YopJ activity may lead to *Yersinia* innate immune recognition and caspase-8 activation [70]. YopM inhibits macrophage pyrin-dependent caspase-1 activation and pyroptosis, a form of inflammatory cell death [71]. Similarly, YopK prevents excess entry of YopB and YopD into the host cytoplasm, limiting pyroptosis via a poorly-defined pathway [72].

In general, pathogenic bacteria activate the expression of virulence genes by sensing different environmental cues such as oxygen, pH, osmolarity, temperature, and iron availability [9]. As with many other mammalian bacterial pathogens, *Yersinia* upregulates many of its virulence genes at 37°C, host body temperature. Surprisingly, early studies in *Y. pestis* from the mid-1950s showed that activation of the T3SS correlated with growth restriction when the bacteria was cultured at 37°C in Ca^{2+}-deprived media [33]. This observation was termed the low calcium response (LCR) [73]. Expression of the majority of the pYV-encoded virulence genes is controlled by the AraC-type DNA-binding protein LcrF (low calcium response F). LcrF is thermoregulated at both the transcriptional and translational levels. At the transcriptional

level, LcrF depends on the binding of the thermo-labile protein YmoA [74]. At the translational level it depends on an intergenic RNA thermometer that melts at 37°C, enabling access of the ribosome to the ribosome binding site [75]. This tight regulation of LcrF ensures maximal pathogenicity in *Y. pseudotuberculosis* [34]. In the mouse model of the intragastric *Y. pseudotuberculosis* infection, mice infected with different *lcrF* RNA thermometer mutant strains did not show any signs of disease and were still alive after fourteen days of infection, in contrast to mice infected with the wild type strain, which died between three and six days post-infection [34]. Disrupting delivery of Yop proteins affects the virulence of pathogenic *Yersinia* by making them more susceptible to the host immune response. Therefore, it is important to understand how *Yersinia* use host environmental cues to fine-tune expression of the T3SS.

Co-regulation of host-adapted metabolism and virulence

The gastrointestinal tract in mammals is considered as a very rich but challenging environment for pathogenic bacteria to grow. Different factors such as nutrient supply, ion concentration, oxygen tension, and pH can vary significantly in different portions of the gut [76]. In addition to the varying levels of these factors, pathogens have to compete with resident flora for resources. Enteropathogenic *Yersinia* encounter a heterogeneous bacterial community of around 10^{14} bacteria from more than 400 species [76]. During infection, the immune system induces inflammation and hypoxic conditions, which changes considerably the availability of nutrients and ions [77]. As pathogenic *Yersinia* face varying environmental conditions during their life cycle, tight regulation and coordination of multiple metabolic pathways is required. An example of this is the ability of *Yersinia* to sense changes in nutrient supplies, especially sugars and amino acid limitation, which trigger the activation of virulence factors via the cAMP receptor protein, and the stringent response through Crp and (p)ppGpp, respectively [78]. In 2010 Vadyvaloo et al. conducted an *in vivo* transcriptomic study of *Y. pestis*, which revealed that some of the most important virulence factors were repressed when the bacteria resided in the

flea gut: the T3SS, the virulence regulator RovA, the fimbriae gene PsaA, the iron siderophore (low molecular weight molecules with high affinity for Fe^{3+} ions) yersiniabactin (Ybt), and the iron transport system Yfe [79]. Conversely, when *Y. pestis* virulence gene expression was studied in the rat model of pneumonic infection, expression of iron acquisition systems, such as a hemin uptake operon, as well as T3SS genes were induced [80]. These results highlight the ability of *Yersinia* to adapt to different environments and fine-tune metabolic and virulence genes to successfully colonize its host. Understanding the relationship of host-adapted bacterial metabolism and virulence will help us identify key metabolic and pathogenic pathways as potential targets for the design of antimicrobial methods.

Iron metabolism and virulence

Iron (Fe) ions serve as metabolic cofactors for many proteins that play roles in crucial processes, such as respiration, oxidative stress resistance, gene expression regulation, and virulence gene production [7]. Iron is able to adopt two stable valences, ferric and ferrous, providing iron-containing proteins with a considerable oxidation-reduction potential [6]. The level of iron required for optimal bacterial growth is ~10^{-6} M. However, within mammals the level of free iron is significantly less, with an average of 10^{-18} M [81]. This is because iron in mammals is mostly found inside cells as heme, metalloproteins, or is stored in ferritin [6]. During infection, the amount of iron decreases even further due to sequestration of iron from invading pathogens in a process termed nutritional immunity [82]. For example, lactoferrin is a molecule found in bodily secretions and neutrophil granules whose expression is induced during an inflammatory response and acts to sequester iron [83]. In addition, as a response specific to enteric pathogens, the inflamed intestine produces siderocalin/lipocalin-2, which is an antimicrobial protein that captures the bacterial siderophore enterobactin, the primary siderophore of many enteric bacteria. Studies show that mice laking siderocalin have an increased sensitivity to bacterial pathogens that rely on this siderophore [84]. The importance of nutritional immunity in the case of iron limitation is exemplified by the increased susceptibility of individuals with iron

overload, including ß-thalassemia, sideroblastic anemia, and hemochromatosis, some of the most common genetic diseases in humans, to systemic infections with pathogenic *Yersinia*, *Vibrio parahemolyticus* and several other pathogens [85, 86]

Numerous bacterial pathogens use iron depletion as an indication to tell when they are within their vertebrate host and must adjust the production of virulence factors. For example, the pathogens *Corynebacterium diphtheriae* and *Shigella spp* inhibit expression of their toxins through the iron-activated global repressors DtxR and Fur, respectively [76]. An interesting example of a pathogen that has evolved to survive host iron withholding is *Bordetella burgorferi,* which causes Lyme disease. This pathogen substitutes iron with manganese in its metal-requiring enzymes [84].

It is important to note that although iron is necessary for most living cell, excess iron is toxic, especially if it is not bound to protein or chelated. In the presence of oxygen, free iron can act as a catalyst for the Haber-Weiss reaction, where superoxides convert ferric iron to ferrous iron (Fe^{2+}). In the Fenton reaction, Fe^{2+} reacts with peroxide to produce highly reactive hydroxyl radicals [87]. Hydroxyl radicals can cause substantial cell damage or even death because they can damage DNA, unsaturated lipids, and proteins. As oxygen plays an important role in iron availability and iron toxicity, bacteria have evolved to regulate their iron metabolic pathways in response to varying levels of iron and oxygen [6].

Fur

Enteropathogens have a wide arsenal of uptake systems adapted to the different iron sources and availability, some of which are encoded on pathogenicity islands. To ensure optimal iron uptake, pathogenic *Yersinia* have numerous iron uptake and detoxification mechanisms preferentially activated depending on the environment and iron source they encounter [51]. Due to the deleterious effects of excess iron on bacteria, it is thought that all iron uptake mechanisms are ultimately repressed by iron. This global iron-dependent regulation is largely controlled, directly or indirectly, by the repressor Fur (Ferric Uptake Regulator) [88].

Fur binds as a dimer to specific sequences, known as Fur boxes, upstream of the transcriptional start site of many iron-repressible genes. When iron levels are elevated, Fur binds Fe^{2+}, changing its configuration and allowing it to bind to the Fur boxes of iron-repressible genes, including *fur* itself. Conversely, when iron levels are low, Fe^{2+} is displaced from Fur, subsequently releasing the target DNA sequences [6, 51]. Importantly, there are also genes that have been shown to have higher expression in the presence of Fur, which suggests that Fur can also activate genes, usually encoding proteins that coordinate iron or iron-sulfur clusters [89]. Masse and Gottesman, (2002,2005) determined that the small non-coding RNA RyhB repressed these genes, and that Fur repressed RyhB. Consequently, when the levels of iron are low, RyhB is expressed, which in turn represses a series of genes encoding iron-containing storage proteins, making iron available for essential processes [6]. Other studies have also demonstrated that many iron-repressible genes, including those controlled by *fur*, can be modulated by additional transcription factors in response to environmental changes, such as oxidative stress or siderophore uptake [90]. This co-regulation of iron-dependent genes ensures that pathogens use the most fitting iron uptake system during their passage through the complex environment in the host organism.

Recent studies have determined that Fur/RyhB regulation can have a direct and/or indirect effect on the regulation of specific virulence determinants [91]. Fur and RyhB have a direct effect on genes involved in iron acquisition, an important process for most bacterial pathogens. For example, Studies have shown that RyhB is important for virulence in the pathogen *Vibrio vulnificus*; specifically, the *ryhB* mutant was shown to be less virulent in both the WT and the hemochromatosis mouse model [92]. Another way Fur/RyhB can affect virulence is by targeting transcriptional regulators, such *Shigella dysenteriae* VirB, which inhibits T3SS expression when iron concentration is low, as in *Shigella*'s growth niche of the eukaryotic cytoplasm [93]. This serves to avoid premature lysis of the host cell. Similarly, Fur also controls expression of one of the two T3SSs in *Salmonella Typhimurium* based on iron availability. Since iron availability differs between Salmonella-containing vacuoles in host cells

and the gut lumen, two growth niches of *Salmonella*, Fur enables the pathogen to express its T3SS-1 in the GI tract to invade eukaryotic cells [94]. In addition, by controlling iron homeostasis, *E. coli* Fur and RyhB, regulate the intracellular concentration of iron, which in turn allows the indirect regulation many other genes, including virulence determinants [95]. Lastly, the T3SS of other pathogens such as *Bordetella bronchiseptica* and *Vibrio parahaemolyticus* have been shown to be upregulated by iron starvation, although the mechanisms are still unknown [9, 10]. Importantly, there have been other studies showing that Fur controls other cellular processes that may affect virulence, such as acid shock and redox-stress responses, chemotaxis, and metabolic pathways [96]. However, the mouse model of subcutaneous and intranasal infection of *Y. pestis* using a *ryhB* mutant demonstrated no effect on virulence [97], although a *Y. pestis fur* mutant has not been tested.

Iron uptake systems

Experimental and/or computational evidence have shown that most iron scavenging systems in *Yersinia* are Fur-controlled. Among these systems is the siderophore-dependent yersiniabactin (Ybt) inorganic iron transport system, which has been extensively studied. The Ybt system is encoded on a pathogenicity island and is functional in numerous Gram-negative pathogens [6]. In *Yersinia,* the genes responsible for biosynthesis, transport, and regulation of the Ybt production are clustered on a highly pathogenicity island (HPI) that is located within the pgm locus, a 102-kb region in the chromosome that undergoes spontaneous deletion due to recombination between two IS100 elements flanking the locus. Studies by Perry et al (2010) demonstrated that the Ybt system is functional in *Y. pseudotuberculosis*, although it is absent from several widely-used laboratory strains, including the IP2666 strain used in this thesis [98]. Similarly, the *Y. pseudotuberculosis* YPIII O3 type strain, which is commonly used to study *Yersinia* virulence in mice models, lacks the Ybt system but shows no iron acquisition deficit [99]. Likewise, the *Y. pseudotuberculosis* strains responsible for the Far East Scarlet-like fever epidemic in the Far East Russia and Japan, also lack the *ytb* gene cluster [100]. In contrast, in

experiments using the *Y. pseudotuberculosis* IP2790H strain, mutation of a Ybt biosynthetic gene caused a 1,000-fold or greater loss of virulence in mice infected subcutaneously or intravenously. Conversely, other studies have shown that the orthologous *Y. pestis* mutant is fully virulent when mice were infected intravenously [101]. These finding shed light on the possibility that highly pathogenic *Yersinia* use other siderophore systems when they lack Ybt. Use of alternative siderophores such as pseudochelin (Pch) and yersiniachelin (Ych) has been suggested; however, these siderophores have not yet been shown to be functional [99]. Interestingly, in studies comparing *ybt* gene expression between *Y. pestis* grown in LB media and *in vivo* showed that *ybt* gene expression was increased in the rat bubo after subcutaneous inoculation, as well as in the lungs after intranasal inoculation of mice [19, 102]. Interestingly, there was no upregulation of *ybt* genes in the mouse spleen and liver in the pneumonic model of infection [102]. Conversely, microarray studies comparing *Y. pestis* from blocked flea midgut and the rat bubo showed that *ybt* gene expression is highly upregulated in the rat bubo but not the flea [79]. Collectively, these studies demonstrate that yersiniabactin is important for virulence of certain strains, but *Yersinia* has also evolved other mechanisms to acquire iron during infection of mammals that allow it to colonize its host in the absence of yersiniabactin.

Another iron transport system that has been studied in pathogenic *Yersinia* is the Hmu ABC transporter system. It is composed of the HmuRSTUV proteins, which are identical in all five sequenced *Y. pestis* genomes. *Y. pseudotuberculosis* HmuR has four amino acids residue changes from *Y. pestis* while HmuT has two [103]. HmuTUV comprise an ABC transporter that works with the HmuR outer membrane receptor. Homologues of HmuS are suggested to function as a hemin-binding protein that prevents toxicity. Despite the fact that the Hmu system is necessary for uptake of hemin and other hemoproteins in *Y. pestis,* its mutation does not affect virulence in a mouse model of bubonic plague [104]. *Yersinia* pathogens also possess the haemophore system Has, which is composed of the HasRADEBF proteins. However, *in vitro* studies with *Y. pestis* were unable to demonstrate transport activity for the Has hemophore system [105] Additional experiments with an *Y. pestis hmu-has* double mutant suggested that

these demonstrated and putative hemin uptake systems are not involved in the pathogenesis of bubonic or pneumonic plague, as this double mutant is fully virulent [98].

In addition to heme uptake systems, *Yersinia* have numerous demonstrated and putative inorganic iron uptake systems (Table 1). The Yfe system is an ABC transporter for ferrous iron. It is composed of YfeA, a periplasmic binding protein, two inner membrane permeases, YfeC and YfeD, and the ATPase YfeB. An outer membrane has not yet been identified [103]. In addition, the Feo transporter is found in the majority of the Enterobacteriaceae and plays a role in the transport of ferrous iron under anoxic conditions and/or during intracellular growth [106]. Experiments in the bubonic plague mouse model showed that a single *feoB* mutant was still virulent, but a *yfeAB* mutant had a 8- to 9-fold decrease in virulence [106]. However, a *feoB*/*yfeAB* double mutant displayed a synergistic 98-fold loss of virulence. These results suggest that the two systems might play redundant roles *in vivo.* Conversely, experiments in the pneumonic model of plague showed that the Yfe and Feo systems did not play any role [106]. Based on these studies, we can conclude that during infection, *Yersinia* use different iron transport systems depending on the time of infection, route, and host organs.

T3SS, IscR, and iron

As mentioned previously, the T3SS is one of the main tools *Yersinia* and many other human pathogens use to survive in the face of the host immune response. Recently, a novel screen for *Y. pseudotuberculosis* mutants with defects in the T3SS identified the transcription factor IscR as an essential gene for full T3SS function and virulence in a mouse model of infection [12]. *Yersinia* IscR has 79% identity to the well-studied *E. coli* IscR. This study showed that deletion of IscR leads to a significant loss of T3SS function. IscR is a transcriptional regulator whose DNA-binding activity depends on its association with an iron-sulfur cluster, [2Fe-2S]. It functions as a sensor of the cellular Fe-S cluster status and regulates Fe-S cluster

biogenesis. When it is associated with the [2Fe-2S] cluster (holo-IscR), it binds to two different types of DNA motifs; in contrast, in its apo form, IscR binds only to so-called type 2 DNA sequence motifs. Additionally, the helix-turn helix DNA binding domain and the three cysteines and histidine known to coordinate an Fe-S cluster in *E. coli* IscR are conserved in all three pathogenic *Yersinia*. Importantly, a *Y. pseudotuberculosis iscR* mutant showed significantly decreased virulence in the mouse oral model of infection [12]. In *E. coli,* IscR controls more than 40 genes [107]. In addition, *Vibrio vulnificus* IscR is a global regulator that controls expression of many genes involved in Fe-S biogenesis and other cellular processes [108]. Different studies have shown that factors such as oxidative stress, iron starvation, and oxygen limitation can affect the cellular Fe-S cluster pool, which in turn will modulate the expression of different genes through IscR. In terms of virulence genes, IscR function has been shown to affect the ability for some pathogens to resist oxidative stress and maintain iron homeostasis during host infection [109]. A study with *Pseudomonas aeruginosa* showed that a mutant lacking IscR is hypersensitive to peroxide and paraquat, and displays decreased virulence in an acute infection models, due to the decrease of catalase A (KatA) enzyme activity [110]. In a similar way, deletion of IscR also renders the pathogen *Bulkholderia mallei* less resistant to reactive nitrogen species [111], and protects the intracellular pathogen *Shigella flexneri* against oxidative stress [109]. Moreover, it was shown that IscR regulates bacterial sensitivity to oxidative stress during host coinfection with the bacterium *Haemophilus influenza* and Influenza A virus [112]. Other studies have also demonstrated IscR control over other virulence factors such as motility, adhesion to host cells, and hemolytic activity in *V. vulnificus,* as well as capsular polysaccharide biosynthesis and iron acquisition pathways in *Klebsiella pneumoniae* [108, 113]. Furthermore, a recent study demonstrated that *S. enterica* represses the SPI-1 T3SS in response to low iron or high oxygen conditions through IscR direct regulation of the transcriptional regulator *hilD* [114]. As mentioned above, another study demonstrated that Fur induces expression of *hilD* under iron replete conditions [91]. These studies showed how *Salmonella* regulates expression of the SPI-1 T3SS by two different transcriptional

regulators under the control of iron. All of these examples, in addition to the fact that IscR is not used in plants or mammalian hosts, suggests that IscR is a transcriptional regulator with a potential of being a target for antimicrobial treatment [109]. Understanding how pathogens have evolved to use the limitation of iron as an environmental cue to fine-tune their virulence and pathogenicity will allow us to develop better tools to prevent bacterial diseases.

Table1. *Yersinia* iron/hemin uptake systems.

Proteins	Metal specificity	Major regulators	Species	Role in virulence	Reference
FeoB (inner membrane transporter)	Fe^{2+}	Fur	*Y. pestis* *Y. pstb.* *Y. ent.*	Systemic infection	Perry et al, 2007; Forman et al, 2010
YfeABCDE (ABC transporter)	Fe^{2+}	Fur	*Y. pestis* *Y. Y. pstb.*	No effect in local infection	Bearden and Perry 1999 ; Forman et al. 2007 ; Perry et al. 2003
YiuABC (ABC transporter)	Fe^{2+}	Fur	*Y. pestis*	No effect in local infection	Kirillina et al, 2006
Irp2 (yersiniabactin synthesis)	Fe^{3+}	Fur, YbtA	*Y. pestis* *Y. pstb.*	Effect in local infection	Perry et al, 1999
YfuA (yersiniabactic receptor)	Fe^{3+}	Fur, YbtA	*Y. pestis* *Y. pstb.*	Effect in local infection	Kirillina et al. 2006; Perry et al. 2004 ; Perry and Fetherston 2004, Forman et al, 2010
Hmu (haem receptor)	haem	Fur	*Y. pestis* *Y. pstb.*	No effect in local or systemic infection	Thomsom et al 1999; Rossi et al, 2001
HasR (haemophore receptor)	haem	Fur, HasI, HasS	*Y. pestis*	No effect in local or	Rossi et al, 2001; Forman et al, 2010

				systemic infection	
Ybt (yersiniabactin)	Fe^{3+}	Fur, YbtA	*Y. pestis* *Y. pstb.* *Y. ent.*	Effect in local infection	Bearden et al. 1997; Bearden and Perry 1999 ; Fetherston et al. 1999; Carniel et al. 1992 ; Karlyshev et al. 2001

References

1. Boutayeb A. The double burden of communicable and non-communicable diseases in developing countries. Transactions of the Royal Society of Tropical Medicine and Hygiene. 2006;100(3):191-9. doi: 10.1016/j.trstmh.2005.07.021.

2. Staskawicz BJ, Mudgett MB, Dangl JL, Science G-JE. Common and contrasting themes of plant and animal diseases. Science. 2001. doi: 10.1126/science.1062013.

3. Cartwright GE, Lauritsen MA, of … J-PJ. The anemia of infection. I. Hypoferremia, hypercupremia, and alterations in porphyrin metabolism in patients. The Journal of clinical investigation. 1946. **doi.** 10.1172/JCI101690

4. Bullen JJ, Leigh LC, Immunology R-HJ. The effect of iron compounds on the virulence of Escherichia coli for guinea-pigs. Immunology. 1968.

5. Cartwright GE, Lauritsen MA, Jones PJ. The anemia of infection. I. Hypoferremia, hypercupremia, and alterations in porphyrin metabolism in patients. The Journal of clinical investigation. 1946. doi: 10.1172/JCI101690. PubMed Central PMCID: PMC1946.

6. Carpenter C, Payne SM. Regulation of iron transport systems in Enterobacteriaceae in response to oxygen and iron availability. J Inorg Biochem. 2014;133:110-7. Epub 2014/02/04. doi: 10.1016/j.jinorgbio.2014.01.007. PubMed PMID: 24485010; PubMed Central PMCID: PMCPMC3964178.

7. Heroven AK, in c, infection D-P. Coregulation of host-adapted metabolism and virulence by pathogenic yersiniae. Frontiers in cellular and infection …. 2014.

8. Coburn B, Sekirov I, Finlay BB. Type III Secretion Systems and Disease. Clinical Microbiology Reviews. 2007;20(4):535-49. doi: 10.1128/CMR.00013-07.

9. Kurushima J, Kuwae A, Abe A. Iron starvation regulates the type III secretion system in Bordetella bronchiseptica. Microbiology and Immunology. 2012;56(6):356-62. doi: 10.1111/j.1348-0421.2012.00442.x.

10. Gode-Potratz CJ, of bacteriology C-DM. Calcium and iron regulate swarming and type III secretion in Vibrio parahaemolyticus. Journal of bacteriology. 2010. doi: 10.1128/JB.00654-10.

11. Wilharm G, in c, infection microbiology H-C. Interrelationship between type three secretion system and metabolism in pathogenic bacteria. Frontiers in cellular and infection microbiology. 2014.

12. Miller HK, Kwuan L, Schwiesow L, Bernick DL, Mettert E, Ramirez HA, et al. IscR Is Essential for Yersinia pseudotuberculosis Type III Secretion and Virulence. PLoS Pathogens. 2014;10(6). doi: 10.1371/journal.ppat.1004194.

13. Porcheron G, Garenaux A, Proulx J, Sabri M, Dozois CM. Iron, copper, zinc, and manganese transport and regulation in pathogenic Enterobacteria: correlations between strains, site of infection and the relative importance of the different metal transport systems for virulence. Front Cell Infect Microbiol. 2013;3:90. Epub 2013/12/25. doi: 10.3389/fcimb.2013.00090. PubMed PMID: 24367764; PubMed Central PMCID: PMCPMC3852070.

14. Koornhof HJ, Jr SRA, of Clinical N-M. Yersiniosis II: The Pathogenesis of Yersinia Infections. European Journal of Clinical microbiological infection.1999. PMMID: 10219574

15. Smego RA, Frean J, of Clinical K-HJ. Yersiniosis I: Microbiological and Clinicoepidemiological Aspects of Plague and Non-Plague Yersinia Infections. European Journal of Clinical Microbial infections. 1999.

16. Chlebicz A, of environmental. Campylobacteriosis, salmonellosis, yersiniosis, and listeriosis as zoonotic foodborne diseases: a review. Journal of environmental research and public health 2018. doi: 10.3390/ijerph15050863.

17. Dis S-IW. Twelve diseases that changed our world. Emerg Infect Dis. 2008.

18. Raoult D, Mouffok N, Bitam I, Piarroux R, Drancourt M. Plague: History and contemporary analysis. Journal of Infection. 2013;66(1):18-26. doi: 10.1016/j.jinf.2012.09.010.

19. Sebbane F, Lemaître N, Sturdevant DE, Rebeil R, Virtaneva K, Porcella SF, et al. Adaptive response of Yersinia pestis to extracellular effectors of innate immunity during bubonic plague. 2006;103(31):11766-71. doi: 10.1073/pnas.0601182103 J Proceedings of the National Academy of Sciences.

20. Spinner JL, Cundiff JA, and immunity K-SD. Yersinia pestis type III secretion system-dependent inhibition of human polymorphonuclear leukocyte function. Infection and immunity. 2008. doi: 10.1128/IAI.00385-08.

21. Bottone EJ. Yersinia enterocolitica: the charisma continues. Clinical microbiology reviews. 1997;10(2):257-76.

22. Rahman A, Bonny TS, S-S. Yersinia enterocolitica: epidemiological studies and outbreaks. Journal of pathogens. 2011. doi: 10.4061/2011/239391.

23. Handley SA, Newberry RD, Miller VL. Yersinia enterocolitica Invasin-Dependent and Invasin-Independent Mechanisms of Systemic Dissemination. Infection and Immunity. 2005;73(12). doi: 10.1128/iai.73.12.8453-8455.2005. PubMed Central PMCID: PMC2005.

24. Carter PB. Animal model of human disease. *Yersinia enteritis.* Animal model: oral *Yersinia enterocolitica* infection of mice. The american journal of pathology. 1975.

25. Oellerich MF, Jacobi CA, Freund S, Niedung K, Bach A, Heesemann J, et al. Yersinia enterocolitica Infection of Mice Reveals Clonal Invasion and Abscess Formation. Infection and Immunity. 2007;75(8):3802-11. doi: 10.1128/IAI.00419-07.

26. Jalava K, Hallanvuo S. Multiple outbreaks of Yersinia pseudotuberculosis infections in Finland. Journal of clinical Microbiology. 2004. doi: 10.1128/JCM.42.6.2789-2791.2004.

27. Pujol C, immunology B-JB. Turning Yersinia pathogenesis outside in: subversion of macrophage function by intracellular yersiniae. Clinical immunology. 2005.

28. Barnes PD, Bergman MA, Mecsas J, Isberg RR. Yersinia pseudotuberculosis disseminates directly from a replicating bacterial pool in the intestine. The Journal of Experimental Medicine. 2006;203(6):1591-601. doi: 10.1084/jem.20060905.

29. Trebesius K, Harmsen D,R-A. Development of rRNA-targeted PCR and in situ hybridization with fluorescently labelled oligonucleotides for detection of Yersinia species. Journal of clinical Microbiology. 1998. PMID. 9705392

30. Chauvaux S, Dillies MA, Marceau M. In silico comparison of Yersinia pestis and Yersinia pseudotuberculosis transcriptomes reveals a higher expression level of crucial virulence determinants in the plague bacillus. International Journal of Med Microbiology. 2011. doi.10.1016/j.ijmm.2010.08.013.

31. Achtman M, Zurth K, M-G. Yersinia pestis, the cause of plague, is a recently emerged clone of Yersinia pseudotuberculosis. Proceedings of the National academy of sciences. 1999. doi: 10.1073/pnas.96.24.14043.

32. Lindler LE, Plano GV, Burland V. Complete DNA sequence and detailed analysis of the Yersinia pestis KIM5 plasmid encoding murine toxin and capsular antigen. Infection and Immunity. 1998. PMID:9826348

33. Cornelis GR, Boland A, Boyd AP. The virulence plasmid of Yersinia, an anti-host genome. Microbiol Mol Biol Review. 1998. PMID: 9841674

34. Bohme K, Steinmann R, Kortmann J, Seekircher S, Heroven AK, Berger E, et al. Concerted actions of a thermo-labile regulator and a unique intergenic RNA thermosensor control Yersinia virulence. PLoS Pathog. 2012;8(2):e1002518. Epub 2012/02/24. doi: 10.1371/journal.ppat.1002518. PubMed PMID: 22359501; PubMed Central PMCID: PMCPMC3280987.

35. Marra A, Isberg R. Invasin-dependent and invasin-independent pathways for translocation of Yersinia pseudotuberculosis across the Peyer's patch intestinal epithelium. Infection and immunity. 1997;65(8). PubMed Central PMCID: PMC1997.

36. Clark MA, Hirst BH, and immunity J-MA. M-cell surface β1 integrin expression and invasin-mediated targeting of Yersinia pseudotuberculosis to mouse Peyer's patch M cells. Infection and immunity. 1998.

37. Mikula KM, Kolodziejczyk R, in cellular and G-A. Yersinia infection tools—characterization of structure and function of adhesins. Frontiers in cellular and Infection Microbiology. 2013. doi. 10.3389/fcimb.2012.00169

38. Simonet M, Riot B, Fortineau N, and immunity B-P. Invasin production by Yersinia pestis is abolished by insertion of an IS200-like element within the inv gene. Infection and immunity. 1996.

39. Pederson KJ, and immunity P-DE. Ail expression in Yersinia enterocolitica is affected by oxygen tension. Infection and immunity. 1995.

40. Atkinson S, Fresearch W-P. Yersinia virulence factors-a sophisticated arsenal for combating host defences. F1000Research. 2016.

41. Thomson JJ, Plecha SC, Krukonis ES. Ail provides multiple mechanisms of serum resistance to Yersinia pestis. Molecular Microbiology. 2019;111(1):82-95. doi: 10.1111/mmi.14140.

42. Heise T, Dersch P. Identification of a domain in Yersinia virulence factor YadA that is crucial for extracellular matrix-specific cell adhesion and uptake. Procedures of the National Academy of Sciences. 2006. doi: 10.1073/pnas.0507749103.

43. Tahir EY, of Microbiology S-M. YadA, the multifaceted Yersinia adhesin. International Journal of Medical Microbiology. 2001.

44. Visser LG, Annema A, and immunity VR. Role of Yops in inhibition of phagocytosis and killing of opsonized Yersinia enterocolitica by human granulocytes. Infection and immunity. 1995.

45. Ke Y, Chen Z, in c, infection microbiology Y-R. Yersinia pestis: mechanisms of entry into and resistance to the host cell. Frontiers in cellular and infection microbiology. 2013.

46. Forman S, Wulff CR, and M-M-T. yadBC of Yersinia pestis, a new virulence determinant for bubonic plague. Infection and Immunity. 2008. doi: 10.1128/IAI.00219-07.

47. Paczosa MK, F-ML. Yersinia pseudotuberculosis uses Ail and YadA to circumvent neutrophils by directing Yop translocation during lung infection. Cellular Microbiology. 2014. doi: 10.1111/cmi.12219.

48. Makoveichuk E, Cherepanov P, L-S. pH6 antigen of Yersinia pestis interacts with plasma lipoproteins and cell membranes. Journal of lipid research. 2003. doi: 10.1194/jlr.M200182-JLR200.

49. Leo JC, Oberhettinger P, Schütz M, of L-D. The inverse autotransporter family: intimin, invasin and related proteins. International Journal of …. 2015.

50. Yang Y, Merriam JJ, and … M-JP. The psa locus is responsible for thermoinducible binding of Yersinia pseudotuberculosis to cultured cells. Infection and …. 1996.

51. Marceau M. Transcriptional regulation in Yersinia: an update. Current issues in molecular biology. 2005;7(2):151-77.

52. Dewoody R, Merritt PM, Houppert AS, Marketon MM. YopK regulates the Yersinia pestis type III secretion system from within host cells. Molecular Microbiology. 2011;79(6):1445-61. doi: 10.1111/j.1365-2958.2011.07534.x.

53. Cao SY, Liu WB, Tan YF, Yang HY, Z-TT. An interaction between the inner rod protein YscI and the needle protein YscF is required to assemble the needle structure of the Yersinia type three secretion system. Journal of Biological chemistry. 2017. doi: 10.1074/jbc.M116.743591.

54. Diepold A, Wiesand U, A-M. Assembly of the Yersinia injectisome: the missing pieces. Molecular Microbiology. 2012. doi.10.1111/j.1365-2958

55. Journet L, Agrain C, Broz P, Science C-GR. The needle length of bacterial injectisomes is determined by a molecular ruler. Science. 2003. doi: 10.1126/science.1091422.

56. Mota LJ, Sorg I, microbiology letters C-GR. Type III secretion: the bacteria-eukaryotic cell express. FEMS microbiology letters. 2005. doi: 10.1016/j.femsle.2005.08.036.

57. Allaoui A, Schulte R, microbiology C-GR. Mutational analysis of the Yersinia enterocolitica virC operon: characterization of yscE, F, G, I, J, K required for Yop secretion and yscH encoding YopR. Molecular microbiology. 1995. doi: 10.1111/j.1365-2958.1995.mmi_18020343.x.

58. Kwuan L, Adams W, Auerbuch V. Impact of Host Membrane Pore Formation by the Yersinia pseudotuberculosis Type III Secretion System on the Macrophage Innate Immune Response. Infection and Immunity. 2013;81(3):905-14. doi: 10.1128/IAI.01014-12.

59. Adams W, Morgan J, K-L. Yersinia pseudotuberculosis YopD mutants that genetically separate effector protein translocation from host membrane disruption. Molecular Microbiology. 2015. doi: 10.1111/mmi.12970.

60. Kusmierek M, Hoßmann J, Witte R, Opitz W, Vollmer I, Volk M, et al. A bacterial secreted translocator hijacks riboregulators to control type III secretion in response to host cell contact. PLOS Pathogens. 2019;15(6). doi: 10.1371/journal.ppat.1007813.

61. Dewoody RS, Merritt PM, Marketon MM. Regulation of the Yersinia type III secretion system: traffic control. Frontiers in Cellular and Infection Microbiology. 2013;3. doi: 10.3389/fcimb.2013.00004.

62. Logsdon LK, and immunity M-J. Requirement of the Yersinia pseudotuberculosis effectors YopH and YopE in colonization and persistence in intestinal and lymph tissues. Infection and immunity. 2003.

63. Viboud GI, Bliska JB. YERSINIA OUTER PROTEINS: Role in Modulation of Host Cell Signaling Responses and Pathogenesis. Annual Review of Microbiology. 2005;59(1):69-89. doi: 10.1146/annurev.micro.59.030804.121320.

64. Barbieri JT, Riese MJ, of and A-K. Bacterial toxins that modify the actin cytoskeleton. Annual Review of Cell and Developmental Biology. 2002. doi: 10.1146/annurev.cellbio.18.012502.134748.

65. Songsungthong W, Higgins MC, Rolán HG, Murphy JL, Mecsas J. ROS-inhibitory activity of YopE is required for full virulence of Yersinia in mice. Cellular Microbiology. 2010;12(7):988-1001. doi: 10.1111/j.1462-5822.2010.01448.x.

66. Perry RD, microbiology reviews F-JD. Yersinia pestis--etiologic agent of plague. Clinical microbiology reviews. 1997. doi: 10.1128/CMR.10.1.35.

67. Trülzsch K, Sporleder T, Igwe EI, Rüssmann H, Heesemann J. Contribution of the Major Secreted Yops of Yersinia enterocolitica O:8 to Pathogenicity in the Mouse Infection Model. Infection and Immunity. 2004;72(9):5227-34. doi: 10.1128/IAI.72.9.5227-5234.2004.

68. Aepfelbacher M, Trasak C, W-G. Characterization of YopT effects on Rho GTPases in Yersinia enterocolitica-infected cells. Journal of Biological Chemistry. 2003. doi: 10.1074/jbc.M303349200.

69. Philip NH, in c, infection microbiology B-IE. Cell death programs in Yersinia immunity and pathogenesis. Frontiers in cellular and infection microbiology. 2012.

70. Philip NH, Dillon CP, Snyder AG, Fitzgerald P, Wynosky-Dolfi MA, Zwack EE, et al. Caspase-8 mediates caspase-1 processing and innate immune defense in response to bacterial blockade of NF-κB and MAPK signaling. Proceedings of the National Academy of Sciences. 2014;111(20):7385-90. doi: 10.1073/pnas.1403252111.

71. Chung LK, Bliska JB. Yersinia versus host immunity: how a pathogen evades or triggers a protective response. Current Opinion in Microbiology. 2016; 29:56-62. doi: 10.1016/j.mib.2015.11.001.

72. Zwack EE, Snyder AG, Wynosky-Dolfi MA, Ruthel G, Philip NH, Marketon MM, et al. Inflammasome Activation in Response to the Yersinia Type III Secretion System Requires Hyperinjection of Translocon Proteins YopB and YopD. mBio. 2015;6(1):14. doi: 10.1128/mBio.02095-14.

73. Goguen JD, Yother J, of bacteriology S-SC. Genetic analysis of the low calcium response in Yersinia pestis mu d1 (Ap lac) insertion mutants. Journal of bacteriology. 1984.

74. Jackson MW, Silva-Herzog E, Plano GV. The ATP-dependent ClpXP and Lon proteases regulate expression of the Yersinia pestis type III secretion system via regulated proteolysis of YmoA, a small histone-like protein. Molecular Microbiology. 2004;54(5):1364-78. doi: 10.1111/j.1365-2958.2004.04353.x.

75. Hoe NP, Goguen JD. Temperature sensing in Yersinia pestis: translation of the LcrF activator protein is thermally regulated. Journal of Bacteriology. 1993;175(24):7901-9. doi: 10.1128/jb.175.24.7901-7909.1993.

76. Rohmer L, Hocquet D, Miller SI. Are pathogenic bacteria just looking for food? Metabolism and microbial pathogenesis. Trends Microbiol. 2011;19(7):341-8. Epub 2011/05/24. doi: 10.1016/j.tim.2011.04.003. PubMed PMID: 21600774; PubMed Central PMCID: PMCPMC3130110.

77. Nizet V, Johnson RS. Interdependence of hypoxic and innate immune responses. Nature reviews Immunology. 2009;9(9):609-17. doi: 10.1038/nri2607.

78. Heroven AK, Sest M, P-F. Crp induces switching of the CsrB and CsrC RNAs in Yersinia pseudotuberculosis and links nutritional status to virulence. Frontiers in cellular and Infection Microbiology. 2012. doi:10.3389/fcimb.2012.00158

79. Vadyvaloo V, Jarrett C, Sturdevant DE, Sebbane F, Hinnebusch JB. Transit through the Flea Vector Induces a Pretransmission Innate Immunity Resistance Phenotype in Yersinia pestis. PLoS Pathogens. 2010;6(2). doi: 10.1371/journal.ppat.1000783.

80. Lathem WW, Crosby SD, M-VL. Progression of primary pneumonic plague: a mouse model of infection, pathology, and bacterial transcriptional activity. Proceedings of the National Academy. 2005. doi: 10.1073/pnas.0506840102.

81. Litwin CM, Calderwood SB. Role of iron in regulation of virulence genes. 1993;6(2):137-49. doi: 10.1128/CMR.6.2.137 J Clinical Microbiology Reviews.

82. Hennigar SR, journal of lifestyle M-JP. Nutritional immunity: starving pathogens of trace minerals. American journal of lifestyle 2016. doi: 10.1177/1559827616629117

83. Schaible UE, Kaufmann SHE. Iron and microbial infection. Nature Reviews Microbiology. 2004;2:946. doi: 10.1038/nrmicro1046.

84. Skaar EP. The battle for iron between bacterial pathogens and their vertebrate hosts. PLoS pathogens. 2010;6(8). doi: 10.1371/journal.ppat.1000949.

85. Ganz T, Nemeth E. Iron homeostasis in host defence and inflammation. Nature reviews Immunology. 2015;15(8):500-10. Epub 2015/07/10. doi: 10.1038/nri3863. PubMed PMID: 26160612.

86. Watson KG, Holden DW. Dynamics of growth and dissemination of Salmonella in vivo. Cellular Microbiology. 2010;12(10):1389-97. doi: 10.1111/j.1462-5822.2010.01511.x.

87. Kehrer. The Haber–Weiss reaction and mechanisms of toxicity. Toxicology. 2000. PubMed Central PMCID: PMC2000.

88. Staggs TM, Perry RD. Fur regulation in Yersinia species. Molecular Microbiology. 1992;6(17):2507-16. doi: 10.1111/j.1365-2958.1992.tb01427.x.

89. Fillat MF. The FUR (ferric uptake regulator) superfamily: Diversity and versatility of key transcriptional regulators. Archives of Biochemistry and Biophysics. 2014;546:41-52. doi: 10.1016/j.abb.2014.01.029.

90. Jacobi CA, Gregor S, Rakin A, Heesemann J. Expression Analysis of the Yersiniabactin Receptor Gene fyuA and the Heme Receptor hemR of Yersinia enterocolitica In Vitro and In Vivo Using the Reporter Genes for Green Fluorescent Protein and Luciferase. Infection and Immunity. 2001;69(12):7772-82. doi: 10.1128/iai.69.12.7772-7782.2001.

91. Porcheron G, Dozois CM. Interplay between iron homeostasis and virulence: Fur and RyhB as major regulators of bacterial pathogenicity. Vet Microbiol. 2015;179(1-2):2-14. Epub 2015/04/19. doi: 10.1016/j.vetmic.2015.03.024. PubMed PMID: 25888312.

92. Alice AF, Naka H, Crosa JH. Global Gene Expression as a Function of the Iron Status of the Bacterial Cell: Influence of Differentially Expressed Genes in the Virulence of the Human Pathogen Vibrio vulnificus ▿ †. Infection and Immunity. 2008;76(9):4019-37. doi: 10.1128/IAI.00208-08.

93. Murphy ER, Payne SM. RyhB, an Iron-Responsive Small RNA Molecule, Regulates Shigella dysenteriae Virulence. Infection and Immunity. 2007;75(7):3470-7. doi: 10.1128/IAI.00112-07.

94. Teixidó L, Carrasco B, Alonso JC, Barbé J, Campoy S. Fur Activates the Expression of Salmonella enterica Pathogenicity Island 1 by Directly Interacting with the hilD Operator In Vivo and In Vitro. PLoS ONE. 2011;6(5). doi: 10.1371/journal.pone.0019711.

95. Tobe T, Yen H, Takahashi H, Kagayama Y, Ogasawara N, Oshima T. Antisense Transcription Regulates the Expression of the Enterohemorrhagic Escherichia coli Virulence Regulatory Gene ler in Response to the Intracellular Iron Concentration. PLoS ONE. 2014;9(7). doi: 10.1371/journal.pone.0101582.

96. McHugh JP, Rodriguez-Quinones F, Abdul-Tehrani H, Svistunenko DA, Poole RK, Cooper CE, et al. Global iron-dependent gene regulation in Escherichia coli. A new mechanism for iron homeostasis. J Biol Chem. 2003;278(32):29478-86. Epub 2003/05/15. doi: 10.1074/jbc.M303381200. PubMed PMID: 12746439.

97. Deng Z, Meng X, Su S, Liu Z, Ji X, Zhang Y, et al. Two sRNA RyhB homologs from Yersinia pestis biovar microtus expressed in vivo have differential Hfq-dependent stability. Research in Microbiology. 2012;163(6-7):413-8. doi: 10.1016/j.resmic.2012.05.006.

98. Forman S, Paulley JT, Fetherston JD, Cheng Y-QQ, Perry RD. Yersinia ironomics: comparison of iron transporters among Yersinia pestis biotypes and its nearest neighbor, Yersinia pseudotuberculosis. Biometals : an international journal on the role of metal ions in biology, biochemistry, and medicine. 2010;23(2):275-94. doi: 10.1007/s10534-009-9286-4.

99. Rakin A, Schneider L, in cellular and P-O. Hunger for iron: the alternative siderophore iron scavenging systems in highly virulent Yersinia. Frontiers in cellular and …. 2012.

100. Amphlett A. Far East scarlet-like fever: a review of the epidemiology, symptomatology, and role of superantigenic toxin: Yersinia pseudotuberculosis-derived mitogen A. Open forum infectious diseases. 2016.

101. Carniel E, Guiyoule A, G-I. Molecular cloning, iron-regulation and mutagenesis of the irp2 gene encoding HMWP2, a protein specific for the highly pathogenic Yersinia. Molecular Biology 1992. doi: 10.1111/j.1365-2958.1992.tb01481.x.

102. Liu H, Wang H, Qiu J, Wang X, G-Z. Transcriptional profiling of a mice plague model: insights into interaction between Yersinia pestis and its host. Journal of basic Microbiology. 2009. doi: 10.1002/jobm.200800027.

103. Bearden SW, Staggs TM, of bacteriology P-RD. An ABC Transporter System of Yersinia pestis Allows Utilization of Chelated Iron by Escherichia coliSAB11. Journal of bacteriology. 1998.

104. Thompson JM, Jones HA, and immunity P-RD. Molecular Characterization of the Hemin Uptake Locus (hmu) from Yersinia pestis and Analysis ofhmu Mutants for Hemin and Hemoprotein Utilization. Infection and immunity. 1999.

105. Perry RD, Bobrov AG, Metallomics F-JD. The role of transition metal transporters for iron, zinc, manganese, and copper in the pathogenesis of Yersinia pestis. Metallomics. 2015. doi: 10.1039/C4MT00332B.

106. Fetherston JD, Mier I, T-H. The Yfe and Feo transporters are involved in microaerobic growth and virulence of Yersinia pestis in bubonic plague. Infection and Immunity. 2012. doi: 10.1128/IAI.00086

107. Schwartz CJ, Giel JL, Patschkowski T, Luther C, Ruzicka FJ, Beinert H, et al. IscR, an Fe-S cluster-containing transcription factor, represses expression of Escherichia coli genes encoding Fe-S cluster assembly proteins. Proc Natl Acad Sci U S A. 2001;98(26):14895-900. Epub 2001/12/14. doi: 10.1073/pnas.251550898. PubMed PMID: 11742080; PubMed Central PMCID: PMCPMC64955.

108. Lim JG, Choi SH. IscR is a global regulator essential for pathogenesis of Vibrio vulnificus and induced by host cells. Infect Immun. 2014;82(2):569-78. Epub 2014/01/31. doi: 10.1128/IAI.01141-13. PubMed PMID: 24478072; PubMed Central PMCID: PMCPMC3911388.

109. Santos JA, Pereira PJ, Macedo-Ribeiro S. What a difference a cluster makes: The multifaceted roles of IscR in gene regulation and DNA recognition. Biochim Biophys Acta.

2015;1854(9):1101-12. Epub 2015/02/03. doi: 10.1016/j.bbapap.2015.01.010. PubMed PMID: 25641558.

110. Kim S-H. IscR Modulates Catalase A (KatA) Activity, Peroxide Resistance, and Full Virulence of Pseudomonas aeruginosa PA14. Journal of Microbiology and Biotechnology. 2009;19(12):1520-6. doi: 10.4014/jmb.0906.06028.

111. Jones-Carson J, Laughlin J, Hamad MA, one S-AL. metalloproteins mediates nitric oxide-dependent killing of Burkholderia mallei. PloS one. 2008. doi: 10.1371/journal.pone.0001976.

112. Wong SM, Bernui M, Shen H, Akerley BJ. Genome-wide fitness profiling reveals adaptations required by Haemophilus in coinfection with influenza A virus in the murine lung. Proc Natl Acad Sci U S A. 2013;110(38):15413-8. Epub 2013/09/05. doi: 10.1073/pnas.1311217110. PubMed PMID: 24003154; PubMed Central PMCID: PMCPMC3780910.

113. Wu CC, Wang CK, Chen YC, Lin TH, Jinn TR, Lin CT. IscR regulation of capsular polysaccharide biosynthesis and iron-acquisition systems in Klebsiella pneumoniae CG43. PLoS One. 2014;9(9):e107812. Epub 2014/09/23. doi: 10.1371/journal.pone.0107812. PubMed PMID: 25237815; PubMed Central PMCID: PMCPMC4169559.

114. Vergnes A, Viala J, Ouadah-Tsabet R, Pocachard B, Loiseau L, Méresse S, et al. The iron–sulfur cluster sensor IscR is a negative regulator of Spi1 type III secretion system in Salmonella enterica. Cellular Microbiology. 2016. doi: 10.1111/cmi.12680.

Chapter 2

Mouse Models of Yersiniosis

By Diana Hooker-Romero, Leah Schwiesow, Yahan Wei, and Victoria Auerbuch

Summary/Abstract

Yersiniosis is common food-borne gastrointestinal disease caused by the enteric pathogens *Yersinia enterocolitica* and *Yersinia pseudotuberculosis.* The mouse model of oral infection serves as a useful tool to study enteropathogenic *Yersinia* infection in mammals. The following protocol describes two distinct oral infection methods: the commonly used oral gavage method in which the bacterial inoculum is instilled directly into the mouse stomach using a feeding needle, and an alternative method in which mice are fed bread soaked with *Yersinia* culture.

1. Introduction

Yersiniosis is a food-borne, self-limiting gastrointestinal disease caused by the Gram negative bacterial pathogens *Yersinia enterocolitica* and *Yersinia pseudotuberculosis*, which are usually transmitted via the fecal-oral route ***(1)***. Although both *Y. pseudotuberculosis* and *Y. enterocolitica* cause disease, most cases in humans are associated with *Y. enterocolitica* ***(1)***. In otherwise healthy individuals, yersiniosis is characterized by mild, self-limiting diarrhea, enteritis, ileocolitis, and mesenteric lymphadenitis, and can affect the appendix tissue and mimic appendicitis ***(1)***. In immunocompromised patients, or in patients with iron overload ***(2)***, *Yersinia* can disseminate to the spleen and liver. The *Yersinia* mouse model of oral infection is the most widely used animal model to study enteric *Yersinia* infections, as it reflects the natural route of infection where the pathogen is exposed to the mucosal immune environment of the small intestine before disseminating into deeper tissues ***(3, 4)***. Specifically, the mouse model of oral infection mimics human disseminated infection in that the spleen and liver become colonized.

The oral infection model was first established by Phil Carter and Frank Collins in 1974 when they demonstrated that after oral gavage, mice displayed similar symptoms to those

observed in humans, such as formation of abscesses in Peyer's patches, mesenteric lymph nodes, spleen, and liver ***(5, 6)***. These abscesses can resolve in animals that survive the infection ***(5–8)***. After ingestion, *Yersinia* adheres to the apical surface of microfold (M) cells within the small intestinal lining, where the bacteria cross the epithelial barrier to the underlying Peyer's patches ***(9, 10)***. Within the Peyer's patches, *Yersinia* replicate extracellularly and disseminate to distal lymphoid tissues such as the mesenteric lymph nodes ***(1)***. However, *Yersinia* can also replicate in the intestinal lumen and a Peyer's patch independent route of dissemination from the gut lumen to the spleen and liver has been described for *Y. pseudotuberculosis*, although the mechanism remains unclear ***(11)***. This Peyer's patch independent route enables successful colonization of the spleen and liver, where monoclonal microabscesses are formed ***(7, 11)***.

Numerous studies using the mouse oral infection model have identified a number of virulence factors needed for infection and survival in the host ***(8, 10, 12–20)***. In addition, a recent study showed that virulence factor expression can vary within an abscess, depending on proximity to immune cells and other parameters ***(8)***. Other studies have provided a better understanding of how the host immune system recognizes and reacts to *Yersinia* ***(17, 19, 21–27)***. The dynamic interplay between a variety of host cells and *Yersinia* capable of sensing environmental cues to control virulence gene expression underscores the importance of studying the host-pathogen interaction in the context of a natural infection model. Studies like the one by Nuss *et al*, which analyzed the interaction between *Y. pseudotuberculosis* and the murine host by performing a dual RNAseq technique on infected mouse Peyer's patches ***(26)***, will help fill in the gaps of our understanding.

The following protocols describe two different methods of orally inoculating mice with enteropathogenic *Yersinia.* The first method, oral gavage, which introduces the bacterial inoculum directly into the stomach, is the most commonly used procedure. The second

method, bread feeding, is a new protocol recently developed for *Listeria monocytogenes* infection by Ghanem *et al (2013),* in which bacterial culture is resuspended in melted butter and soaked into a small piece of white bread ***(28)***. Our lab has adapted this method to use with *Y. pseudotuberculosis* infection of mice because it resembles a more natural route of oral infection and prevents possible physical trauma to the lining of the esophagus, which could cause direct entrance of the inoculum into the bloodstream ***(28)***. This method also limits stress on the animal subjects during delivery of the infectious dose. However, one limitation is that, depending on the mouse genotype and susceptibility to *Yersinia* infection, it can be challenging to deliver a large enough inoculum. Therefore, we have performed this method successfully in 129S1/SvImJ mice (*see* **Figure 1***)* but not in C57Bl/6 mice, which require a higher dose ***(4).***

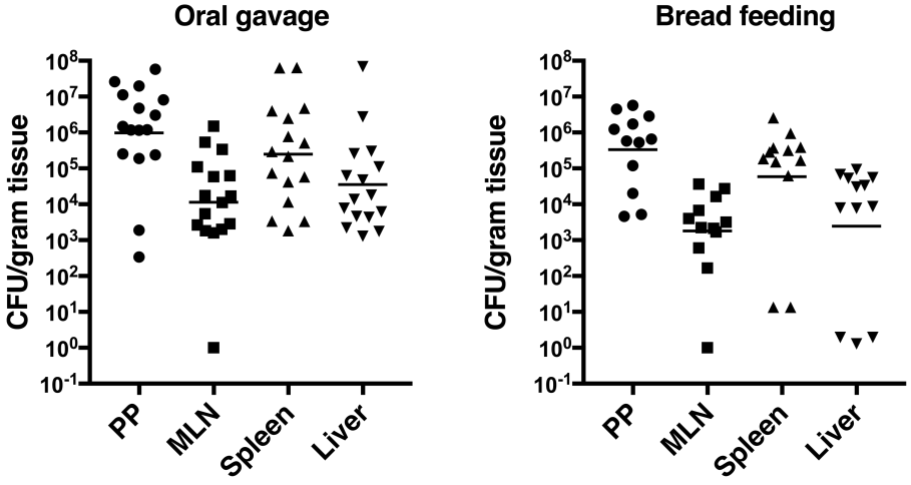

Fig. 1. Bacterial load in the different organs is comparable after oral infection of Yersinia pseudotuberculosis by oral gavage or bread feeding. Mice were infected with 2 $X10^8$ CFU of WT Y. pseudotuberculosis IP2666 and after 5 days the mesenteric lymph nodes, Peyer's patches, livers, and spleens were harvested, homogenized, and plated for CFU determination. Oral gavage data points were previously published in Miller et al. [20, 21]

The oral mouse models of infection described here can be used to determine virulence kinetics of different *Y. pseudotuberculosis* or *Y. enterocolitica* strains or mutants. Dissemination can be analyzed by plating homogenates of mouse organs and counting colony forming units (CFU), or by sectioning mouse organ tissue and analyzing microabscess formation by immunohistochemistry. This latter approach is usually done after infecting mice with fluorescently labeled bacteria ***(7, 8, 19)***

2. Materials

2.1. Oral gavage.

1. Sterile 1ml syringes and gauge 10, stainless-steel 2-inch feeding needles with a smooth, 3 mm ball on the end.
2. Luria Broth (LB) medium.
3. Sterile 1X Phosphate-buffered saline (1X PBS).
4. *Yersinia* strains to be used during infection. (*see* **note 1*)***
5. 8-10 week old 129X1/Sjv mice. (*see* **note 2)** (*see* **note 3**)
6. LB agar plates supplemented with irgasan (1μg/ml).
7. Sterile 1X PBS.
8. Sterile spreading glass beads.
9. 1.5 ml Eppendorf tubes.

2.2. Oral infection via ingestion of contaminated bread.

1. Sterile 1X PBS.
2. LB medium.
3. *Yersinia* strains to be used during infection.
4. Salted sweet cream butter
5. White sliced bread.

6. Sterile scalpel.
7. Sterile 1.5 ml microcentrifuge tubes.
8. 8-10 week old 129X1/Sjv mice. (*see* **note 4**)
9. LB agar plates supplemented with irgasan (1μg/ml).
10. Sterile 1X PBS.
11. Sterile spreading glass beads.
12. 1.5 ml Eppendorf tubes

2.3. Dissemination analysis

1. 15 ml Conical tubes.
2. LB agar plates supplemented with irgasan (1μg/ml). Approximately 6 plates per organ per mouse.
3. Cotton balls.
4. Sterile 1X PBS.
5. Isoflurane.
6. Sterile spreading glass beads.
7. Sterile 1.5 ml Eppendorf tubes.
8. Sterile scalpel, forceps, and scissors for mice tissue dissection.
9. Sterile 5ml culture tubes or 15ml conical tubes to collect mice tissues and perform homogenization.
10. Scale.
11. Plastic Tupperware with cover.
12. Omni Tissue Homogenizer with stainless steel probe (125 watt, speed 5,000 – 35,000rpm).
13. 70% (v/v) ethanol.
14. 100% ethanol.

15. 50 ml conical tubes
16. Fresh 4% Paraformaldehyde in 1X PBS
17. 30% sucrose in 1X PBS
18. Leica Cryostat
19. OCT compound-freezing media
20. Positively charged slides
21. ProLong Gold Antifade Mountant
22. Clear nail polish
23. Coverslips
24. 2-methyl butane
25. Dry ice

3. Methods

3.1. Oral gavage.

1. 15-18 h prior to infection, fast mice by removing chow. Continue providing water ad libitum. (*see* **note 5**)
2. 15-18 h prior to infection, inoculate 2 ml of LB media with *Yersinia* strain. Grow at 26°C with agitation.
3. Take OD of the overnight culture and calculate amount of culture needed to inoculate 2 $x10^8$ bacteria per mouse (*see* **note 6)**. Transfer culture to Eppendorf tube and spin down for 5 minutes at 835 x g. Decant supernatant and resuspend bacterial culture in 1X PBS to approximately 2 x 10^9 bacteria/ml. Each mouse will get 200 μl aliquots of 2 $x10^8$ bacteria per inoculum. (*see* **note 7**)
4. Uptake the bacterial suspension into the syringe and position the feeding needle securely.

5. Restrain the mouse securely by the scruff and hold mouse in an upright position, preventing the mouse from moving its head. (*see* **note 8**)
6. Locate the mouse's last rib, this is the position of the stomach. With the ball tip at the last rib, place the needle alongside the mouse and look at where the shaft meets the mouse's incisors, this is the point at which you would stop advancing the needle.
7. Introduce the feeding needle into the mouse mouth slowly and guide the ball tip along the roof of the mouth and towards the back of the throat, incline the syringe so that it is parallel with the mouse body and gently guide the needle down the esophagus. Never force the needle. Remove the needle and try again if you get resistance. Once the needle tip is in the stomach, inject 200μl slowly. Control mice can be inoculated with sterile 1X PBS.
8. Remove the needle straight up slowly.
9. Return mouse to cage and monitor for any signs of respiratory distress or injury, which would indicate unintended injury during gavage.
10. Provide food and water *at libitum.*
11. Verify inoculum by plating 10-fold serial dilutions onto LB plates with irgasan 1μg/ml, as it selects for *Yersinia* species. For the dilutions, add 900 μl of 1X PBS into 1.5 ml Eppendorf tubes. Take 100 μl of inoculum and pipet into the first Eppendorf tube, vortexing vigorously for 15 sec, for a 1:10 dilution. Take 100 μl of the 1:10 dilution and add it to the next tube containing 900 μl sterile 1X PBS to make the 1:100 dilution. Repeat these steps to make 5 dilutions for each organ.

12. Add 100 μl of each dilution to a previously labeled LB plate supplemented with irgasan, add spreading beads and shake plate for 30 seconds to spread the bacteria. Remove the beads.
13. Incubate plates at 26°C for 48hr, then count colonies.

3.2. Oral infection via ingestion of contaminated bread.

1. 15-18 h prior to infection, fast mice by removing chow. Continue providing water ad libitum.
2. 15-18 h prior to infection, inoculate 2 ml of LB media with *Yersinia* strain. Grow at 26°C with agitation.
3. Remove crust from bread and cut into small 3-4mm cubes with the sterile scalpel blade. (*see* **note 9)** (*see* **figure 2**)
4. Cut butter into 0.5-1 cm cubes and place into 1.5 ml microcentrifuge tube. (*see* **note 9)**

Fig. 2 Measurement of the bread size for mouse infection. After cutting the crusts, the bread is sliced with a sterile scalpel. Pieces should be cubes of about 3–4 mm^3

5. Incubate microcentrifuge tube with 2 ml aliquot of 1X PBS in water bath at 55°C.
6. Incubate microcentrifuge tube with previously cut butter in water bath at 55°C.
7. Once the overnight culture is ready, take OD and calculate number of bacteria needed for an infectious dose of 2 x 10^8 per mouse. For example, to inoculate 10 mice, transfer 2 x 10^9 cells to an Eppendorf tube.
8. Spin down culture at 835 x g for 5 minutes, then aspirate supernatant.
9. Each inoculum needs to be resuspended in 2 μl of previously incubated at 55°C 1X PBS and 3 μl of melted butter. For 10 inoculums, resuspend the 2 x 10^9 cells in 20 μl of warm 1X PBS and 30 μl of melted butter. Mix thoroughly and rapidly pipet the 5 μl onto a bread cube (*see* **note 10)**. Store tubes with inoculated bread on ice until ready to do infection.
10. Place each mouse in an empty cage and provide the bread piece. Wait until the animal has eaten the entire piece of bread. This usually takes a few minutes. (*see* **Note 11**)
11. After infection, return mouse to original cage.
12. Provide food and water *at libitum.*
13. Verify inoculum by placing an inoculated bread piece in 1ml of warm 1X PBS and vortexing vigorously for 30 seconds.
14. Serially dilute bread homogenate by a 10 fold factor by adding 100 μl of it into 900μl of 1X PBS. Continue serially diluting to 10^{-7}.
15. Plate the last four dilutions onto LB plates supplemented with irgasan by pipetting 100 μl and spreading with sterile glass beads.

3.3. Methods for studying bacterial dissemination

After inoculation, check mice daily for signs of distress. Inspect daily for any inactivity, lack of responsiveness to stimulation, reduced eating or drinking, hunched posture, or ruffled fur, which can be indicative of severe illness. If mice display any of those signs, euthanize immediately to avoid suffering. Tissues can be harvested between 1 and 5 days post-inoculation.

3.3.1. Bacterial enumeration in infected tissues

1. Label and weigh one 15 ml conical tube for each tissue that will be harvested.
2. Euthanize mice by an American Veterinary Medical Association approved method.
3. Pin mouse to dissecting board and spray ventral side with 70% ethanol.
4. Make an incision along the abdomen with sterile scissors.
5. Place intestines on one side, without damaging the mesentery, so that the mesenteric lymph nodes are exposed. (*see* **note 12**) (*see* **figure 3**)

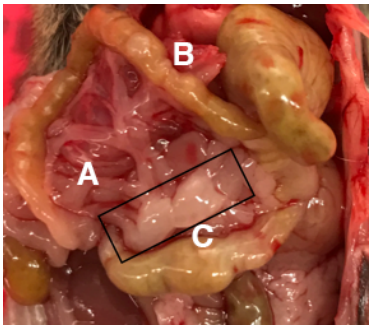

Fig. 3 Location of the inflamed mesenteric lymph nodes and Peyer's patches. Once the intestines are exposed, lift the intestinal coils on the mouse's right side and shift over to the left to find the mesentery (a). Find the mesenteric lymph nodes nestled in the mesentery (b). They will look like small white oval plump structures. The Peyer's patches are located along

the intestine walls (c). They look like pearly white raised dots on the surface of the small intestine.

6. Using aseptic technique, remove the mesenteric lymph nodes and place them on ice in a previously weighed conical tube.
7. Remove the Peyer's patches along the small intestine (*see* **figure 3)** by using scissors to cut each Peyer's patch away from the small intestinal tissue, taking care not to include luminal contents. Place the Peyer's patch in a previously weighed conical tube. Incubate on ice. Peyer's patches belonging to the same mouse are placed into the same tube.
8. Remove spleen and liver and place on ice in individual previously weighed conical tubes. (*see* **note 13**)
9. Weigh the tubes containing the organs.
10. Add 1ml of sterile 1X PBS to the tubes holding the livers and 500 μl to the tubes holding the remaining organs. (*see* **note 14**)
11. Homogenize organs for 30 seconds with tissue homogenizer at 20,000 rpm. Smaller organs such Peyer's patches and mesenteric lymph nodes are homogenized first, then the spleen is homogenized, followed by the liver. Homogenization should be done in a laminar air flow hood since bacteria can be aerosolized. Wash homogenizer between each set of organs by running the homogenizer at 20,000 rpm for 15 seconds in a 50 ml conical tube filled with 1X PBS, followed by a run in 100% ethanol, and then 1X PBS again. A fresh set of washing tubes is used for each mouse.

16. Serially dilute homogenate by a 10-fold factor by adding 100 μl of it into 900 μl of 1X PBS. Continue serially dilution from 10^{-1} to 10^{-4}.

12. Use undiluted homogenate as well as the 10^{-1} to 10^{-4} dilutions for Peyer's patches, mesenteric lymph nodes, liver, and spleen. Plate onto LB plates supplemented with irgasan by pipetting 100 μl and spreading it with sterile glass beads.
13. Incubate plates at 26°C for 48 hours.
14. Count colony forming units (CFU) and calculate CFU per gram of tissue using the formula below. (*see* figure 1)

$$CFU/_{gr\ Organ} = \left(\frac{CFU}{Vol.plated}\right)\left(\frac{total\ vol.PBS}{Weight\ of\ organ}\right)(dilution\ factor)$$

3.3.2. Immunofluorescence analysis of infected tissues

If mice have been infected with fluorescent *Yersinia* strains, bacterial dissemination can also be examined by microscopy.

1. Harvest tissues as described in 3.3.1 steps 1 to 4.
2. Place organs in 15 ml conical tubes containing 1ml 1X PBS. Swirl the tube slowly for 15 seconds, decant PBS and repeat wash with fresh PBS two more times.
3. Fix organs by placing them in a 15 ml conical tube and adding 1 ml of fresh 4% PFA in PBS. Incubate for 3 hours.
4. Wash tissue by transferring each organ to a new 15 ml conical tube with 1 ml 1X PBS and incubating for 5 minutes at room temperature. Repeat once more.
5. Incubate in 2 ml of 30% sucrose overnight at 4°C.
6. To freeze-embed the tissue, add about 2 ml of tissue freezing media to a cryogenesis cuvette, then add the organ and completely cover with more freezing media. Make sure to add media slowly to avoid any bubbles.

7. Submerge the cuvette in a flask filled with ~200 ml of 2-methylbutane over dry ice. (*See* **note 15)**
8. Cut 10 μm sections with a cryostat microtome and affix to slides. Store slides in dark slide box at 4°C until ready to stain.
9. Stain tissues with Hoechst at a 1:10,000 dilution in 1X PBS. Incubate for 30 minutes in the dark at room temperature.
10. Wash two times by tilting the slide to 45° and slowly pipetting 1X PBS to the top of the slide and letting it drip over the tissue slice.
11. Affix coverslips with an antifade mountant such as ProLong Gold, and seal the sides of the coverslip with clear nail polish.
12. Let the ProLong Gold cure and nail polish dry overnight by storing in the dark at room temperature.
13. Examine by fluorescence microscopy.

4. Notes

1. *Y. pseudotuberculosis* and *Y. enterocolitica* are considered potentially hazardous. Biosafety Level 2 practices and facilities are required when working with these pathogens.
2. All experimental procedures using live animals must be approved by the relevant Institutional Animal Care and Use Committee (IACUC).
3. Yersiniosis oral model studies usually use mice between 7 to 12 weeks old, as infant mice do not develop systemic infection ***(29)***. The three main inbred mouse strains used for *Yersinia* oral infection are C57BL/6, BALB/c, and 129X1/Sjv. A study comparing the three mouse strains showed no difference in dissemination patterns and tissue pathology; however, mesenteric lymph nodes of C5BL/6 mice displayed a lower bacterial load, compared to the other two strains. Additionally, this study also reported high variability in spleen colonization in C57BL/6 and BALB/c mice ***(4)***. LD_{50}

analysis showed that BALB/c mice are more susceptible, and that C57BL/6 are more resistant.

4. We have performed this method with 8 to10-week-old 129S1 mice only and have not tested the optimal inoculum for other mouse inbred strains. As the infectious dose used to infect C57Bl/6 is higher due to higher resistance, the pieces of bread fed to these animals would need to be larger to soak up the larger *Yersinia* pellet resuspension. This can be challenging given the small size of the mouse stomach. Additionally, a bigger bacterial pellet might also be hard to resuspend in such a small amount of butter, making the suspension very sticky and hard to get off of the tube.
5. Sodium chloride or sodium bicarbonate can be supplemented before inoculation. Pretreatment of mice with sodium bicarbonate can reduce gastric acid and thus resistance to gastric infection ***(30)***. However, another study giving different concentrations of sodium chloride to mice before orally inoculating them with *Yersinia enterocolitica* suggested that neutralization of gastric acidity had no effect on bacterial virulence ***(31)***.
6. Quantity of cells corresponding to a specific OD can be calculated by growing an overnight culture of the strains to be inoculated, taking the OD with a spectrophotometer and then performing a 10-fold serial dilution, from which 100 μl are plated on LB plates. CFU can be counted after 48 hrs incubation at 26°C
7. Different studies using *Yersinia pseudotuberculosis* strains IP2666, YPIII, and IP32953 have shown that the ideal inoculum is between 1×10^8 to 8×10^8 CFU for C57BL/6 and 129X1/Sjv mice, and about 2×10^7 for BALB/c mice. However, dose depends on bacterial serotype, as some serotypes can be more virulent than others.
8. Mice can be lightly anesthetized using a vaporizer to deliver a small dose of isoflurane before performing oral gavage. This can minimize stress on the mice and prevent mice from moving during gavage. After gavage, mice are monitored for

several minutes after they regain consciousness to ensure they do not show any signs of distress or discomfort. Isoflurane usage should be performed in a ducted biosafety cabinet or in the presence of an isoflurane scavenger system to avoid accidental inhalation.

9. Store individual bread pieces in a microcentrifuge tube or small petri dish at -20C. This can be done up to a day before inoculation of the bread. Butter can also be stored ahead of time in an Eppendorf tube at -20C.To avoid fast cooling of the butter, bacterial resuspension in warm butter and PBS can be done in batches. Avoid doing more than 10 pieces at the time or the butter will solidify. To keep the butter melted in between bread inoculations, rapidly dip bacterial suspension tube in a 55˚C water bath for a couple seconds and pipette several times to mix bacterial suspension. Make sure this is done rapidly so as not affect bacterial viability.
10. If mouse does not eat the piece of bread within 15 minutes, mouse can be left undisturbed in the cage for up to 2 hours.
11. Mesenteric lymph nodes are usually removed first before disrupting the mesentery. Once the intestines are exposed, lift the intestinal coils on the mouse's right side and shift over to the left to find the mesentery. Find the mesenteric lymph nodes nestled in the mesentery. They will look like small white oval plump structures. (*See* **Figure 3**)
12. It is also possible to analyze *Yersinia* within the small intestine and feces. When plating the small intestine, squeeze out the contents with forceps and plate that separately from the small intestinal tissue. Cecal content and fecal pellets can also be homogenized and analyzed for bacterial content.
13. PBS can be added prior to weighing the tubes. NP-40 detergent can also be added to PBS to lyse open the mouse cells. No difference between the use of PBS and PBS with NP-40 has been found in terms of CFU ***(27)***.

14. 2-methyl buthane should be previously incubated at -70°C the night before tissue embedding.

Acknowledgements

We thank Susannah McKay and Daniel Portnoy for technical advice in establishing the bread feeding model in *Yersinia*. D.H.-R. is supported by a Ford Foundation fellowship. The mouse infection data shown are taken from work supported by the National Institute of Allergy and Infectious Diseases of the National Institutes of Health under Award Numbers R21AI099747 and R01AI119082 (to V

References

1. Galindo C, Rosenzweig J, Kirtley M, et al (2011) Pathogenesis of *Y. enterocolitica* and *Y. pseudotuberculosis* in Human Yersiniosis. J Pathogens 2011:182051

2. Weinberg E (2000) Microbial pathogens with impaired ability to acquire host iron. Biometals 13:85–89

3. Lawrenz M (2010) Model Systems to Study Plague Pathogenesis and Develop New Therapeutics. 1:119

4. Handley S, Dube P, Revell P, et al (2004) Characterization of Oral *Yersinia enterocolitica* Infection in Three Different Strains of Inbred Mice. Infect Immun 72:1645–1656

5. Carter P (1975) Animal model of human disease. *Yersinia* enteritis. Animal model: oral Yersinia enterocolitica infection of mice. Am J Pathology 81:703–6

6. Carter P and Collins F (1974) Experimental *Yersinia enterocolitica* infection in mice: kinetics of growth. Infect Immun 9:851–7

7. Trülzsch K, Oellerich M, and Heesemann J (2007) Invasion and dissemination of *Yersinia enterocolitica* in the mouse infection model. 603:279–85

8. Davis K, Mohammadi S, and Isberg R (2015) Community Behavior and Spatial Regulation within a Bacterial Microcolony in Deep Tissue Sites Serves to Protect against Host Attack. Cell Host Microbe 17:21–31

9. Grützkau A, Hanski C, Hahn H, et al (1990) Involvement of M cells in the bacterial invasion of Peyer's patches: a common mechanism shared by *Yersinia enterocolitica* and other enteroinvasive bacteria. Gut 31:1011-1015

10. Marra A and Isberg R (1997) Invasin-dependent and invasin-independent pathways for translocation of *Yersinia pseudotuberculosis* across the Peyer's patch intestinal epithelium. Infect Immun 65:3412–21

11. Barnes P, Bergman M, Mecsas J, et al (2006) *Yersinia pseudotuberculosis* disseminates directly from a replicating bacterial pool in the intestine. J Exp Medicine 203:1591–1601

12. Handley S, Newberry R, and Miller V (2005) *Yersinia enterocolitica* invasin-dependent and invasin-independent mechanisms of systemic dissemination. Infect Immun 73:8453-8455

13. Mecsas J, Bilis I, and Falkow S (2001) Identification of attenuated *Yersinia*

pseudotuberculosis strains and characterization of an orogastric infection in BALB/c mice on day 5 postinfection by signature-Tagged Mutagenesis. Infect Immun 69:2779-2787

14. Clark M, Hirst B, and Jepson M((1998) M-cell surface β1 integrin expression and invasin-mediated targeting of *Yersinia pseudotuberculosis* to mouse Peyer's patch M cells. Infect Immun 66:1237-1243

15. Trülzsch K, Sporleder T, Igwel E et al (2004) Contribution of the major secreted yops of *Yersinia enterocolitica* O: 8 to pathogenicity in the mouse infection model. Infect Immun 72:5227-5234

16. Trcek J, Berschl K, and Trülzsch K (2010) In vivo analysis of *Yersinia enterocolitica* infection using luxCDABE. Fems Microbiol Lett 307:201–6

Pepe J, Wachtel M, Wagar E, et al (1995) Pathogenesis of defined invasion mutants of *Yersinia enterocolitica* in a BALB/c mouse model of infection. Infect Immun 63:4837–48

18. Balada-Llasat J and Mecsas J (2006) *Yersinia* Has a Tropism for B and T Cell Zones of Lymph Nodes That Is Independent of the Type III Secretion System. Plos Pathog 2:e86

19. Crimmins G, Mohammadi S, Green E, et al (2012) Identification of MrtAB, an ABC Transporter Specifically Required for *Yersinia pseudotuberculosis* to Colonize the Mesenteric Lymph Nodes. Plos Pathog 8:e1002828

20. Miller H, Kwuan L, Schwiesow L, et al (2014) IscR Is Essential for *Yersinia pseudotuberculosis* Type III Secretion and Virulence. Plos Pathog 10:e1004194

21. Miller H, Schwiesow L, Au-Yeung W, et al (2016) Hereditary Hemochromatosis Predisposes Mice to *Yersinia pseudotuberculosis* Infection Even in the Absence of the Type III Secretion System. Frontiers Cell Infect Microbiol 6:69

22. Autenrieth I, Kempf V, Sprinz T, et al (1996) Defense mechanisms in Peyer's patches and mesenteric lymph nodes against *Yersinia enterocolitica* involve integrins and cytokines. Infect Immun 64:1357–68

23. Autenrieth I, Beer M, Bohn E, et al (1994) Immune responses to *Yersinia enterocolitica* in susceptible BALB/c and resistant C57BL/6 mice: an essential role for gamma interferon. Infect Immun 62:2590-2599

24. Westermark L, Fahlgren A, and Fällman M (2014) *Yersinia pseudotuberculosis* Efficiently Escapes Polymorphonuclear Neutrophils during Early Infection. Infect Immun 82:1181–1191

25. Costa T, Amer A, Farag S, et al (2013) Type III secretion translocon assemblies that attenuate *Yersinia* virulence. Cell Microbiol 15:1088–1110

26. Nuss A, Beckstette M, Pimenova M, et al (2017) Tissue dual RNA-seq allows fast discovery of infection-specific functions and riboregulators shaping host–pathogen transcriptomes. Proc National Acad Sci 114:E791–E800

27. Auerbuch V, Golenbock D, and Isberg R (2009) Innate Immune Recognition of *Yersinia pseudotuberculosis* Type III Secretion. Plos Pathog 5:e1000686

28. Ghanem E , Myers-Morales T, Jones G, et al (2013) Oral Transmission of *Listeria monocytogenes* in Mice via Ingestion of Contaminated Food. J Vis Exp (74):e50381

29. Echeverry A, Schesser K, and Adkins B (2007) Murine Neonates Are Highly Resistant to Yersinia enterocolitica following Orogastric Exposure. Infect Immun 75:2234–2243

30. Tennant S, Hartland E, Phumoonna T , et al (2008) Influence of Gastric Acid on Susceptibility to Infection with Ingested Bacterial Pathogens. Infect Immun 76:639–645

31. Singh A, McFeters G (1987) Survival and virulence of Copper and chlorine-stressed *Yersinia enterocolitica* in experimentally infected mice. Appl Environ Microb 53: 1768-74

Chapter 3.

Iron availability and oxygen tension regulate the *Yersinia* Ysc type III secretion system through IscR to enable disseminated infection

By Diana Hooker-Romero, Erin Mettert, Leah Schwiesow, David Balderas, Anadin Kicin, Azuah Gonzalez, Gregory Plano, Patricia J. Kiley, Victoria Auerbuch

Abstract

In *E. coli*, IscR is a [2Fe-2S] cluster-containing transcription factor whose levels and activity are controlled by Fe-S cluster demand, which in turn is regulated by iron availability and oxygen tension. We recently showed that IscR is required for expression of a major *Yersinia* virulence factor, the Ysc type III secretion system (T3SS). In *Yersinia*, IscR binds to the promoter of the T3SS master regulator LcrF and promotes *lcrF* transcription, type III secretion (T3S), and virulence. However, iron and oxygen have not previously been shown to control the *Yersinia* T3SS, although *Y. pseudotuberculosis* and *Y. pestis* are known to encounter fluctuating iron and oxygen availability in host tissues. In this study, we show that the *Y. pseudotuberculosis* T3SS is expressed under aerobic conditions regardless of iron availability. However, T3S can only be detected anaerobically if bacteria are depleted of iron or if IscR is mutated to prevent Fe-S cluster coordination, leading to ectopic IscR overexpression through disruption of a negative feedback loop. *Yersinia* T3S under both aerobic and anaerobic conditions is dependent on IscR binding to the *lcrF* promoter. Importantly, a mutation that prevents this binding leads to decreased disseminated infection in a *Y. pseudotuberculosis* bread-feeding mouse model but does not perturb bacterial colonization of the intestinal lumen. The IscR binding site in the *lcrF* promoter is completely conserved between *Y. pseudotuberculosis* and *Y. pestis*, and deletion of *iscR* in *Y. pestis* leads to drastic disruption of T3S. We propose that pathogenic *Yersinia* use IscR to sense iron and oxygen availability to control T3SS expression during infection.

Author summary

The *Yersinia* T3SS is critical for dampening host defenses and promoting virulence of the enteropathogens *Yersinia pseudotuberculosis* and *Y. enterocolitica* as well as *Y. pestis*, the causative agent of plague. Yet active type III secretion in *Yersinia* induces growth arrest and the T3SS is an object of innate immune recognition. In order to express the T3SS only when needed, pathogenic *Yersinia* have evolved to tightly regulate T3SS expression, for example,

by responding to changes in temperature when transitioning from the environment into the host. Here we show that T3SS expression in *Yersinia* is also regulated by iron availability and oxygen tension, which fluctuate over the course of *Yersinia* infection within the mammalian host. For example, iron is predicted to be more available to enteropathogenic *Yersinia* in the lumen of the intestine compared to in deeper tissues, where nutritional immunity maintains iron at vanishingly low levels. In addition, the oxygen gradient within intestinal tissue is critical for maintaining gut homeostasis and is disrupted in a number of inflammatory diseases. In this study, we show that eliminating the ability of *Yersinia* to control their T3SS in response to iron and oxygen leads to avirulence. These data suggest that *Yersinia* dynamically sense multiple cues during their life cycle to shape expression of critical factors promoting virulence.

Introduction

Iron (Fe) ions serve as metabolic cofactors for many proteins that play roles in crucial processes such as respiration, oxidative stress resistance, gene expression regulation, and virulence factor production [1]. Iron is able to adopt two stable valences, ferric and ferrous, providing iron-containing proteins with a considerable oxidation-reduction potential [2]. The level of iron required for optimal bacterial growth is ~10^{-6} M. However, the level of free iron in mammalian tissues is typically ~10^{-18} M [3]. This is because iron in mammals is mostly found inside cells associated with heme or metalloproteins or stored in ferritin. Furthermore, the trace amounts of extracellular iron are bound to the high affinity glycoproteins lactoferrin and transferrin [2, 3]. During infection, the host immune system withholds Fe from invading pathogens even more stringently. For example, expression of lactoferrin, found in bodily secretions and neutrophil granules, is induced during an inflammatory response and acts to sequester iron [4]. In addition, neutrophils in the inflamed intestine produce lipocalin-2, an antimicrobial protein that captures enterobactin, the primary siderophore of many enteric bacteria. The importance of nutritional immunity is exemplified by the increased susceptibility

of individuals with iron overload, including β-thalassemia, sideroblastic anemia, and hemochromatosis, to systemic infections with pathogenic *Yersinia, Vibrio parahaemolyticus*, and several other pathogens [5, 6].

Enteropathogens have evolved an extensive armory of uptake systems tailored to different iron sources and availability. To ensure optimal iron uptake, pathogenic *Yersinia* have numerous iron uptake and detoxification mechanisms preferentially activated depending on the environment and iron source they encounter [7]. However, in most bacteria, iron levels are homeostatically regulated through repression of these iron uptake systems to avoid the deleterious effects of excess iron. This global iron-dependent regulation is largely controlled by the repressor Fur (Ferric Uptake Regulator), which represses target gene expression under iron replete conditions [8]. Other studies in different bacterial species have also demonstrated that many iron responsive genes, including *fur* itself, can be regulated by other transcription factors in response to environmental changes such as oxidative stress or siderophore uptake [9]. This co-regulation of iron-dependent genes ensures that pathogens use the most fitting iron uptake system during their passage through the complex environment of the host organism and maintain iron homeostasis.

Many bacterial pathogens use iron availability to sense entry into the vertebrate host and adjust production of virulence factors important for growth or survival in host tissues [10]. The type III secretion system (T3SS) is a virulence factor used by nearly two dozen human pathogens, including *Yersinia* species, to modulate host defenses [11]. Recently, the transcription factor *iscR* was shown to be required for full *Y. pseudotuberculosis* Ysc T3SS function and virulence in a mouse model of infection [12]. This study showed that IscR binds to the promoter of the operon encoding the LcrF master regulator of the T3SS. IscR is a transcriptional regulator whose DNA-binding activity is regulated by its association with an iron-sulfur cluster [2Fe-2S]. IscR functions as a sensor of cellular Fe-S cluster status and regulates Fe-S cluster biogenesis mediated by the housekeeping Isc pathway and the stress-responsive Suf pathway. The [2Fe-2S] cluster holo-form of IscR binds to two distinct DNA motifs (type I

and type II). In contrast, the clusterless apo-IscR form binds only type II motifs. In *E. coli*, IscR negatively regulates its own promoter and directly or indirectly controls more than 40 genes [13]. *Vibrio vulnificus* IscR is also a global regulator that controls expression of many genes involved in Fe-S biogenesis and other cellular processes [14]. Likewise, over 200 genes are differentially expressed in the presence or absence of IscR in *Y. pseudotuberculosis* [12]. Therefore, whether the severe attenuation of the *Y. pseudotuberculosis* Δ*iscR* mutant in mice stems specifically from its defect in type III secretion or more broadly from altered regulation of multiple IscR-regulated genes remains unknown.

Studies in different Gram-negative organisms have shown that IscR regulates the expression of a number of genes, including its own operon, in response to environmental factors such as oxidative stress, iron starvation, and oxygen limitation [14-17]. These factors can affect the cellular Fe-S cluster pool, which in turn will modulate IscR association with Fe-S clusters. A recent study in *Salmonella enterica* serovar Typhimurium suggested that IscR leads to induction of the SPI-1 T3SS in response to iron sufficiency. Considering the SPI-1 T3SS is required for *Salmonella* to invade intestinal epithelial cells, this suggests that *Salmonella* uses IscR to sense the gut environment, upregulate the SPI-1 T3SS, and cross the gut barrier [17]. Although IscR is known to be essential for T3SS regulation and virulence in *Y. pseudotuberculosis* [12], how *Yersinia* regulates its T3SS in response to iron or oxygen is unknown. In this current study we determine the environmental conditions that affect IscR regulation of the *Yersinia* T3SS. Specifically, we demonstrate that iron insufficiency or the presence of oxygen lead to upregulation of T3SS expression in *Yersinia,* contrary to what is observed for *Salmonella* IscR control of the SPI-1 T3SS but in agreement with *Yersinia* requiring its Ysc T3SS after crossing the intestinal barrier.

Results

IscR binding to the *lcrF* promoter is critical for type III secretion. To investigate the environmental cues that impact IscR in *Yersinia*, we constructed a mutation in the *lcrF* promoter

predicted to disrupt IscR binding (*lcrF*^{pNull}) [18]. As IscR is a global regulator in *Yersinia [12]*, the *lcrF*^{pNull} mutant should only be defective in T3SS control while a Δ*iscR* mutant displays additional T3SS-independent phenotypes (unpublished observations). As predicted, purified *E. coli* apo-IscR bound the WT *lcrF* promoter region but not the mutated *lcrF*^{pNull} promoter (Fig. 1A), indicating that IscR binding was ablated by this mutation. Consistent with our previous results showing that IscR is essential for type III secretion under standard aerobic conditions [12], the *lcrF*^{pNull} mutant was as deficient as the Δ*iscR* mutant in Yop secretion (Fig. 1B). At the environmental temperature of 26°C, the *lcrF*^{pNull} mutant displayed the same growth rate as both the wild type (WT) strain and a strain lacking the pYV plasmid encoding the T3SS (pYV^{-}). However, at the mammalian body temperature of 37°C, the *lcrF*^{pNull} mutant grew at a rate in between that of WT and the pYV^{-} mutant (Fig. S1). This is consistent with our previous results showing that the Δ*iscR* mutation partially rescues the growth restriction associated with active type III secretion [12]. Therefore, although the *lcrF*^{pNull} mutant retains a wildtype IscR allele, it is defective in the IscR-LcrF-T3SS pathway, making it suitable for assessing the role of IscR in direct regulation of the T3SS.

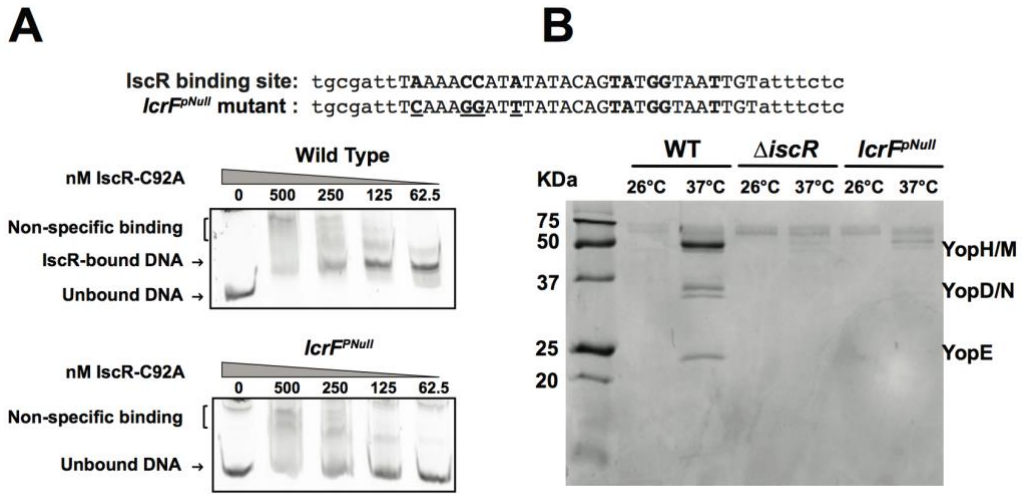

Fig. 1. Mutation of the identified IscR binding site in the *lcrF* promoter disrupts apo-IscR binding and type III secretion. (A) Nucleotide sequences of the IscR binding site in

the WT strain (top) and the *lcrF*^{pNull} mutant (bottom). Bases previously shown to be important for IscR binding are in bold. [18]. Mutated residues are underlined. Electrophoretic mobility shift assays (EMSAs) were performed on DNA fragments (206 bp) containing the WT and *lcrF*^{pNull} mutant promoter sequences upstream of the *yscW-lcrF* operon. Concentrations of *E. coli* apo IscR, afforded by the IscR-C92A mutant protein, are denoted above the gel lanes. One representative experiment out of two is shown. **(B)** *Y. pseudotuberculosis* was grown in low calcium 2xYT media containing iron and the T3SS was induced at 37°C for 2 hours. T3SS cargo proteins secreted into culture supernatant and precipitated with TCA were visualized with Coomassie blue. One representative experiment out of three is shown.

Oxygen induces Ysc T3SS expression. To examine the effect of oxygen on the regulation of *Yersinia iscR* and the Ysc T3SS, *Y. pseudotuberculosis* was grown under either aerobic or anaerobic conditions, and T3SS expression and activity was analyzed. Importantly, the WT, Δ*iscR,* and *lcrF*^{pNull} strains displayed similar growth under anaerobic conditions at 26°C, with a doubling time of ~2 hours (Fig. 2A). After shifting cultures to 37°C, we observed that *iscR* mRNA levels were induced 38-fold ($p<0.0001$) under aerobic conditions relative to anaerobic conditions (Fig. 2B). Similarly, *lcrF* expression was induced 138-fold ($p<0.0001$) in response to oxygen. In addition, IscR and LcrF protein levels as well as T3SS activity, as measured by observing relative secreted levels of the T3SS effector protein YopE, were higher under aerobic conditions than anaerobic conditions (Fig. 2C), consistent with previously published data [19]. Taken together, these data demonstrate that IscR, LcrF, and T3SS expression is induced in the presence of oxygen and that LcrF expression correlates with IscR expression.

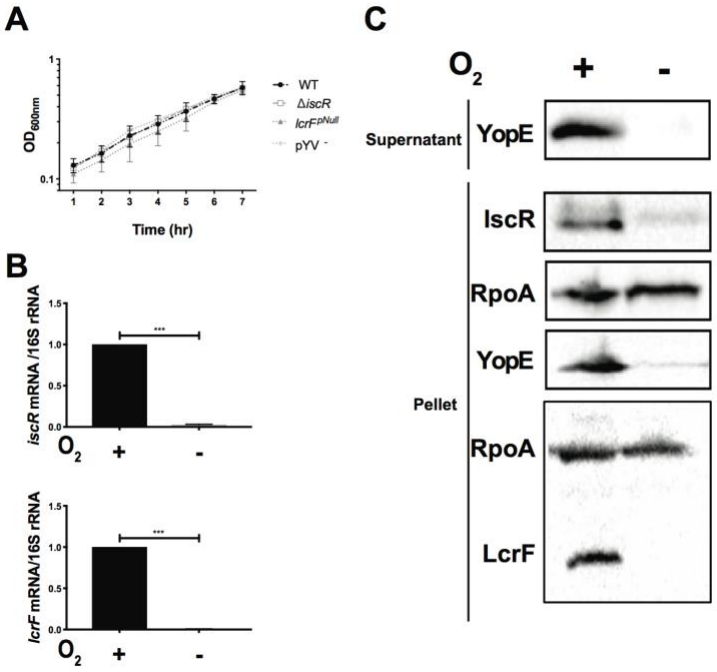

Fig. 2. The *Yersinia* Ysc type III secretion system is induced by oxygen. (A) *Y. pseudotuberculosis* was grown under anaerobic, iron replete conditions at 26°C and the optical density at 600 nm (OD_{600nm}) measured every hour. *Y. pseudotuberculosis* pYV^- lacks the pYV virulence plasmid and serves as a T3SS-deficient control strain. Data shown represent an average of three biological replicates. **(B-C)** *Y. pseudotuberculosis* WT was grown in M9/high glucose (iron replete) in the presence or absence of oxygen and type III secretion induced by shifting to 37˚C for 4 hrs. **(B)** RNA was extracted from the bacterial cultures and *iscR* and *lcrF* gene expression analyzed using qPCR. Relative mRNA levels for each gene of interest were normalized to 16S rRNA levels. Data shown represent the average of three independent experiments. **** $p \leq 0.0001$, as determined by unpaired t-test. **(C)** Equal amounts of cell lysates were probed with antibodies for RpoA, IscR, YopE, and LcrF. T3SS cargo proteins secreted into culture supernatant and precipitated with TCA were probed with YopE antibody. All samples shown are from the same experiment, with each lysate split into two gels, one subsequently used for IscR and YopE probing and the other for LcrF probing. RpoA was blotted on each membrane as a loading control. One representative experiment out of three is shown.

Since IscR has been shown to differentially regulate genes in response to iron limiting conditions in *E. coli* and *Pseudomonas aeruginosa* [15, 20, 21], we sought to determine the effect of iron on the expression of both *iscR* and T3SS genes in *Yersinia*. We previously developed a protocol for limiting *Y. pseudotuberculosis* for iron and demonstrated induction of a Fur-repressed gene [22], indicating efficacy of the iron limitation. To mimic host temperature and activate expression of the T3SS, iron-starved *Y. pseudotuberculosis* was incubated at 37°C under aerobic and anaerobic conditions in media that contained either 6.58 μM $FeSO_4$ (iron replete) or 0.0658 μM $FeSO_4$ (iron limited). qPCR analysis revealed that expression of *iscR* mRNA levels did not significantly change in response to iron under aerobic conditions (Fig. 3A). Similarly, IscR protein levels were similar in iron replete and iron limited aerobic conditions (Fig. 3B). While *lcrF* expression was decreased by ~1.4-fold under iron limited conditions (Fig. 3A, p= 0.0 005), this decrease did not lead to a change in LcrF protein levels (Fig. 3C) nor any significant change in expression (Figs. 3A, 3D) or secretion (Figs. 3C, S2) of the LcrF target genes *yopE* and *yopH*. However, the Δ*iscR* and the *lcrF*^{pNull} mutants displayed a significant decrease in *lcrF* and *yopE* mRNA levels (Fig. 3A), *yopH* expression (Fig. 3D), and LcrF, YopE and YopD protein levels compared to WT (Fig. 3C), consistent with the apo form of IscR playing a major role in regulation of the *Yersinia* T3SS under aerobic conditions, where the apo form of IscR predominates [23]. Collectively, these data show that under aerobic conditions, *Yersinia* IscR and LcrF expression as well as T3SS activity are not affected by iron availability.

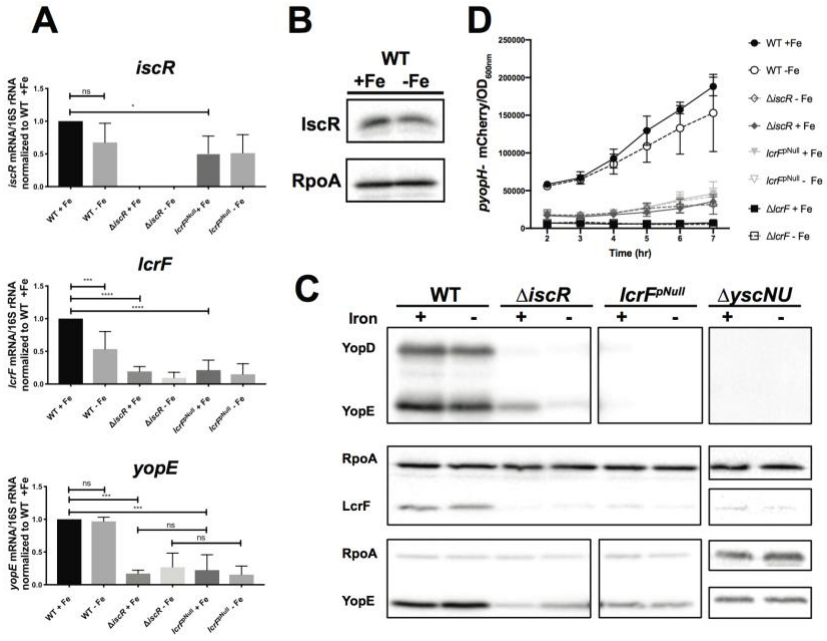

Fig. 3. Iron limitation does not affect IscR, LcrF, YopH, or YopE expression in the presence of oxygen. M9/high glucose iron limited aerobic cultures of *Y. pseudotuberculosis* were subsequently grown in iron replete (+Fe) or iron limited (-Fe) aerobic conditions and type III secretion induced by shifting to 37°C for 4 hrs. **(A)** RNA was isolated and qPCR used to determine relative expression of *iscR, yopE,* and *lcrF* by normalizing to 16S rRNA levels. Data shown represent the average of four independent experiments. ***p≤0.001, as determined by one-way ANOVA with Tukey post-test. **(B)** IscR and RpoA protein levels were determined by Western blot analysis. One representative experiment out of four is shown. **(C)** T3SS cargo proteins secreted into culture supernatant and precipitated with TCA were probed with antibodies for YopE and YopD. Cell lysates were probed with antibodies for RpoA, YopE, YopD, and LcrF. The Δ*yscNU* negative control strain does not express a functional T3SS. All samples shown are from the same experiment, with each lysate split into two gels, one subsequently used for LcrF probing and the other for YopE probing. RpoA was used as a loading control. One representative experiment out of four is shown. **(D)** *Y. pseudotuberculosis* P*yopH*-mCherry was used to assess *yopH* expression under M9/high glucose aerobic iron

replete (+Fe) or iron limited (-Fe) conditions at 37°C, in the genetic backgrounds indicated. mCherry fluorescence intensity normalized to OD_{600} is shown, with T=0 being the start of incubation at 37˚C . Data shown represent the average of three independent experiments.

Iron limitation induces type III secretion under anaerobic conditions. In order to test whether iron availability affects IscR, LcrF, and T3SS expression in the absence of oxygen, iron limited *Yersinia* were incubated anaerobically without any alternative terminal electron acceptors for 12 hrs. The doubling times of the WT, Δ*iscR*, and *lcrF*^{pNull} strains were similar at 37˚C under iron repletion versus limitation (~10 hours; Fig. S3). In contrast to our observations under aerobic conditions, under these anaerobic fermentative conditions, iron limitation induced expression of *iscR* by 430-fold when compared to iron replete conditions (Fig. 4A). Similarly, expression of *lcrF* was induced 260-fold by iron limitation. LcrF protein levels were also upregulated by iron limitation (Figs. 4B, S4). Likewise, iron limitation upregulated expression of the LcrF target gene *yopE* by 1190-fold (p<0,0001; Fig. 4A), and significantly induced Yop expression and secretion, as measured by detecting YopE and YopD protein levels in the pellet and supernatant (Figs. 4B, S4). Additionally, shorter incubation under anaerobic conditions (4 hrs) led to similar results in type III secretion (Fig. S5), indicating that growth phase did not affect the observed phenotype. These results show that iron depletion under anaerobic conditions leads to a shift from [2Fe-2S]-IscR to apo-IscR, de-repressing *iscR* expression and in turn inducing expression of LcrF, which then activates T3SS expression.

When grown under anaerobic respiration conditions, in M9 media lacking glucose but supplemented with mannitol as a carbon source and nitrate as an alternative terminal electron acceptor, we observed the same trend of increased IscR expression and T3SS activity under iron limited conditions (Figs. 5, S6). Taken together, these data suggest that IscR expression is induced under aerobic conditions or by iron limitation under anaerobic conditions (during

respiration or fermentation), and that this correlates with LcrF expression and ultimately T3SS activity.

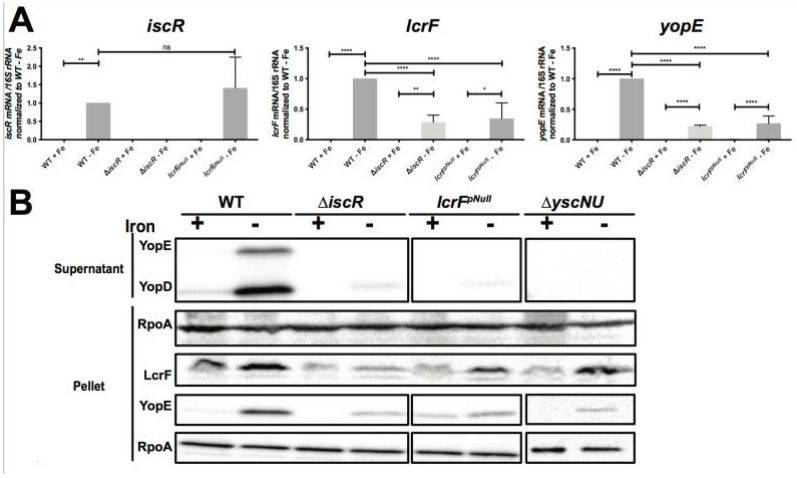

Fig. 4. Iron limitation induces *iscR*, *lcrF*, and *yopE* expression and type III secretion under fermentative conditions. Iron limited *Y. pseudotuberculosis* was shifted to iron replete (+Fe) or iron limited (-Fe) M9/high glucose media in the absence of oxygen and type III secretion induced at 37˚C for 4 hrs. **(A)** RNA was isolated and qPCR used to determine relative expression of *iscR, lcrF*, and *yopE* by normalizing to 16S rRNA levels. Data shown represent the average of four independent experiments. ***p≤0.001 (One-Way ANOVA with Tukey post-test) **(B)** T3SS cargo proteins secreted into culture supernatant and precipitated with TCA were probed with antibodies for YopE and YopD. Cell lysates were probed with antibodies for RpoA, YopE, and LcrF. All samples shown are from the same experiment, with each lysate split into two gels, one subsequently used for LcrF probing and the other for YopE probing. RpoA was used as a loading control. One representative experiment out of four is shown.

IscR control of LcrF is critical for type III secretion under anaerobic conditions. In order to assess the role of IscR in the increased T3SS activity observed anaerobically in response to iron limitation, we examined gene expression and T3SS activity in the Δ*iscR* and *lcrF*^{pNull} mutants. Under iron limited anaerobic conditions, *lcrF* expression was reduced ~3-fold in both the Δ*iscR* or the *lcrF*^{pNull} mutant (Fig. 4A) compared to WT, indicating a role of IscR in the upregulation of LcrF under these conditions. Indeed, there was no significant difference in *lcrF* expression between the Δ*iscR* and *lcrF*^{pNull} mutants in any of the conditions tested (Figs. 3A, 4A), indicating a direct role of IscR binding to the *lcrF* promoter to increase *lcrF* transcription under both aerobic and anaerobic conditions. Surprisingly, iron limitation induced a low level of expression of *lcrF* and *yopE* mRNA in the Δ*iscR* and *lcrF*^{pNull} mutants in the absence of oxygen, but this led to only trace amount of secreted YopE and no detectable YopD in the supernatant of the mutants (Figs. 4B, S4, 5). These data suggest a minor IscR-independent mechanism of LcrF upregulation in response to iron limitation under anaerobic conditions. Taken all together, these results show that anaerobically-grown *Yersinia* increase T3SS expression in response to iron limitation through a predominantly IscR-dependent mechanism that requires IscR binding site in the *lcrF* promoter.

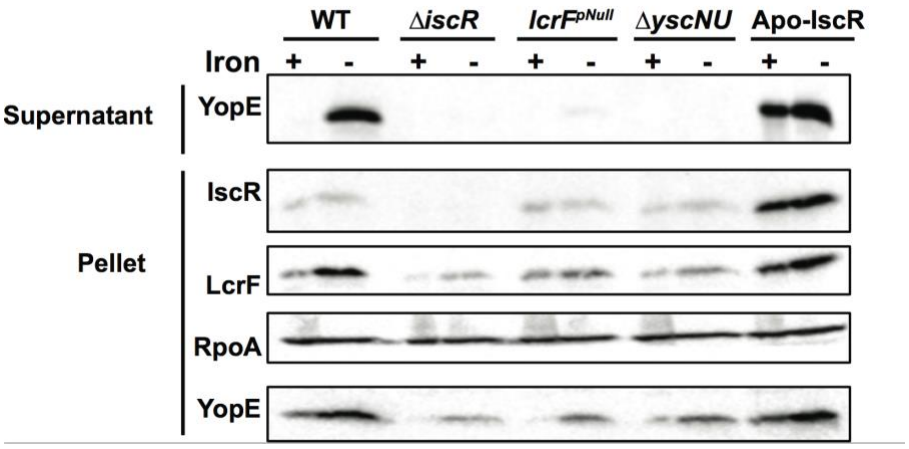

Fig. 5. Iron limitation induces *iscR*, *lcrF*, and *yopE* expression under anaerobic respiration conditions. Iron limited *Y. pseudotuberculosis* was shifted to iron replete (+Fe)

or iron limited (-Fe) M9 media supplemented with sodium nitrate and mannitol in the absence of oxygen. Type III secretion was induced at 37˚C for 4 hrs. T3SS cargo proteins secreted into culture supernatant and precipitated with TCA were probed with antibodies for YopE. Cell lysates were probed with antibodies for RpoA, YopE, and LcrF. All samples shown are from the same experiment, with each lysate split into two gels, one subsequently used for LcrF and YopE probing and the other for IscR probing. RpoA was used as a loading control. One representative experiment out of three is shown.

Ectopic induction of IscR under anaerobic conditions is sufficient to drive type III secretion. To test the hypothesis that upregulation of *iscR* expression under anaerobic conditions is sufficient to induce expression of the T3SS regardless of iron availability, we used a *Y. pseudotuberculosis* apo-locked *iscR* mutant (Apo-IscR) in which the three conserved cysteines are mutated to alanines (C93A, C98A, C104A), leading to loss of iron-sulfur cluster coordination. This mutant should constitutively express *iscR*, as it lacks holo-IscR to mediate *isc* promoter repression. We previously showed that under standard aerobic conditions, the Apo-IscR mutant expressed LcrF but was unable to secrete Yops due to a proton motive force defect [12]. As expected, the Apo-IscR mutant had high IscR levels under anaerobic conditions regardless of iron availability (Fig. 5). Importantly, this correlated with high levels of LcrF and secreted YopE under both iron replete and iron limited conditions. Furthermore, in anaerobic cultures never starved for iron, we observed a 5-fold upregulation of IscR protein levels, a 6-fold increase in LcrF, and a 7-fold increase in YopE in the Apo-IscR mutant pellet compared to WT (Fig. 6). Surprisingly, we also observed secreted YopE in the Apo-IscR mutant supernatant (Figs. 5, 6), indicating that either the Apo-IscR mutant does not have a proton motive force defect under anaerobic conditions or that the proton motive force is not required for type III secretion in the absence of oxygen. Interestingly, we observed a small amount of RpoA in the

supernatant of the Apo-IscR mutant (Fig. 6), indicative of cell lysis in this strain under anaerobic conditions. Therefore, it is possible that some of the YopE detected in the supernatant of the Apo-IscR strain is a result of lysis rather than type III secretion. However, the 5-fold greater YopE levels in the pellet of the Apo-IscR mutant compared to WT (Fig. 6) corroborates the hypothesis that this mutant is undergoing type III secretion, as active secretion feeds back on transcription of T3SS genes through a positive feedback loop [24]. These results demonstrate that increasing IscR levels is sufficient to activate T3SS expression under anaerobic conditions.

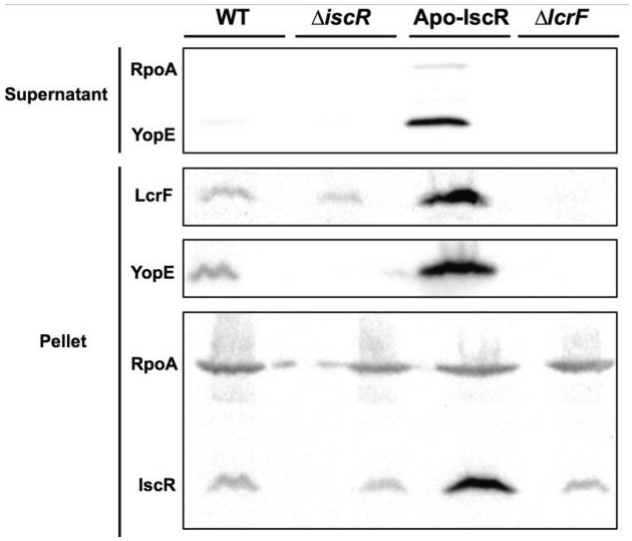

Fig. 6. Ectopic expression of IscR is sufficient to rescue T3SS expression under anaerobic, iron-replete conditions. *Y. pseudotuberculosis* was grown in iron replete M9/high glucose and in the absence of oxygen and type III secretion induced at 37˚C for 4 hrs. T3SS cargo proteins secreted into culture supernatant and precipitated with TCA were probed with an antibody for YopE. Cell lysates were probed with antibodies for RpoA, IscR, YopE, and LcrF. All samples shown are from the same experiment, with each lysate split into two gels, one subsequently used for LcrF and YopE probing and the other for IscR probing. RpoA was used as a loading control. One representative experiment out of three is shown.

Proper regulation of the T3SS by IscR is necessary for disseminated infection. To examine the impact of IscR-mediated regulation of *lcrF* on infection, we performed oral inoculation of mice using a bread feeding model. Consistent with our previous data using an oral gavage model [12], the Δ*iscR* mutant displayed decreased colonization in the Peyer's patches (PP, p=0.0059) and a trend toward decreased colonization of the mesenteric lymph nodes (MLN) that was not statistically significant (p=0.0689). This mutant also displayed a 10,000-fold defect in bacterial burden in the spleen and liver (p<0.0001) (Fig. 7). Although the *lcrF*^{pNull} mutant had a trend of lower PP and MLN colonization compared to WT (100-fold and 10-fold, respectively), this was not statistically significant (p=0.0837 and p=0.0942, respectively). Importantly, the *lcrF*^{pNull} mutant exhibited severe defects in disseminated infection (1,000-fold in the spleen and 100-fold in the liver; p=0.0009 and p=0.0006, respectively). Interestingly, the Δ*iscR* mutant was also defective at colonizing the small intestine, while the *lcrF*^{pNull} mutant was comparable to WT. These results suggest that IscR binding to the *lcrF* promoter is critical for *Yersinia* disseminated infection while IscR itself is also important for *Yersinia* colonization of the intestine and Peyer's patches.

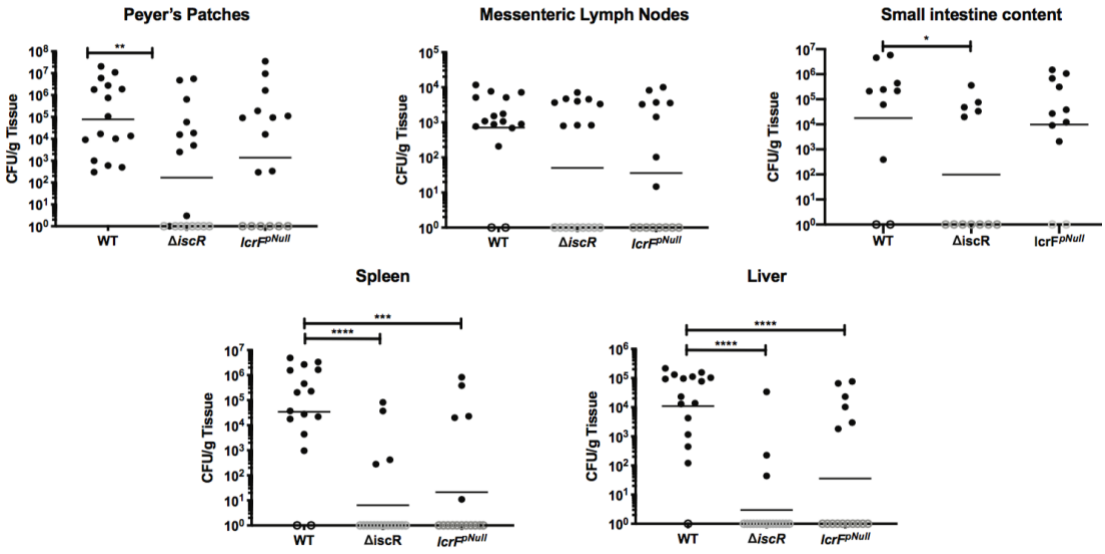

Fig. 7. Proper regulation of *lcrF* by IscR is necessary for disseminated infection. Mice were infected with ~2x10^8 *Y. pseudotuberculosis* using a bread feeding model, and organs

and intestinal contents harvested 5 days post-inoculation. CFUs were normalized to the weight of the organ in grams. Each symbol represents one animal. Unfilled symbols indicate that CFU were below the limit of detection. These data represent five independent experiments. **p<0.01, *** p<0.001, ****p <0.0001 was determined by an unpaired Mann-Whitney rank sum test. Dashes represent geometric mean.

IscR is required for type III secretion in *Yersinia pestis*. The region containing the IscR binding site upstream of *lcrF* is 100% identical between *Y. pseudotuberculosis and Y. pestis* [25]. Therefore, we sought to determine if T3SS activity in *Y. pestis* also required IscR despite the difference in *Yersinia* life cycles carried out by enteropathogenic *Yersinia* compared to *Y. pestis*. To assess T3SS activity *in vitro* we incubated the WT and Δ*iscR* strains of pgm$^-$ *Y. pestis* in BHI media at 37˚C, to mimic host temperature, in the presence of oxygen. Calcium depletion serves as a host-cell independent trigger of type III secretion *in vitro* [26]. Importantly, deletion of *iscR* led to significantly decreased YopE secretion (Fig. 8), indicating that IscR is a critical regulator of the T3SS in both *Y. pseudotuberculosis* and *Y. pestis*.

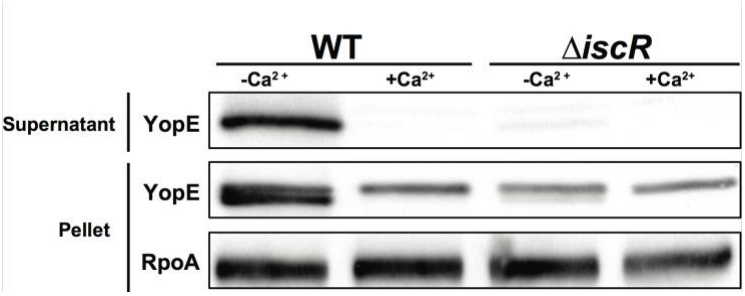

Fig. 8. IscR is critical for type III secretion system in *Y. pestis.* *Y. pestis* pgm- was grown in BHI low calcium or high calcium media at 37˚C. Proteins in the bacterial culture supernatant were precipitated with TCA and type III secretion probed using an anti-YopE antibody . Results are representative of three independent experiments.

Discussion

A recent study suggested that anaerobiosis may repress the Ysc T3SS expression *in vitro* [19], although the mechanism underlying this regulation was unknown. Here we show that the *Y. pseudotuberculosis* global transcription factor IscR regulates the Ysc T3SS in response to oxygen and iron availability and is dependent upon IscR binding to the promoter of the T3SS master regulator *lcrF.* Specifically, we show that aerobic conditions induce IscR expression and, in turn, IscR upregulates LcrF and subsequently the T3SS. Furthermore, iron depletion under anaerobic conditions causes upregulation of IscR, LcrF, and T3SS activity. IscR regulation of LcrF and the T3SS is critical for *Y. pseudotuberculosis* disseminated infection and is conserved between *Y. pseudotuberculosis* and *Y. pestis*. These data provide a mechanism by which oxygen and iron control expression of the *Yersinia* T3SS.

Previous studies in *E. coli* provide a framework for explaining the oxygen and iron dependent regulation invoked by *Yersinia* IscR observed in our studies. In *E. coli*, IscR controls the expression of genes involved in iron-sulfur biogenesis as well as more than 40 other genes [13, 23]. Depending on its association with its [2Fe-2S] cluster, IscR can bind two different DNA motif sequences. Type I motifs can only be bound by holo-IscR, and type II motifs can be bound by both holo and apo-IscR [18, 23]. *iscR* is the first gene in the operon encoding the Isc Fe-S cluster biogenesis pathway. IscR regulates this operon, including its own gene, through a negative feedback loop that requires binding of holo-IscR to two type I motifs upstream of the *isc* promoter [13]. Indeed, Δ*iscR Y. pseudotuberculosis* displays enhanced expression of the *isc* operon, suggesting that this negative regulation is also present in *Yersinia* [12]. This suggests that under conditions where Fe-S cluster turnover is low, such as in the absence of oxygen, holo-IscR should repress *isc* transcription, maintaining low overall IscR levels as found in *E. coli*. Conversely, under conditions where Fe-S cluster demand is high, such as high oxygen tension or under oxidative stress, the majority of IscR should be clusterless, de-repressing IscR [23]. In this study we demonstrated that IscR expression is induced under

aerobic conditions when compared to anaerobic conditions. However, under anaerobic conditions IscR can be induced by depletion of iron, presumably as a result of holo-IscR depletion leading to derepression of *isc* transcription and ultimately an increase in apo-IscR levels. As shown here, these changes in the amount of apo-IscR under oxygen and iron limiting conditions cause downstream changes in the expression of the T3SS though direct transcriptional control of the major regulator LcrF.

LcrF is an AraC-like DNA binding transcriptional regulator of the T3SS in *Yersinia*, controlling expression of the majority of T3SS structural and regulatory proteins, as well as the Yop effector proteins [27, 28]. We previously demonstrated that IscR is essential for LcrF expression and binds to a type II motif just upstream of the *lcrF* promoter [12]. In addition, LcrF is known to be tightly regulated both at the transcriptional and translational level in response to temperature and calcium. LcrF expression is upregulated at 37°C, mammalian host body temperature, and upon calcium depletion, which is thought to mimic contact with host cells [26, 28-31]. LcrF thermal control is mediated by host temperature dependent degradation of the negative regulator YmoA to activate transcription and an RNA thermometer that represses translation only at environmental temperatures [25, 28, 31, 32]. A recent study showed that low calcium or host cell contact lead to secretion of a T3SS cargo protein and regulator, YopD, that ultimately affects *lcrF* mRNA stability [33]. However, in this study, we demonstrated that, in addition to temperature and calcium serving as environmental signals controlling the *Yersinia* T3SS, IscR regulates *Yersinia* T3SS expression in response to iron and oxygen availability, and that IscR control of LcrF is important for pathogenesis. Under anaerobic, low iron conditions we also observed a minor upregulation of type III secretion in the Δ*iscR* and the *lcrF*^{pNull} mutants, suggesting that an additional regulator may further enhance type III secretion under these conditions.

The need for *Yersinia* to use IscR to control T3SS expression may reflect the nature of the different tissues these pathogens encounter within the mammalian host. For example, upon ingestion, *Y. pseudotuberculosis* is exposed to the mucosal environment of the gastrointestinal tract, and, once in the lumen of the small intestine, it binds to the apical surface of microfold (M) cells to subsequently translocate into the Peyer's patches, where it replicates extracellularly and colonizes mesenteric lymph nodes (MLN) [34, 35]. The *Y. pseudotuberculosis* T3SS is not necessary for colonization of the MLN [36], consistent with the lack of a statistically significant defect for the *Y. pseudotuberculosis* Δ*iscR* and *lcrF*^{pNull} mutants in MLN colonization. However, colonization of the Peyer's patches and MLN is not required for *Y. pseudotuberculosis* disseminated infection [37]. Instead, *Y. pseudotuberculosis* intestinal replication is required for subsequent successful infection of the spleen and liver through an unknown pathway [37, 38]. Interestingly, a recent publication postulated the existence of a "gut vascular barrier" that only allows passage of small antigens under 70 kDa from the gut lumen, across the blood endothelial cells, and to the bloodstream. However, infection of *S. enterica* serovar Typhimurium disrupts this barrier, allowing bacteria to cross into the bloodstream and disseminate to the spleen and liver [39]. Notably, our data demonstrated that the *Y. pseudotuberculosis* Δ*iscR* mutant was defective in colonization of the small intestinal lumen, Peyer's patches, spleen, and liver. Therefore, it is possible the Δ*iscR* mutant may be unable to initiate the undefined colonization pathway from the intestinal lumen to the spleen and liver in addition to being defective for growth in Peyer's patches, spleen, and liver. In contrast, the *lcrF*^{pNull} mutant did not display an intestinal colonization defect but failed to cause disseminated infection, as significantly lower hepatosplenic burden was observed compared to WT. These data support the hypothesis that IscR regulates multiple factors required for colonization of mammalian tissues but that IscR regulation of LcrF and the T3SS specifically disrupts the ability to establish successful disseminated infection.

Previous studies suggest that *Yersinia* encounter differing oxygen tension and iron availability during transit through the mammalian host, providing important context for IscR control of the T3SS *in vivo*. Jacobi et al. suggested that iron and heme uptake systems are downregulated in *Y. enterocolitica* in the lumen of the intestine, suggesting that iron is readily available in that tissue [40]. A recent study by Nuss and colleagues found that during *Y. pseudotuberculosis* infection, nutritional immunity factors are among the highest expressed genes in infected lymphatic tissue. Specifically, the iron sequestration molecules haptoglobin and lipocalin-2 were >100-fold induced during infection [41]. This study also showed that during infection, neutrophil influx and iron sequestration were some of the host responses *Y. pseudotuberculosis* encountered once it crossed the epithelial barrier. The authors concomitantly observed an upregulation of *Yersinia* iron uptake systems, as well as genes involved in anaerobic growth. When comparing *Y. pseudotuberculosis* metabolism in PP to that of *Y. pestis* during rat bubo colonization, the data suggest that the different lymphatic tissues constitute a similar nutritional environment, i.e.-iron limited anaerobic conditions [41, 42], conditions we have shown *in vitro* to induce *Yersinia* type III secretion through IscR. Interestingly, a recent study by Davis and colleagues demonstrated that when *Y. pseudotuberculosis* grows in microcolonies in the spleen, subpopulations within a microcolony express different genes in response to distinct environmental cues [43]. For example, only the bacteria localized at the microcolony periphery actively expressed the T3SS. Thus, even within the same tissue, environmental conditions can vary, affecting virulence factor expression. Further studies will be needed to determine *iscR* and *lcrF* expression during infection of different organs as well as within subpopulations of established microcolonies.

IscR may have additional roles in *Yersinia* pathogenesis beyond regulating the T3SS.

Indeed, IscR controls virulence gene expression in a number of different bacteria. For example, in *Klebsiella pneumonia*, IscR regulates capsular polysaccharide biosynthesis as well as iron uptake systems in response to iron availability [44]. Similarly, enterotoxigenic *E. coli* regulates

colonization factor antigen I (CFA/I) fimbriae through IscR in response to iron starvation [20]. Recently, a study in *Salmonella enterica* serovar Typhimurium revealed that IscR regulates the SPI-1 T3SS in response to iron and oxygen availability. Specifically, a type II DNA binding motif was identified upstream of the *hilD* gene, the master regulator of the SPI-1 T3SS. These data suggested that IscR represses *hilD* expression during iron depletion or aerobic conditions, when IscR is upregulated, but favor *hilD* expression under anaerobic conditions when IscR levels are decreased. This would allow *S. enterica* to upregulate SPI-1 T3SS expression in the anaerobic environment of the small intestine in order for *Salmonella* to invade the intestinal epithelium. Once *Salmonella* gains entry into the iron-depleted environment of the host cell, *Salmonella* no longer requires the SPI-1 T3SS. Iron depletion would upregulate IscR expression and this should in turn repress expression of *hilD* and, subsequently, the SPI-1 T3SS [17]. Interestingly, these conditions are distinct from those that trigger IscR-induced T3SS expression in *Y. pseudotuberculosis*, which requires its T3SS once the bacteria have crossed the intestinal epithelium and, presumably, encounter increased oxygen tension or iron limitation under hypoxic conditions. It is noteworthy that two bacterial pathogens have coopted IscR, which is found in numerous pathogenic and non-pathogenic bacteria, to regulate T3SS genes encoded on horizontally-acquired genetic elements in a way that promotes their unique life cycles.

Materials and methods

Bacterial Strains and Growth Conditions. The strains used in this study are listed in Table 1. For standard *Y. pseudotuberculosis* growth and T3SS induction (Fig. 1B), bacteria were grown overnight in 2xYT media, subcultured in 2xYT plus 20 mM sodium oxalate (to chelate calcium and induce type III secretion) and 20 mM $MgCl_2$ to an optical density at 600 nm (OD_{600}) of 0.2, grown at 26˚C for 1.5 hrs followed by 37˚C for another 1.5 hrs. For growing *Yersinia*

under various iron and oxygen condition, casamino acid-supplemented M9 media, referred to as M9 below, was used [45].

Growth of cultures to vary oxygen tension (Figs. 2 and 6) was achieved by first diluting 26˚C overnight aerobic cultures of *Y. pseudotuberculosis* to an OD_{600} of 0.1 in fresh M9 minimal media supplemented with 0.9% glucose (referred to as M9/high glucose) to maximize growth rate and energy production under anaerobic conditions, and incubating for 12 hrs under either aerobic or anaerobic conditions at 26°C. Anaerobic cultures were then shifted to 37°C and incubated for 4 hrs in a vinyl anaerobic chamber with a gas mix of 90%N, 5%CO_2, 5% H_2 (Coy Laboratory Products, Inc). Aerobic cultures were instead diluted to an OD_{600} of 0.2, grown with agitation for 2 hrs at 26°C, and then shifted to 37°C for 4 hrs. Where indicated, to test for effect of anaerobic respiration, M9 media was supplemented with 40 μM sodium nitrate as an alternative electron acceptor and 40 μM mannitol as a carbon source instead of glucose.

Growth of cultures to vary iron availability (Figs. 4 and 5) was achieved by first growing *Y. pseudotuberculosis* aerobically in M9/high glucose media treated with Chelex® 100 resin to remove all traces of iron in acid-washed glassware, as previously described [22]. Specifically, iron replete overnight cultures (M9+6.58 μM $FeSO_4$) grown at 26˚C aerobically were diluted to an OD_{600} of 0.1 into Chelex-treated M9/high glucose media and grown for 8 hrs at 26˚C aerobically with agitation. Cultures were then diluted a second time to OD_{600} 0.1 in fresh Chelex-treated M9/high glucose, and grown for 12 hrs at 26˚C with agitation. Subsequently, cultures were then diluted a third time to OD_{600} 0.2 in M9/high glucose supplemented with 6.58 μM $FeSO_4$ (iron replete) or with 0.0658 μM $FeSO_4$ (iron limitation), grown for 2 hrs at 26°C with agitation, and then shifted to 37°C for 4 hrs with agitation to induce type III secretion. For anaerobic cultures, the cultures were instead diluted a second time to OD_{600} 0.1 in M9/high glucose supplemented with 6.58 μM $FeSO_4$ (iron replete,) or with 0.0658 μM $FeSO_4$ (iron

limitation), and transferred to a vinyl anaerobic chamber where they were grown at 26˚C for 12 hrs (most experiments) or 4 hrs (experiment shown in Fig. S5). Rezasurin redox indicator was used to monitor oxygen levels in the anaerobic chamber. By 4 hrs after introduction of cultures to the anaerobic chamber, the dye color changed from pink to clear, indicating an absence of residual oxygen. Cultures were then shifted to 37°C for another 4 hrs to induce type III secretion.

Y. pestis KIM D27 pgm$^-$ was grown in BHI (brain heart infusion) at 26°C with agitation overnight. Cultures were diluted into low-calcium medium (BHI plus 20 mM sodium oxalate and 20 mM $MgCl_2$) or high-calcium medium (BHI plus 2.5 mM $CaCl_2$) to OD_{600} of 0.1 and grown for 3 hrs at 26°C with agitation, followed by 2 hrs at 37°C with agitation to induce type III secretion.

Type III secretion assays. Visualization of T3SS cargo secreted in broth culture was performed as previously described [46]. Briefly, 5 mL of each culture were pelleted at 13,200 rpm for 15 min at room temperature. Supernatants were removed, and proteins precipitated by addition of trichloroacetic acid (TCA) at a final concentration of 10%. Samples were incubated on ice overnight and pelleted at 13,200 rpm for 15 min at 4°C. Resulting pellets were washed twice with ice-cold 100% acetone and subsequently resuspended in final sample buffer (FSB) containing 20% dithiothreitol (DTT). Samples were boiled for 5 min prior to running on a 12.5% SDS-PAGE gel.

Western Blot Analysis. In parallel, after the supernatant was collected, bacterial pellets were resuspended in FSB plus 20% DTT. Pellet samples were boiled for 15 min. At the time of loading, samples were normalized to the same number of cells. Cytosolic and secreted protein samples were run on a 12.5% SDS-PAGE gel and transferred to a blotting membrane (Immobilon-P) with a wet mini trans-blot cell (Bio-Rad). Blots were blocked for an hour in Tris-buffered saline with Tween 20 and 5% skim milk, and probed with the goat anti-YopE antibodies

(Santa Cruz Biotechnology), rabbit anti-YopD (gift from Alison Davis and Joan Mecsas), rabbit anti-RpoA (gift from Melanie Marketon), rabbit anti-LcrF [28], rabbit anti-IscR [18], and horseradish peroxidase-conjugated secondary antibodies (Santa Cruz Biotech). Following visualization, quantification of the bands was performed with Image Lab software (Bio-Rad).

Construction of *Yersinia* Mutant Strains. For the *Y. pseudotuberculosis lcrF*^{pNull} mutant strain, the *lcrF* promoter region was amplified by PCR using 5'/3' *lcrF*^{pNull} which contained the mutations in the IscR binding site (see Table 2, underlined nucleotides). Amplified PCR fragments were cloned into a *Bam*HI- and SacI-digested pSR47s suicide plasmid (λpir-dependent replicon, kanamycin^R, *sacB* gene conferring sucrose sensitivity) using the NEBuilder HiFi DNA Assembly kit (New England Biolabs, Inc) [47, 48]. Recombinant plasmids were transformed into *E. coli* S17-1 λpir competent cells and later introduced into *Y. pseudotuberculosis* IP2666 via conjugation. The resulting Kan^R, irgansan^R (*Yersinia* selective antibiotic) integrants were grown in the absence of antibiotics and plated on sucrose-containing media to select for clones that had lost *sacB* (and by inference, the linked plasmid DNA). Kan^S, sucrose^R, congo red-positive colonies were screened by PCR and sequencing. The *Y. pestis* Δ*iscR* strain was generated using a pSR47S:Δ*iscR* suicide plasmid as described previously for *Y. pseudotuberculosis* [12], except using BHI plates instead of LB plates. The pSR47S:Δ*iscR* suicide plasmid was used because the *iscR* gene and the 700 bp regions upstream and downstream encoded on the plasmid are 100% identical between *Y. pestis* and *Y. pseudotuberculosis.*

Mouse Model. All animal use procedures were in strict accordance with the NIH Guide for the Care and Use of Laboratory Animals and were approved by the UC Santa Cruz Institutional Animal Care and Use Committee. 15-18 h prior to infection, food was withheld from eleven to twelve weeks old 129S1/SvImJ mice, but water provided ad libitum. Mice were then inoculated with $2x10^8$ by bread feeding [49]. Briefly, *Y. pseudotuberculosis* cultures were grown in LB

media overnight at 26°C. Cultures were diluted to the appropriate OD_{600} to obtain $2x10^8$ bacteria per mouse. Dilutions were spun down and pellets resuspended in a mixture of 2 μl of 1X PBS and 3 μl melted butter, and this mixture was then pipetted onto a small piece of bread. Mice were given a piece of *Yersinia*-soaked bread and provided food and water *at libitum.* Five days post-inoculation, mice were euthanized and Peyer's patches, mesenteric lymph nodes, spleens, and livers were isolated and homogenized for 30 s in PBS followed by serial dilution and plating on LB supplemented with 1 mg/mL irgasan for CFU determination. Significant difference in colonization was determined by an unpaired Mann-Whitney rank sum test to compare each mutant strain against WT.

Electrophoretic mobility shift assays (EMSAs). *E. coli* IscR-C92A protein that lacks the [2Fe-2S] cluster was isolated as previously described [18, 23] and subsequently used in electrophoretic mobility shift assays (EMSAs) because this apo form of IscR binds exclusively to type 2 sites. DNA fragments containing the wild-type *Y. pseudotuberculosis lcrF* promoter [-206 to +12 bp relative to the +1 transcription start site (TSS)], or its *lcrF*^{pNull} variant in which the IscR binding site is disrupted, were isolated from pPK12778 and pPK12779, respectively, after digestion with *Hind*III and *Bam*HI, and EMSAs were carried out with purified IscR-C92A as previously described [22]. After incubation at 30°C for 1 hr, samples were loaded onto a non-denaturing 6% polyacrylamide gel in 0.5× Tris-borate-EDTA buffer and run at 100 V for 2.5 hrs at 4°C. The gel was stained with SYBR Green EMSA nucleic acid gel stain (Molecular Probes) and visualized using a Typhoon FLA 900 imager (GE).

YopH-mCherry transcriptional reporter assay. Overnight bacterial cultures grown in M9 media were back diluted and iron starved as described above, and then shifted to 37°C to induce type III secretion. Starting at 2 hrs after shift, 1.5 mL of cells were spun down at 3.5 rcf for five minutes, resuspended in 200μl of 1x PBS, and mCherry fluorescence measured in

black bottom 96 well plates (Costar). In parallel, optical density was measured in clear bottom 96 well plates (Costar). Fluorescence and optical density were both measured using a Perkin Elmer Victor X3 plate reader.

RNA Isolation and Quantitative PCR (qPCR) analysis. A total of 3 mL of culture from each condition were pelleted by centrifugation for 5 minutes at 4,000 rpm. The supernatant was removed, and pellets were resuspended in 500 µL of media and treated with 1 mL Bacterial RNA Protect Reagent (Qiagen) according to the manufacturer's protocol. Total RNA was isolated using the RNeasy Mini Kit (Qiagen) per the manufacturer's protocol. After harvesting total RNA, genomic DNA was removed via the TURBO-DNA-free kit (Life Technologies/Thermo Fisher). cDNA was generated for each sample by using the M-MLV Reverse Transcriptase (Invitrogen) according to the manufacturer's instructions, as previously described [12]. Each 20 µl qPCR assay contained 5 µl of 1:10 diluted cDNA sample, 10 µl of Power CYBR Green PCR master mix (Thermo Fisher Scientific), and primers (Table 2) with optimized concentrations. The expression levels of each target gene were normalized to that of 16S rRNA present in each sample and calculated by the ΔΔCt method. Three independent biological replicates were analyzed for each condition

Table 1. Strains used in this study.

Strain	Background	Mutation(s)	Reference
WT	IP2666	Naturally lacks full-length YopT	Bliska *et al, 1991*
Δ*iscR*	IP2666	Δ*iscR*	Miller *et al,* 2014

Δ*yscNU*	IP2666	Δ*yscNU*	Balada-Llasat and Mecsas, 2006
***lcrF*^{pNull}**	IP2666	Point mutations in lscR binding site on p*lcrF*	This study
Δ*iscR*	*Y. pestis* KIM D27 pgm-	Lacks pgm locus, Δ*iscR*	This study
WT	*Y. pestis* KIM D27 pgm-	Lacks pgm locus	Lahteenmaki *et al,* 1998
p*yopH*-mCherry	IP2666	pMMB67EH expressing mCherry under the control of the YopH promoter	Morgan *et al,* 2018

Table 2. Primers used in this study.

Name	Name Sequence Reference	Reference
FqyopE	CCATAAACCGGTGGTGAC	(Morgan et al. 2017)
RqyopE	CTTGGCATTGAGTGATACTG	(Morgan et al. 2017)
Fq16s	AGCCAGCGGACCACATAAAG	(Merriam et al. 1997)
Rq16s	AGTTGCAGACTCCAATCCGG	(Merriam et al. 1997)
FqlcrF	GGAGTGATTTTCCGTCAGTA	(Miller et al. 2014)
RqlcrF	CTCCATAAATTTTTGCAACC	(Miller et al. 2014)
FqiscR	CAGGGCGGAAATCGCTGCCT	This study
RqiscR	ATTAGCCGTTGCGGCGCCTAT	This study

3' *lcrF*^{pNull}	TGTATAAATCCTTTGAAATCGCA TCATATATTCCTAATAT	This study
5' *lcrF*^{pNull}	GATTTCAAAGGATTTATACAGTA TGGTAATTGTATTTCT	This study

Acknowledgments.

We thank Todd Lowe and Chad Saltikov for help setting up the Vinyl anaerobic chamber, Fitnat Yildiz for advice on experimental design, Hanh Lam for assistance with data analysis, Ana Gallego for advice on RNA extraction optimization, and Virginia Miller for technical advice on construction of the *Y. pestis* Δ*iscR* mutant.

References

1. McHugh JP, Rodriguez-Quinones F, Abdul-Tehrani H, Svistunenko DA, Poole RK, Cooper CE, et al. Global iron-dependent gene regulation in Escherichia coli. A new mechanism for iron homeostasis. J Biol Chem. 2003;278(32):29478-86. Epub 2003/05/15. doi: 10.1074/jbc.M303381200. PubMed PMID: 12746439.

2. Carpenter C, Payne SM. Regulation of iron transport systems in Enterobacteriaceae in response to oxygen and iron availability. J Inorg Biochem. 2014;133:110-7. Epub 2014/02/04. doi: 10.1016/j.jinorgbio.2014.01.007. PubMed PMID: 24485010; PubMed Central PMCID: PMCPMC3964178.

3. Litwin CM, microbiology reviews C-SB. Role of iron in regulation of virulence genes. Clinical microbiology reviews. 1993. doi: 10.1128/CMR.6.2.137.

4. Schaible UE, Kaufmann SHE. Iron and microbial infection. Nature Reviews Microbiology. 2004;2:946. doi: 10.1038/nrmicro1046.

5. Nemeth E, Ganz T. Regulation of Iron Metabolism by Hepcidin. 2006;26(1):323-42. doi: 10.1146/annurev.nutr.26.061505.111303. PubMed PMID: 16848710.

6. Ganz T, Nemeth E. Iron homeostasis in host defence and inflammation. Nature reviews Immunology. 2015;15(8):500-10. Epub 2015/07/10. doi: 10.1038/nri3863. PubMed PMID: 26160612.

7. Marceau M. Transcriptional regulation in Yersinia: an update. Current issues in molecular biology. 2005;7(2):151-77.

8. Staggs TM, Perry RD. Fur regulation in Yersinia species. Molecular Microbiology. 1992;6(17):2507-16. doi: 10.1111/j.1365-2958.1992.tb01427.x.

9. Fillat MF. The FUR (ferric uptake regulator) superfamily: Diversity and versatility of key transcriptional regulators. Archives of Biochemistry and Biophysics. 2014;546:41-52. doi: 10.1016/j.abb.2014.01.029.

10. Skaar EP. The battle for iron between bacterial pathogens and their vertebrate hosts. PLoS pathogens. 2010;6(8). doi: 10.1371/journal.ppat.1000949.

11. Coburn B, Sekirov I, Finlay BB. Type III Secretion Systems and Disease. Clinical Microbiology Reviews. 2007;20(4):535-49. doi: 10.1128/CMR.00013-07.

12. Miller HK, Kwuan L, Schwiesow L, Bernick DL, Mettert E, Ramirez HA, et al. IscR Is Essential for Yersinia pseudotuberculosis Type III Secretion and Virulence. PLoS Pathogens. 2014;10(6). doi: 10.1371/journal.ppat.1004194.

13. Schwartz CJ, Giel JL, Patschkowski T, Luther C, Ruzicka FJ, Beinert H, et al. IscR, an Fe-S cluster-containing transcription factor, represses expression of Escherichia coli genes encoding Fe-S cluster assembly proteins. Proc Natl Acad Sci U S A. 2001;98(26):14895-900. Epub 2001/12/14. doi: 10.1073/pnas.251550898. PubMed PMID: 11742080; PubMed Central PMCID: PMCPMC64955.

14. Lim JG, Choi SH. IscR is a global regulator essential for pathogenesis of Vibrio vulnificus and induced by host cells. Infect Immun. 2014;82(2):569-78. Epub 2014/01/31. doi: 10.1128/IAI.01141-13. PubMed PMID: 24478072; PubMed Central PMCID: PMCPMC3911388.

15. Giel JL, Nesbit AD, Mettert EL, Fleischhacker AS, Wanta BT, Kiley PJ. Regulation of iron–sulphur cluster homeostasis through transcriptional control of the Isc pathway by [2Fe–2S]–IscR in Escherichia coli. Molecular Microbiology. 2013;87(3):478-92. doi: 10.1111/mmi.12052.

16. Santos JA, Pereira PJ, Macedo-Ribeiro S. What a difference a cluster makes: The multifaceted roles of IscR in gene regulation and DNA recognition. Biochim Biophys Acta. 2015;1854(9):1101-12. Epub 2015/02/03. doi: 10.1016/j.bbapap.2015.01.010. PubMed PMID: 25641558.

17. Vergnes A, Viala J, Ouadah-Tsabet R, Pocachard B, Loiseau L, Méresse S, et al. The iron–sulfur cluster sensor IscR is a negative regulator of Spi1 type III secretion system in Salmonella enterica. Cellular Microbiology. 2016. doi: 10.1111/cmi.12680.

18. Nesbit AD, Giel JL, Rose JC, Kiley PJ. Sequence-Specific Binding to a Subset of IscR-Regulated Promoters Does Not Require IscR Fe–S Cluster Ligation. Journal of Molecular Biology. 2009;387(1):28-41. doi: 10.1016/j.jmb.2009.01.055.

19. Avican K, Fahlgren A, Huss M, Heroven AK, Beckstette M, Dersch P, et al. Reprogramming of Yersinia from Virulent to Persistent Mode Revealed by Complex In Vivo RNA-seq Analysis. PLOS Pathogens. 2015;11(1). doi: 10.1371/journal.ppat.1004600.

20. Haines S, Arnaud-Barbe N, Poncet D, Reverchon S, Wawrzyniak J, Nasser W, et al. IscR Regulates Synthesis of Colonization Factor Antigen I Fimbriae in Response to Iron Starvation in Enterotoxigenic Escherichia coli. J Bacteriol. 2015;197(18):2896-907. Epub 2015/07/01. doi: 10.1128/JB.00214-15. PubMed PMID: 26124243; PubMed Central PMCID: PMCPMC4542172.

21. Romsang A, Duang-Nkern J, Wirathorn W, Vattanaviboon P, Mongkolsuk S. Pseudomonas aeruginosa IscR-Regulated Ferredoxin NADP(+) Reductase Gene (fprB) Functions in Iron-Sulfur Cluster Biogenesis and Multiple Stress Response. PLoS One. 2015;10(7):e0134374. Epub 2015/08/01. doi: 10.1371/journal.pone.0134374. PubMed PMID: 26230408; PubMed Central PMCID: PMCPMC4521836.

22. Schwiesow L, Mettert E, Wei Y, Miller HK, Herrera NG, Balderas D, et al. Control of hmu Heme Uptake Genes in Yersinia pseudotuberculosis in Response to Iron Sources. Front

Cell Infect Microbiol. 2018;8:47. Epub 2018/03/10. doi: 10.3389/fcimb.2018.00047. PubMed PMID: 29520342; PubMed Central PMCID: PMCPMC5827684.

23. Giel JL, Rodionov D, Liu M, Blattner FR, Kiley PJ. IscR-dependent gene expression links iron-sulphur cluster assembly to the control of O2-regulated genes in Escherichia coli. Molecular Microbiology. 2006;60(4):1058-75. doi: 10.1111/j.1365-2958.2006.05160.x.

24. Kusmierek M, Hoßmann J, Witte R, Opitz W, Vollmer I, Volk M, et al. A bacterial secreted translocator hijacks riboregulators to control type III secretion in response to host cell contact. PLOS Pathogens. 2019;15(6). doi: 10.1371/journal.ppat.1007813.

25. Schwiesow L, Lam H, Dersch P, Auerbuch V. Yersinia type III secretion system master regulator LcrF. Journal of Bacteriology. 2016. doi: 10.1128/JB.00686-15. PubMed Central PMCID: PMC2016.

26. Straley SC, Plano GV, Skrzypek E, Haddix PL, Fields KA. Regulation by Ca2+ in the Yersinia low-Ca2+ response. Molecular Microbiology. 1993;8(6):1005-10. doi: 10.1111/j.1365-2958.1993.tb01644.x.

27. Wattiau P, Cornelis GR. Identification of DNA sequences recognized by VirF, the transcriptional activator of the Yersinia yop regulon. Journal of Bacteriology. 1994;176(13):3878-84. doi: 10.1128/jb.176.13.3878-3884.1994.

28. Bohme K, Steinmann R, Kortmann J, Seekircher S, Heroven AK, Berger E, et al. Concerted actions of a thermo-labile regulator and a unique intergenic RNA thermosensor control Yersinia virulence. PLoS Pathog. 2012;8(2):e1002518. Epub 2012/02/24. doi:

10.1371/journal.ppat.1002518. PubMed PMID: 22359501; PubMed Central PMCID: PMCPMC3280987.

29. Sample AK, Fowler JM, Brubaker RR. Modulation of the low-calcium response in Yersinia pestis via plasmid-plasmid interaction. Microbial Pathogenesis. 1987;2(6):443-53. doi: 10.1016/0882-4010(87)90051-9.

30. Hoe NP, Goguen JD. Temperature sensing in Yersinia pestis: translation of the LcrF activator protein is thermally regulated. Journal of Bacteriology. 1993;175(24):7901-9. doi: 10.1128/jb.175.24.7901-7909.1993.

31. Cornells GR, Sluiters C, Delor I, Geib D, Kaniga K, Rouvroit LC, et al. ymoA, a Yersinia enterocolitica chromosomal gene modulating the expression of virulence functions. Molecular Microbiology. 1991;5(5):1023-34. doi: 10.1111/j.1365-2958.1991.tb01875.x.

32. Jackson MW, Silva-Herzog E, Plano GV. The ATP-dependent ClpXP and Lon proteases regulate expression of the Yersinia pestis type III secretion system via regulated proteolysis of YmoA, a small histone-like protein. Molecular Microbiology. 2004;54(5):1364-78. doi: 10.1111/j.1365-2958.2004.04353.x.

33. Holmström A, Pettersson J, Rosqvist R, Håkansson S, Tafazoli F, Fällman M, et al. YopK of Yersinia pseudotuberculosis controls translocation of Yop effectors across the eukaryotic cell membrane. Molecular Microbiology. 1997;24(1):73-91. doi: 10.1046/j.1365-2958.1997.3211681.x.

34. Marra A, Isberg R. Invasin-dependent and invasin-independent pathways for translocation of Yersinia pseudotuberculosis across the Peyer's patch intestinal epithelium. Infection and immunity. 1997;65(8). PubMed Central PMCID: PMC1997.

35. Grützkau A, Hanski C, Hahn H, Gut R-EO. Involvement of M cells in the bacterial invasion of Peyer's patches: a common mechanism shared by Yersinia enterocolitica and other enteroinvasive bacteria. Gut. 1990. doi: 10.1136/gut.31.9.1011.

36. Balada-Llasat J-M, Mecsas J. Yersinia Has a Tropism for B and T Cell Zones of Lymph Nodes That Is Independent of the Type III Secretion System. PLoS Pathogens. 2006;2(9). doi: 10.1371/journal.ppat.0020086.

37. Barnes PD, Bergman MA, Mecsas J, Isberg RR. Yersinia pseudotuberculosis disseminates directly from a replicating bacterial pool in the intestine. The Journal of Experimental Medicine. 2006;203(6):1591-601. doi: 10.1084/jem.20060905.

38. Oellerich MF, Jacobi CA, Freund S, Niedung K, Bach A, Heesemann J, et al. Yersinia enterocolitica Infection of Mice Reveals Clonal Invasion and Abscess Formation. Infection and Immunity. 2007;75(8):3802-11. doi: 10.1128/IAI.00419-07.

39. Spadoni I, Zagato E, Bertocchi A, Paolinelli R, Hot E, Sabatino A, et al. A gut-vascular barrier controls the systemic dissemination of bacteria. Science. 2015;350(6262):830-4. doi: 10.1126/science.aad0135.

40. Jacobi CA, Gregor S, Rakin A, Heesemann J. Expression Analysis of the Yersiniabactin Receptor Gene fyuA and the Heme Receptor hemR of Yersinia enterocolitica

In Vitro and In Vivo Using the Reporter Genes for Green Fluorescent Protein and Luciferase. Infection and Immunity. 2001;69(12):7772-82. doi: 10.1128/iai.69.12.7772-7782.2001.

41. Nuss AM, Beckstette M, Pimenova M, Schmühl C, Opitz W, Pisano F, et al. Tissue dual RNA-seq allows fast discovery of infection-specific functions and riboregulators shaping host–pathogen transcriptomes. Proceedings of the National Academy of Sciences. 2017;114(5). doi: 10.1073/pnas.1613405114.

42. Sebbane F, Lemaître N, Sturdevant DE, Rebeil R, Virtaneva K, Porcella SF, et al. Adaptive response of Yersinia pestis to extracellular effectors of innate immunity during bubonic plague. 2006;103(31):11766-71. doi: 10.1073/pnas.0601182103 J Proceedings of the National Academy of Sciences.

43. Davis KM, Mohammadi S, Isberg RR. Community Behavior and Spatial Regulation within a Bacterial Microcolony in Deep Tissue Sites Serves to Protect against Host Attack. Cell Host & Microbe. 2015;17(1):21-31. doi: 10.1016/j.chom.2014.11.008.

44. Wu CC, Wang CK, Chen YC, Lin TH, Jinn TR, Lin CT. IscR regulation of capsular polysaccharide biosynthesis and iron-acquisition systems in Klebsiella pneumoniae CG43. PLoS One. 2014;9(9):e107812. Epub 2014/09/23. doi: 10.1371/journal.pone.0107812. PubMed PMID: 25237815; PubMed Central PMCID: PMCPMC4169559.

45. Cheng LW, Anderson DM, Schneewind O. Two independent type III secretion mechanisms for YopE in Yersinia enterocolitica. Molecular microbiology. 1997;24(4):757-65. PubMed PMID: 9194703.

46. Auerbuch V, Golenbock DT, Isberg RR. Innate Immune Recognition of Yersinia pseudotuberculosis Type III Secretion. PLoS Pathogens. 2009;5(12). doi: 10.1371/journal.ppat.1000686.

47. Andrews HL, Vogel JP, Isberg RR. Identification of linked Legionella pneumophila genes essential for intracellular growth and evasion of the endocytic pathway. Infection and immunity. 1998;66(3):950-8. PubMed PMID: 9488381; PubMed Central PMCID: PMC108001.

48. Merriam JJ, Mathur R, Maxfield-Boumil R, Isberg RR. Analysis of the Legionella pneumophila fliI gene: intracellular growth of a defined mutant defective for flagellum biosynthesis. Infection and immunity. 1997;65(6):2497-501. PubMed PMID: 9169800; PubMed Central PMCID: PMC175352.

49. Hooker-Romero D, Schwiesow L, Wei Y, Auerbuch V. Mouse Models of Yersiniosis. Pathogenic Yersinia, Methods and Protocols. 2019:41-53. doi: 10.1007/978-1-4939-9541-7_4.

50. Goverde RLJ, Kusters JG, Veld HJHJ. Growth rate and physiology of Yersinia enterocolitica; influence of temperature and presence of the virulence plasmid. Journal of Applied Microbiology. 1994;77(1):96-104. doi: 10.1111/j.1365-2672.1994.tb03050.x.

Supporting information

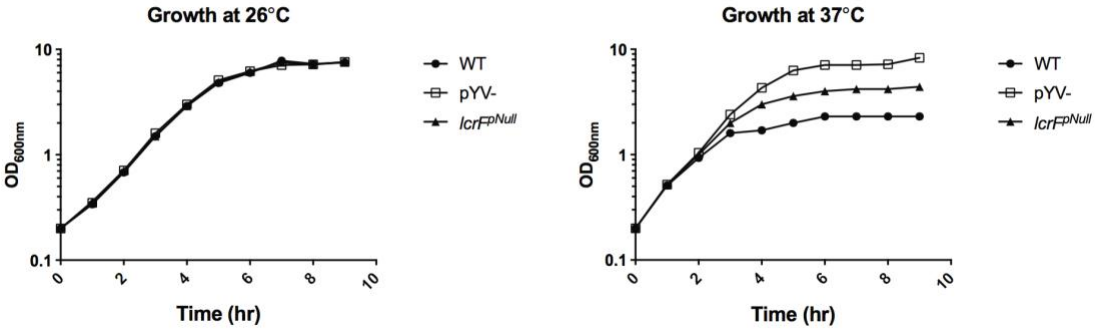

S1. Fig. *Y. pseudotuberculosis lcrF^{pNull}* mutant does not display a growth defect.

Overnight bacterial cultures were subcultured into fresh M9 media containing iron and grown under aerobic condtions for 9 hrs at either 26˚C or 37˚C. OD_{600} was measured every hour. Note that the pYV^{-} mutant lacking all T3SS genes does not undergo the normal growth arrest seen in wildtype *Yersinia* following T3SS induction at 37˚C [50].

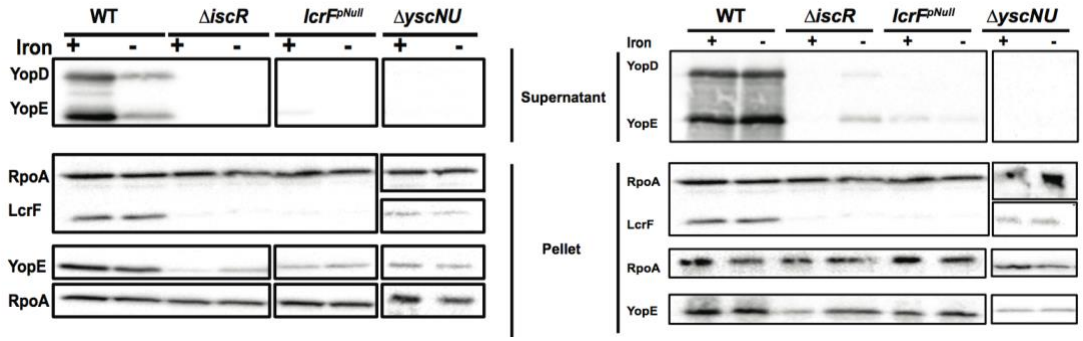

S2. Fig. Iron availability does not impact type III secretion under aerobic conditions.

Two additional independent replicates of the results shown in Fig. 3 are provided. Iron limited *Y. pseudotuberculosis* and mutant variants were induced for the T3SS under aerobic iron

replete (+Fe) or iron limited (-Fe) conditions as described in Fig. 3 and assayed for proteins by Western blots. Top panels, supernatant. Bottom panels, cell pellet.

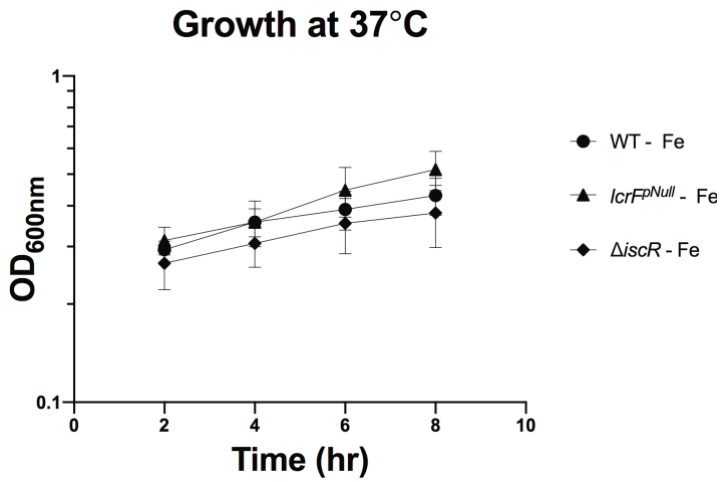

S3. Fig. *Y. pseudotuberculosis lcrF^{pNull}* displays similar growth rate to the WT and Δ*iscR* strains under iron limited, anaerobic conditions. *Y. pseudotuberculosis* strains were iron starved under anaerobic conditions and OD_{600} was measured every hour after shifting to 37ºC. Data shown represent the average of three independent experiments.

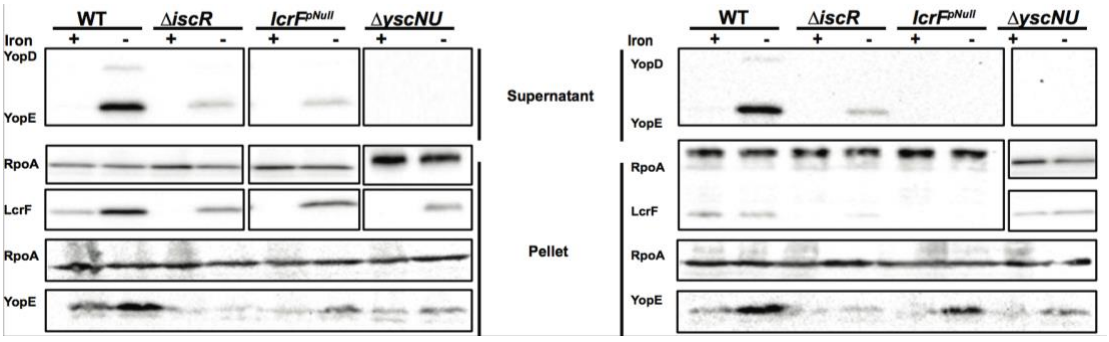

S4. Fig. Type III secretion is induced by iron limitation following 12 hours of anaerobic growth. *Y. pseudotuberculosis* was iron starved and grown for 12 hours in the absence of oxygen prior to inducing the T3SS by shifting to 37˚C, as in Fig. 4. Two additional independent replicates are shown. Top panels, supernatant. Bottom panels, cell pellet.

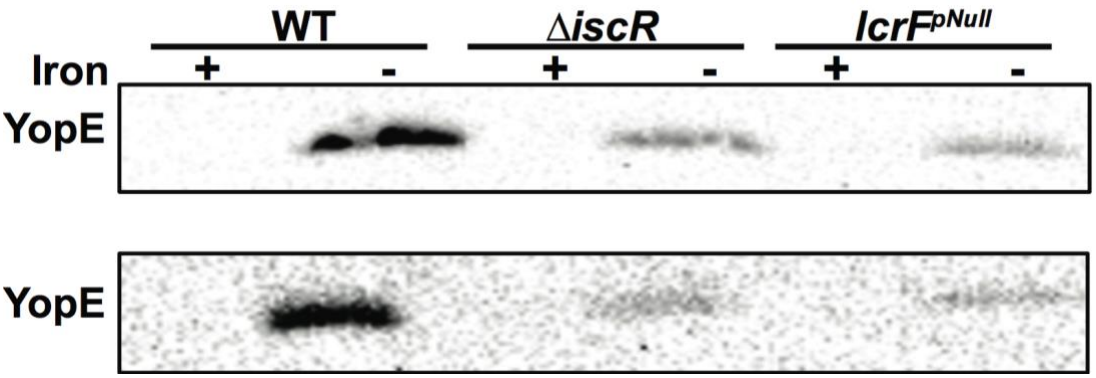

S5. Fig. Type III secretion is induced by iron limitation following only 4 hrs of anaerobic growth. *Y. pseudotuberculosis* was iron starved and grown for only four hours in the absence of oxygen prior to inducing the T3SS by shifting to 37˚C. Secreted proteins were precipitated with TCA and analyzed by Western blot. Two independent experiments are shown.

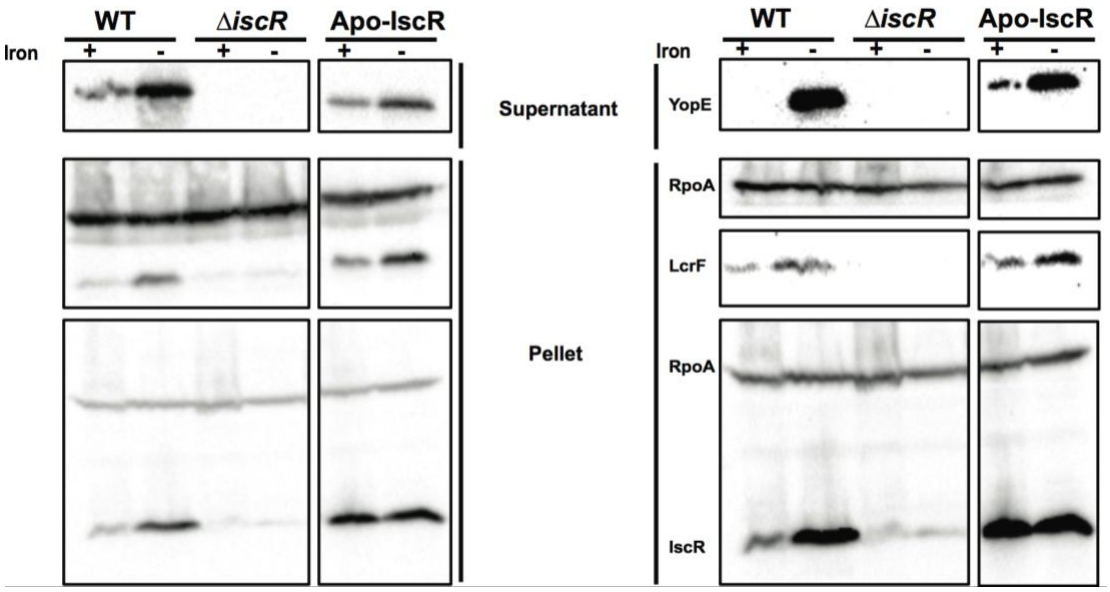

S6. **Fig. Iron depletion induces IscR, LcrF and YopE expression during anaerobic respiration.** Iron starved *Y. pseudotuberculosis* was grown under anaerobic conditions in M9 supplemented with nitrate and mannitol instead of glucose to support anaerobic respiration. Cultures were then shifted to 37˚C and both secreted and intracellular proteins were analyzed by Western blot, as in Fig. 5. Two additional independent replicates are shown. Top panels, supernatant. Bottom panels, cell pellet.

Appendix to Chapter 3

Characterization of a *Yersinia pseudotuberculosis fur* mutant

By Diana Hooker-Romero, Patricia Kiley and Victoria Auerbuch

Introduction

The main transcriptional regulator most bacterial species use to control iron uptake and utilization is the ferric uptake regulator, Fur. Fur controls expression of iron uptake systems, siderophores, iron storage proteins, and numerous virulence factors in pathogens [1]. When iron availability is high, Fur binds Fe^{2+}, and holo-Fur binds to a DNA fragment consisting of a 19 bp inverted repeat located in the promoter region of Fur-regulated genes [2, 3]. Recent studies in *Yersinia pestis* have identified a number of genes regulated by Fur in response to iron depletion, including genes encoding virulence factors such as the *ail* gene, required for serum resistance and invasion, as well as siderophore and heme uptake systems [4, 5]. In Chapter 3 we determined the effect of iron on regulation of the *Yersinia* T3SS; specifically, both oxygen and iron depletion induce upregulation of the T3SS. Importantly, we showed that although IscR is the main player in this upregulation, there may be additional factor(s) that further amplify the response to iron under anaerobic conditions. In this appendix, we aimed to determine if Fur plays a role in regulation of the *Yersinia* T3SS in response to iron.

Results

fur* deletion does not affect growth of *Yersinia pseudotuberculosis. To determine if deletion of the *fur* gene had any effect on *Y. pseudotuberculosis* fitness, we assessed the growth of different strains under aerobic conditions in both rich media and after iron starvation. Importantly the Δ*fur* mutant did not display a growth defect at 26°C in LB media (Fig. 1). Additionally, expression of *fur* in either the WT or the Δ*fur* genetic backgrounds also did not affect growth.

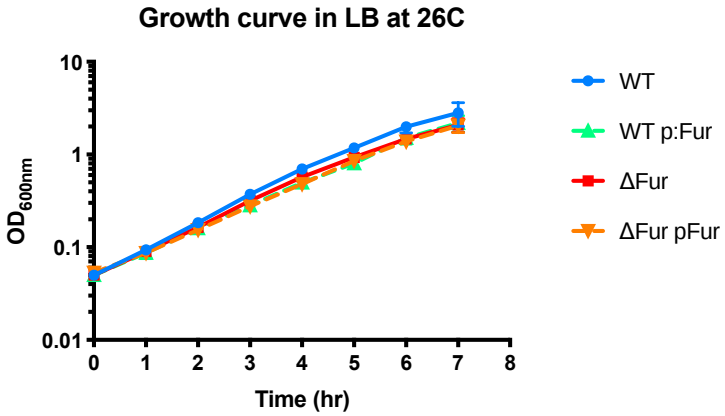

Fig 1. Deletion of *fur* does not affect growth *in vitro* at 26°C in rich media. Overnight *Y. pseudotuberculosis* cultures were diluted into fresh LB and incubated at 26°C for 7 hrs. Optical density (OD_{600nm}) was measured every hour.

***fur* deletion does not affect T3SS activity under aerobic standard laboratory conditions.** Bioinformatic analysis of the *lcrF* promoter sequence upstream of *yscW-lcrF* revealed putative Fur boxes in proximity to the identified IscR binding site (Fig. 2). To determine if Fur plays a role in regulation of *lcrF* expression, the in-frame *fur* deletion mutant was tested for secretion under standard laboratory conditions. Briefly, overnight *Y. pseudotuberculosis* cultures were diluted into 2xYT media and grown for 1.5 hrs at 26°C, then they were shifted to 37°C for 2 hrs to induce T3SS expression. Secreted proteins were precipitated out of the culture supernatant and run on an SDS-PAGE gel. Our results suggest that *fur* deletion does not have an effect on type III secretion under aerobic conditions. However, the strains carrying a plasmid constitutively expressing *fur* (pACYC:*fur*) display a decrease in secretion, suggesting that overexpression of *fur* has a negative effect on secretion (Fig. 3). However, EMSA analysis using purified *E. coli* Fur protein suggested that Fur does not bind to the promoter region upstream of the *yscW-ycrF* operon (Fig. 4). Purified *E. coli* Fur was utilized in this assay, as complementation of the *Y. pseudotuberculosis* Δ*fur* mutant strain with *E. coli fur* fully restored repression of the Fur regulated gene *hmuR* (Fig.

5). This EMSA analysis was carried out using a fragment covering +1 to-205 relative to the transcriptional start site, which includes the potential Fur boxes shown in Figure 2. However, the EMSA should be repeated using a larger DNA fragment that includes an additional potential Fur box downstream of the -10 region, spanning residues +1 to +18 (data not shown). Taken together these data suggest that Fur may negatively impact type III secretion but is unlikely to act directly through binding to the *yscW-ycrF* promoter region.

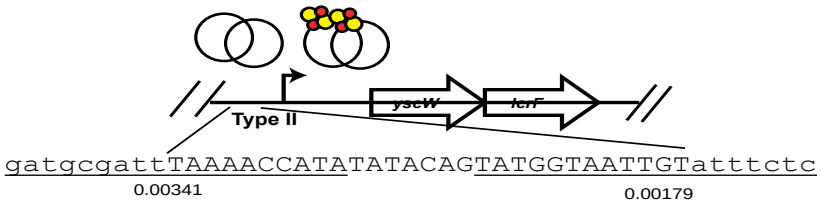

Fig 2. Bioinformatic analysis suggests putative Fur binding sites overlapping the IscR binding site on P_{lcrF} . IscR binding site is in CAPS and putative Fur binding sites are underlined. The IscR type II site is positioned 97 residues upstream of the -10 region. p-values for each binding site are given.

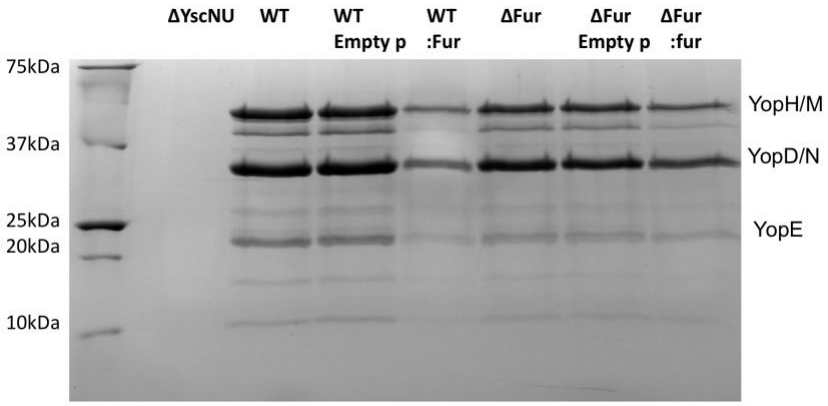

Fig 3. Overexpression of *fur* decreases T3SS activity under standard aerobic conditions. *Y. pseudotuberculosis* was grown in low calcium 2xYT media and the T3SS was induced at

37°C for 2 hours. T3SS cargo proteins secreted into culture supernatant and precipitated with TCA were visualized with Coomassie blue. One representative experiment out of three is shown.

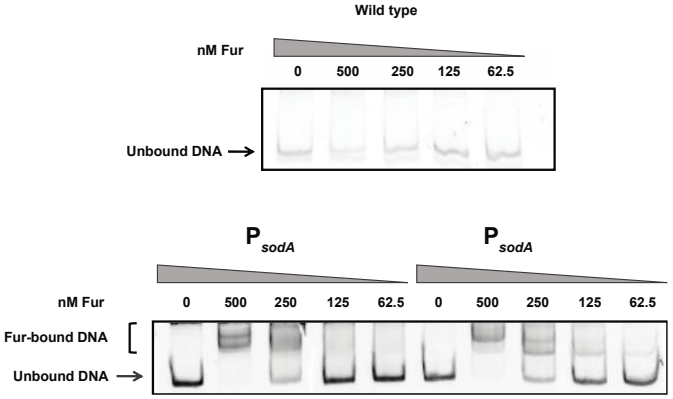

Fig. 4. Fur does not bind to the *lcrF* promoter *in vitro.* Electrophoretic mobility shift assays (EMSAs) were performed on DNA fragments containing the WT promoter region upstream of *yscW-lcrF.* Concentrations of purified *E. coli* Fur protein are denoted above gel lanes. Figure represents one of two independent experiments.

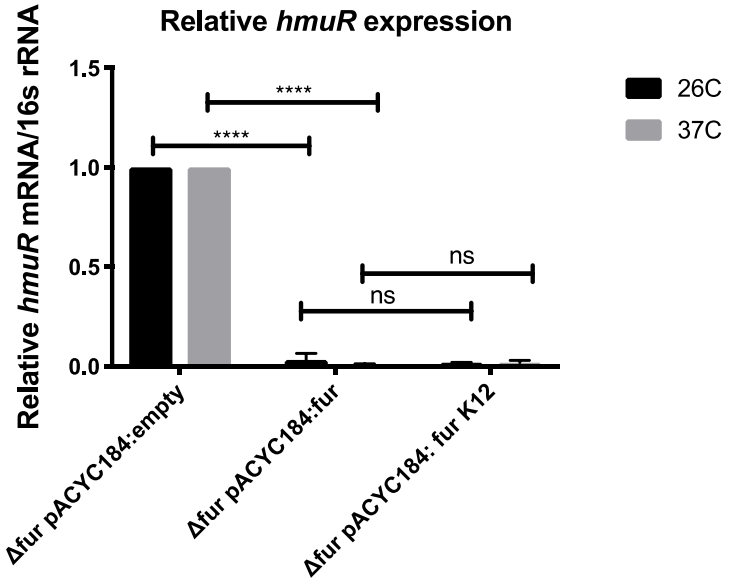

Fig. 5*. E. coli* Fur is functional in *Y. pseudotuberculosis.* *E. coli K12* and *Y. pseudotuberculosis fur* gene sequence plus 600 bp upstream of the start codon were cloned into plasmid pACYC184. Recombinant plasmids were introduced into either WT or ***Δfur*** *Y. pseudotuberculosis.* RNA was isolated at 2 hr after growth at 26ºC or 37ºC. qPCR was performed to determine *hmuR* and 16S gene expression. Relative mRNA levels for each gene were normalized to 16S rRNA levels in the same sample, and calculated by the ΔΔCt method.

Fur does not contribute to induction of type III secretion in response to iron limitation under anaerobic conditions To determine if Fur plays a role in regulation of the T3SS in response to iron availability, the *Y. pseudotuberculosis* Δ*fur* and Δ*iscR*/Δ*fur* strains were tested for secretion under varying iron and oxygen conditions. Under aerobic conditions, the Δ*fur* mutant displayed *iscR, lcrF*, and *yopE* gene expression to the same level as WT (Fig 6), but secreted higher levels of YopE protein than the WT under both iron replete and iron limited conditions. Furthermore, LcrF protein levels were also increased in the Δ*fur* mutant compared to WT.

In contrast to what was observed in the presence of oxygen, under anaerobic conditions, the Δ*fur* mutant secreted YopE similarly to WT. Importantly, very little YopE secretion was observed in a Δ*fur*/Δ*iscR* double mutant, suggesting that T3SS expression remains IscR-dependent in the absence of Fur (Fig. 6). One surprising finding was that YopE protein levels in the cell pellet (unsecreted YopE) were detected under iron replete anaerobic conditions in the Δ*fur* mutant but not in WT**.** Taken together, these data suggest that, while IscR is essential for Yop secretion under all conditions tested, Fur is dispensable. However, Fur may play a role in repressing YopE expression at the post-transcriptional level and/or YopE secretion.

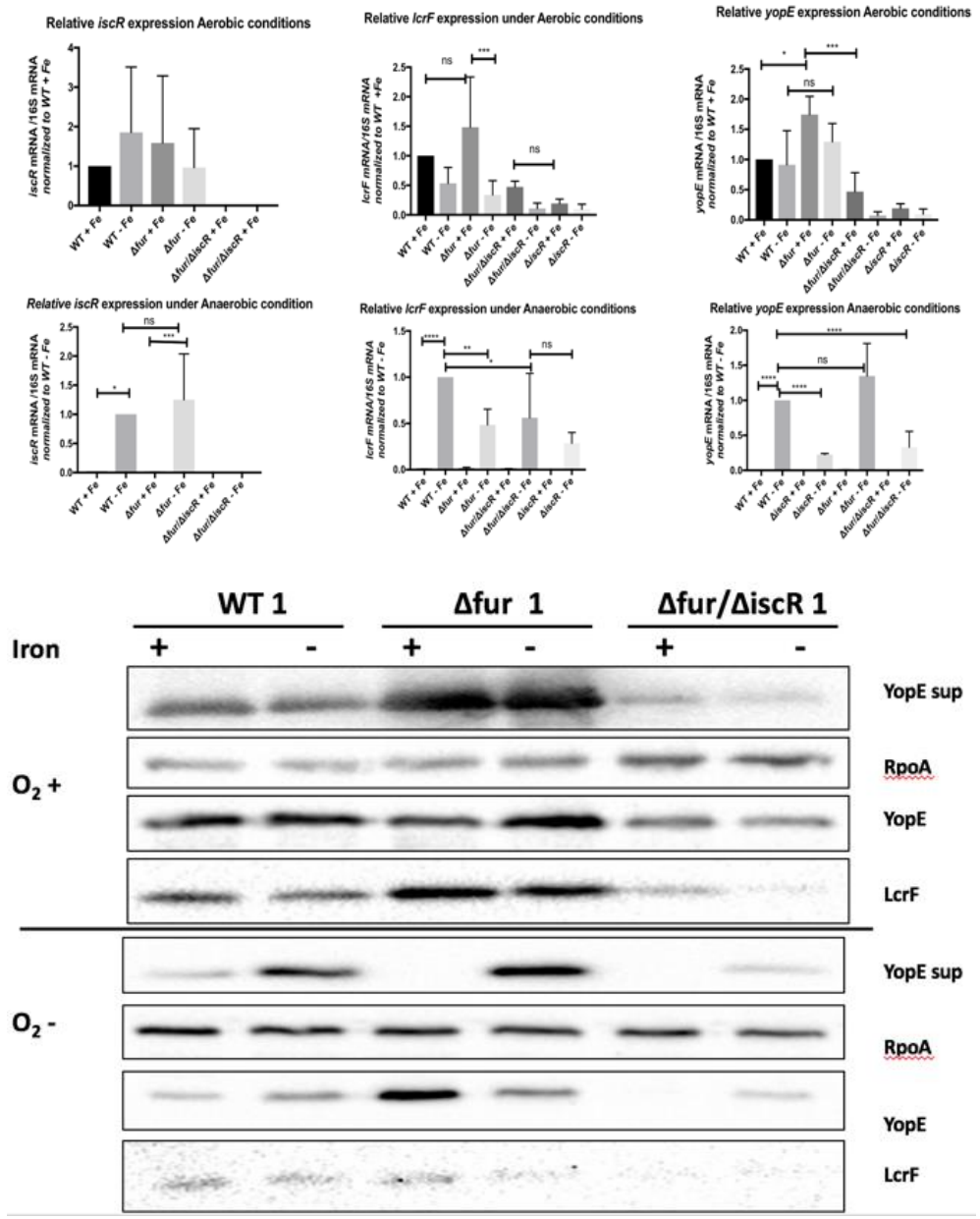

Fig. 6. Deletion of *fur* does not affect the T3SS response to iron and oxygen. *Y. pseudotuberculosis* was grown under iron starvation conditions as previously described under aerobic or anaerobic conditions (12 hrs), in 6.58 µM $FeSO_4$ (iron replete, "+Fe") or with 0.0658 µM $FeSO_4$ (iron limitation, "-Fe"). T3SS was induced by shifting to 37°C for 4hrs. Cell

lysates were probed with antibodies for RpoA, LcrF, and YopE. T3SS cargo proteins secreted into culture supernatant and precipitated with TCA were probed with antibodies for YopE. One representative experiment out of three is shown.

Discussion

Previous studies in *Yersinia pestis* have elucidated the Fur regulon [6, 7], but the role of Fur in enteropathogenic *Yersinia* virulence is not well understood. Interestingly, a recent transcriptomics study of mouse lungs infected with *Y. pestis* revealed an upregulation of the Fur regulated small RNAs RyhB1 and RyhB2 [8]. In addition, a recent study in *E. coli* showed that oxygen availability affects the regulon of Fur and RyhB [2]. However, we show here that a *Y. pseudotuberculosis fur* deletion plays a minor role in Yop secretion in response to iron and oxygen. Interestingly, we observed an upregulation of YopE protein in the absence of Fur. However, although *yopE* is an LcrF target gene, we could not detect binding of *E. coli* Fur to the *lcrF* promoter, suggesting that any repressive activity of Fur on YopE expression is independent of Fur directly binding the *lcrF* promoter.

Our preliminary data suggests that *Y. pseudotuberculosis fur* is not necessary for infection (Y. Wei and V. Auerbuch, data not shown). We reason that if Fur or the Fur-regulated sRNA RyhB had a major role in type III secretion, then the *fur* mutant would display a virulence defect because the T3SS is important for virulence. Nevertheless, the role of Fur in T3SS regulation remains incompletely understood, and further studies are necessary. One possibility is that Fur deletion is indirectly affecting regulation of *yopE* post-transcriptionally, as qPCR data does not show a change in mRNA levels, or that additional regulators controlled by Fur affect secretion of YopE (and possibly expression of other T3SS components). One possible future direction would be to use RNAseq to compare WT and the Δ*fur* mutant under varying oxygen and iron conditions, to determine Fur-regulated genes under these conditions.

References.

1. Fillat MF. The FUR (ferric uptake regulator) superfamily: Diversity and versatility of key transcriptional regulators. Archives of Biochemistry and Biophysics. 2014;546:41-52. doi: 10.1016/j.abb.2014.01.029.

2. Beauchene NA, Myers KS, Chung D, Park DM, Weisnicht AM, Keleş S, et al. Impact of Anaerobiosis on Expression of the Iron-Responsive Fur and RyhB Regulons. mBio. 2015;6(6):15. doi: 10.1128/mBio.01947-15.

3. Lavrrar JL, McIntosh MA. Architecture of a fur binding site: a comparative analysis. Journal of bacteriology. 2003;185(7):2194-202. doi: 10.1128/jb.185.7.2194-2202.2003.

4. Pieper R, Huang S-TT, Parmar PP, Clark DJ, Alami H, Fleischmann RD, et al. Proteomic analysis of iron acquisition, metabolic and regulatory responses of Yersinia pestis to iron starvation. BMC microbiology. 2010;10:30. doi: 10.1186/1471-2180-10-30.

5. Zhou D, Qin L, Han Y, Qiu J, Chen Z, Li B, et al. Global analysis of iron assimilation and fur regulation in Yersinia pestis. FEMS Microbiology Letters. 2006;258(1):9-17. doi: 10.1111/j.1574-6968.2006.00208.x.

6. Staggs TM, Perry RD. Fur regulation in Yersinia species. Molecular Microbiology. 1992;6(17):2507-16. doi: 10.1111/j.1365-2958.1992.tb01427.x.

7. Staggs TM, Fetherston JD, Perry RD. Pleiotropic effects of a Yersinia pestis fur mutation. Journal of bacteriology. 1994;176(24):7614-24. doi: 10.1128/jb.176.24.7614-7624.1994.

8. Deng Z, Meng X, Su S, Liu Z, Ji X, Zhang Y, et al. Two sRNA RyhB homologs from Yersinia pestis biovar microtus expressed in vivo have differential Hfq-dependent stability. Research in Microbiology. 2012;163(6-7):413-8. doi: 10.1016/j.resmic.2012.05.006.

Chapter 4.

Mutation of the *lcrF* promoter to examine why IscR control of the *Yersinia* type III secretion system is important for virulence.

By Diana Hooker-Romero , Patricia Kiley and Victoria Auerbuch

Introduction

Using a *Y. pseudotuberculosis* mutant where the IscR binding site in the *lcrF* promoter was ablated (*lcrF*^{pNull}), we showed in Chapter 3 that *Y. pseudotuberculosis* IscR binding to the *lcrF* promoter is critical for regulating T3SS expression in response to changes in iron and oxygen (Hooker et al., under review). In order to understand the physiological role of this regulation, we chose to construct a more nuanced mutation in the *lcrF* promoter predicted to bind holo-IscR, but not apo-IscR. Studies have shown that IscR binds to both type I and type II DNA motifs depending on its association with its [2Fe-2S] cluster [1, 2]. Therefore, we constructed an *lcrF* promoter mutant where the type II binding site is mutated to a type I binding site *lcrF*^{pTypeI}. Studies in *Escherichia coli* have demonstrated that only IscR-[2Fe2S] (holo-IscR) binds to type I sites [2]. We predicted that the *lcrF*^{pTypeI} mutant should upregulate T3SS expression under conditions where holo-IscR is present, i.e.-when [2Fe2S] clusters are more stable, such as low oxygen/oxidative stress and iron replete environments. Studying how proper regulation of the T3SS in response to environmental cues affects *Y. pseudotuberculosis* virulence will allow us to understand the importance of why pathogens fine-tune their virulence factors in response to different environment signals.

We first sought to investigate the effect of the presence of a type I binding site on the promoter region of *lcrF* under standard laboratory conditions: aerobic conditions in iron replete media. Additionally, we also conducted the iron starvation protocol described in Chapter 3 to test if iron and oxygen presence had an effect on T3SS expression in this mutant. Finally, we determined how regulation of the T3SS in the *lcrF*^{pTypeI} mutant affected virulence and dissemination. Results of this study suggest that standard laboratory conditions do not recapitulate all the host environments that *Y. pseudotuberculosis* encounters during infection.

Materials and Methods

Bacterial Strains and Growth Conditions. The strains used in this study are listed in Table 1. For standard *Y. pseudotuberculosis* growth and T3SS induction (Fig. 1B), bacteria were grown overnight in 2xYT media, subcultured in 2xYT plus 20 mM sodium oxalate (to chelate calcium and induce type III secretion) and 20 mM $MgCl_2$ to an optical density at 600 nm (OD_{600}) of 0.2, grown at 26˚C for 1.5 hrs followed by 37˚C for another 1.5 hrs. For growing *Yersinia* under various iron and oxygen condition, casamino acid-supplemented M9 media, referred to as M9 below, was used [3].

Growth of cultures to vary oxygen tension was achieved by first diluting 26˚C overnight aerobic cultures of *Y. pseudotuberculosis* to an OD_{600} of 0.1 in fresh M9 minimal media supplemented with 0.9% glucose (referred to as M9/high glucose) to maximize growth rate and energy production under anaerobic conditions, and incubating for 12 hrs under either aerobic or anaerobic conditions at 26°C. Anaerobic cultures were then shifted to 37°C and incubated for 4 hrs in a vinyl anaerobic chamber with a gas mix of 90%N, 5%CO_2, 5% H_2 (Coy Laboratory Products, Inc). Aerobic cultures were instead diluted to an OD_{600} of 0.2, grown with agitation for 2 hrs at 26°C, and then shifted to 37°C for 4 hrs.

Growth of cultures to vary iron availability was achieved by first growing *Y. pseudotuberculosis* aerobically in M9/high glucose media treated with Chelex® 100 resin to remove all traces of iron in acid-washed glassware, as previously described [4]. Specifically, iron replete overnight cultures (M9+6.58 µM $FeSO_4$) grown at 26˚C aerobically were diluted to an OD_{600} of 0.1 into Chelex-treated M9/high glucose media and grown for 8 hrs at 26˚C aerobically with agitation. Cultures were then diluted a second time to OD_{600} 0.1 in fresh Chelex-treated M9/high glucose, and grown for 12 hrs at 26˚C with agitation. Subsequently, cultures were then diluted a third time to OD_{600} 0.2 in M9/high glucose supplemented with 6.58 µM $FeSO_4$ (iron replete) or with 0.0658 µM $FeSO_4$ (iron limitation), grown for 2 hrs at

26°C with agitation, and then shifted to 37°C for 4 hrs with agitation to induce type III secretion. For anaerobic cultures, the cultures were instead diluted a second time to OD_{600} 0.1 in M9/high glucose supplemented with 6.58 µM $FeSO_4$ (iron replete,) or with 0.0658 µM $FeSO_4$ (iron limitation), and transferred to a vinyl anaerobic chamber where they were grown at 26°C for 12 hrs. Rezasurin redox indicator was used to monitor oxygen levels in the anaerobic chamber. By 4 hrs after introduction of cultures to the anaerobic chamber, the dye color changed from pink to clear, indicating an absence of residual oxygen. Cultures were then shifted to 37°C for another 4 hrs to induce type III secretion.

Type III secretion assays. Visualization of T3SS cargo secreted in broth culture was performed as previously described [46]. Briefly, 5 mL of each culture were pelleted at 13,200 rpm for 15 min at room temperature. Supernatants were removed, and proteins were precipitated by addition of trichloroacetic acid (TCA) at a final concentration of 10%. Samples were incubated on ice overnight and pelleted at 13,200 rpm for 15 min at 4°C. The resulting pellets were washed twice with ice-cold 100% acetone and subsequently resuspended in final sample buffer (FSB) containing 20% dithiothreitol (DTT). Samples were boiled for 5 min prior to running on a 12.5% SDS-PAGE gel.

Western Blot Analysis. In parallel, after the supernatant was collected, bacterial pellets were resuspended in FSB plus 20% DTT. Pellet samples were boiled for 15 min. At the time of loading, samples were normalized to the same number of cells. Cytosolic and secreted protein samples were run on a 12.5% SDS-PAGE gel and transferred to a blotting membrane (Immobilon-P) with a wet mini trans-blot cell (Bio-Rad). Blots were blocked for an hour in Tris-buffered saline with Tween 20 and 5% skim milk, and probed with the goat anti-YopE antibodies (Santa Cruz Biotechnology), rabbit anti-YopD (gift from Alison Davis and Joan Mecsas), rabbit anti-RpoA (gift from Melanie Marketon), rabbit anti-LcrF [27], rabbit anti-IscR [18], and horseradish peroxidase-conjugated secondary antibodies (Santa Cruz Biotech).

Following visualization, quantification of the bands was performed with Image Lab software (Bio-Rad).

Construction of *Yersinia* Mutant Strains. For the *Y. pseudotuberculosis lcrF*^{pTypeI} mutant strain, the *lcrF* promoter region was amplified by PCR using 5'/3' *lcrF*^{pTypeI} which contained the mutations on the IscR binding site (see Table 1, underlined nucleotides). Amplified PCR fragments were cloned into a *Bam*HI- and SacI-digested pSR47s suicide plasmid (λpir-dependent replicon, kanamycin^{R}, *sacB* gene conferring sucrose sensitivity) using the NEBuilder HiFi DNA Assembly kit (New England Biolabs, Inc) [47, 48]. Recombinant plasmids were transformed into *E. coli* S17-1 λpir competent cells and later introduced into *Y. pseudotuberculosis* IP2666 via conjugation. The resulting Kan^{R}, irgansan^{R} (*Yersinia* selective antibiotic) integrants were grown in the absence of antibiotics and plated on sucrose-containing media to select for clones that had lost *sacB* (and by inference, the linked plasmid DNA). Kan^{S}, sucrose^{R}, and congo red-positive colonies were screened by PCR and sequencing.

Table 1. Primers used in this study

Name	Name Sequence Reference	Reference
FqyopE	CCATAAACCGGTGGTGAC	(Morgan et al. 2017)
RqyopE	CTTGGCATTGAGTGATACTG	(Morgan et al. 2017)
Fq16s	AGCCAGCGGACCACATAAAG	(Merriam et al. 1997)
Rq16s	AGTTGCAGACTCCAATCCGG	(Merriam et al. 1997)
FqlcrF	GGAGTGATTTTCCGTCAGTA	(Miller et al. 2014)
RqlcrF	CTCCATAAATTTTTGCAACC	(Miller et al. 2014)
FqiscR	CAGGGCGGAAATCGCTGCCT	This study
RqiscR	ATTAGCCGTTGCGGCGCCTAT	This study

3' *lcrF*^{ptypeI}	TGTATAAATCCTTTGAAATCGCATCATATATTCCTAATAT	This study
5' *lcrF*^{pTypeI}	GATTTATAGTTGACCAATTTACTCGGGAATTGTAT	This study

Mouse Model. All animal use procedures were in strict accordance with the NIH Guide for the Care and Use of Laboratory Animals and were approved by the UC Santa Cruz Institutional Animal Care and Use Committee. 15-18 hrs prior to infection, food was withheld from eleven to twelve weeks old 129S1/SvImJ mice, but water was provided *ad libitum*. Mice were then inoculated with $2x10^8$ by bread feeding [49]. Briefly, *Y. pseudotuberculosis* cultures were grown in LB media overnight at 26°C. Cultures were diluted to the appropriate OD_{600} to obtain $2x10^8$ bacteria per mouse. Dilutions were spun down and pellets resuspended in a mixture of 2 ml of 1X PBS and 3 ml melted butter, and this mixture was then pipetted onto a small piece of bread. Mice were given a piece of *Yersinia*-soaked bread and provided food and water *ad libitum.* Five days post-inoculation, mice were euthanized and Peyer's patches, mesenteric lymph nodes, spleens, and livers were isolated and homogenized for 30 sec in PBS followed by serial dilution and plating on LB supplemented with 1 mg/mL irgasan for CFU determination.

Electrophoretic mobility shift assays (EMSAs). *E. coli* IscR-C92A protein was purified as previously described [18, 34] and subsequently used in Electrophoretic mobility shift assays (EMSAs). DNA fragments containing the wild-type *Y. pseudotuberculosis lcrF* promoter [-206 to +12 bp relative to the +1 transcription start site (TSS)], or its *lcrF*^{pTypeI} variant in which the IscR binding site is disrupted, were respectively isolated from pPK12778 and pPK12779 after digestion with *Hind*III and *Bam*HI, and EMSAs were carried out with purified IscR-C92A as previously described [22]. After incubation at 30°C for 1 hr, samples were loaded onto a non-

denaturing 6% polyacrylamide gel in 0.5´ Tris-borate-EDTA buffer and run at 100 V for 2.5 hrs at 4°C. The gel was stained with SYBR Green EMSA nucleic acid gel stain (Molecular Probes) and visualized using a Typhoon FLA 900 imager (GE).

RNA Isolation. A total of 3 mL of culture from each condition was pelleted by centrifugation for 5 min at 4,000 rpm. The supernatant was removed, and pellets were resuspended in 500 µL of media and treated with 1 mL Bacterial RNA Protect Reagent (Qiagen) according to the manufacturer's protocol. Total RNA was isolated using the RNeasy Mini Kit (Qiagen) per the manufacturer's protocol.

Quantitative Reverse Transcriptase PCR (qRT-PCR) analysis. After harvesting total RNA, genomic DNA was removed via the TURBO-DNA-free kit (Life Technologies/Thermo Fisher). cDNA was generated for each sample by using the M-MLV Reverse Transcriptase (Invitrogen) according to the manufacturer's instructions, as we previously described [12]. Each 20 µl qRT-PCR assay contained 5 µl of 1:10 diluted cDNA sample, 10 µl of Power CYBR Green PCR master mix (Thermo Fisher Scientific), and primers (Table 2) with optimized concentrations. The expression levels of each target gene were normalized to that of 16S rRNA present in each sample and calculated by the ΔΔCt method. Three independent biological replicates were harvested for each tested condition. For each target transcript, significant differential expression between different bacterial strains were defined by p-value <0.05 of two-way analysis of variance (one-way ANOVA with Tukey post-test)

mCherry fluorescence quantification. *Y. pseudotuberculosis* strains carrying the pMMB67HE:*pyopH*-mCherry construct were grown under iron starvation conditions as mentioned above, either under aerobic or anaerobic conditions. Iron starved cultures were incubated at 37˚C, and every hour a sample was taken from each culture, spun down for 2 min at 3000 rpm, and resuspended in 200µl 1X PBS, and mCherry fluorescence measured in

a black 96 well plate (costar) on a Perkin Elmer Victor X3 plate reader. Optical density was measured in a clear plate (costar) on a Perkin Elmer Victor X3 plate reader.

Results

The *lcrF*^{pTypeI} mutant displays normal T3SS expression under standard aerobic conditions, despite the inability to recruit apo-IscR to the *lcrF* promoter. Previous studies in *E. coli* have shown that only holo-IscR can bind to type I motifs (Nesbit, 2006, Giel, 2009). To confirm this, we conducted DNA-binding assays of *E. coli* apo-IscR protein and the promoter DNA fragment containing the *lcrF*^{pTypeI} mutation. Our results demonstrate that apo-IscR protein cannot bind to the *lcrF*^{pTypeI} promoter region, although apo-IscR can bind to the WT *lcrF* promoter region (Fig. 1). Future experiments should confirm that holo-IscR, which must be purified under anaerobic conditions, binds to the *lcrF*^{pTypeI} promoter region as predicted.

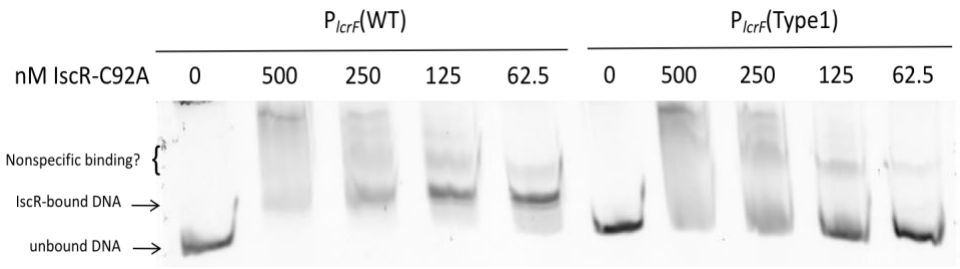

Fig. 1. Mutation of the IscR binding site in the *lcrF* promoter from a type II to a type I motif disrupts apo-IscR binding. Electrophoretic mobility shift assays (EMSAs) were performed on DNA fragments containing the WT and *lcrF*^{pTypeI} mutant promoter region (206 bp) upstream of *yscW* and *lcrF.* Concentration of purified *E. coli* apo-locked IscR-C92A protein used are denoted above the gel lanes. One representative experiment out of two is shown.

Furthermore, to determine how mutating the IscR binding site from a type II to a type I motif could affect T3SS expression, we grew the wild type and the *lcrF*^{pTypeI} mutant strains under aerobic conditions in M9 media at 26°C for 2 hrs and induced T3SS expression by shifting the culture to 37°C. The *lcrF*^{pTypeI} mutant did not display a growth defect compared to the WT strain at either temperature (Fig. 2). Despite the inability of the *lcrF* promoter in this mutant to bind apo-IscR, the secretion pattern of the *lcrF*^{pTypeI} mutant was no different than the WT strain, whose *lcrF* promoter can bind both apo- and holo-IscR (Fig. 3). Consistent with the *lcrF*^{pTypeI} mutant being capable of type III secretion, the *lcrF*^{pTypeI} mutant displayed growth arrest at 37˚C similar to the WT strain, as active type III secretion is associated with growth arrest. These results suggest that, under standard aerobic conditions, holo-IscR is sufficient to drive LcrF expression and subsequently type III secretion. To test this hypothesis, an Δ*iscR*/*lcrF*^{pTypeI} double mutant was constructed. Indeed, T3SS expression was ablated in this mutant (Fig. 4), suggesting that IscR is necessary for T3SS expression in the *lcrF*^{pTypeI} mutant and that sufficient holo-IscR is present under standard aerobic conditions to support LcrF expression and type III secretion.

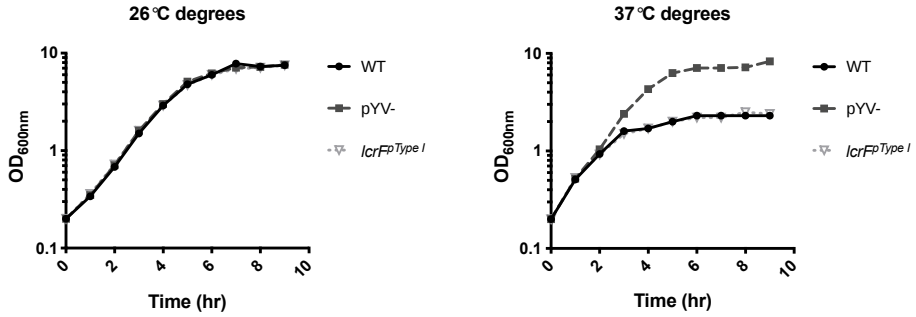

Fig. 2. The *lcrF*^{pTypeI} mutant does not display a growth defect under standard laboratory conditions. *Y. pseudotuberculosis* WT, Δ*iscR*, and *lcrF*$^{pType\ I}$ strains were grown under aerobic standard conditions in M9 media and optical density measured every hour.

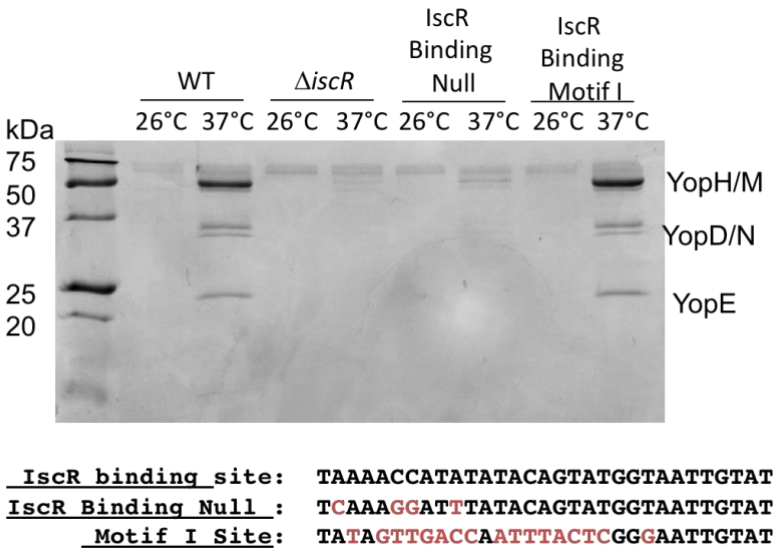

Fig. 3. Mutation of the IscR binding site in the *lcrF* promoter from a type II to a type I motif does not affect T3SS expression under standard aerobic conditions. *Y. pseudotuberculosis* strains were grown in M9 media and the T3SS induced at 37°C for 2 hours. T3SS cargo proteins secreted into the culture supernatant and precipitated with TCA were visualized with Coomassie blue. One representative experiment out of three is shown.

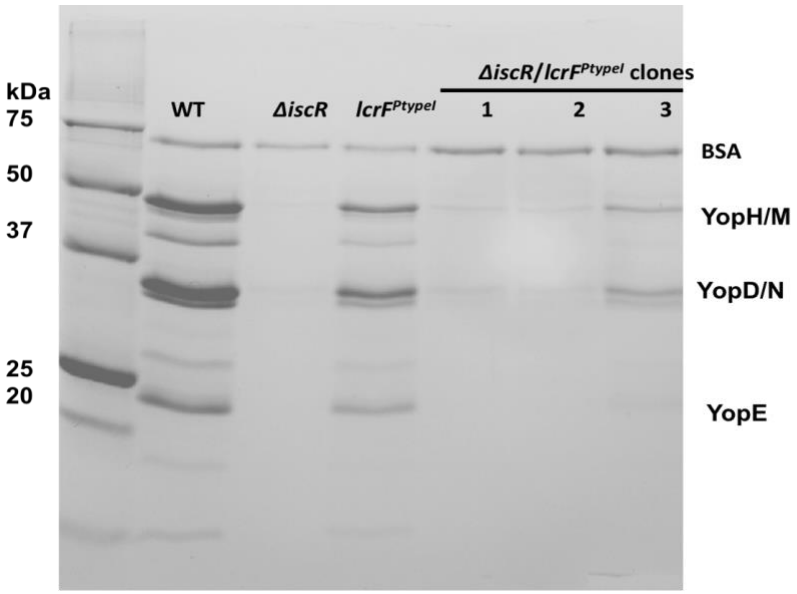

Fig. 4. IscR is necessary for T3SS expression in a *lcrF*^{pTypeI} mutant. *iscR* was deleted from the *lcrF*^{ptypeI} strain, and type III secretion was determined under standard aerobic conditions in M9. Gel depicts TCA precipitation of secreted proteins that were stained by Coomassie blue. Three individual clones of the Δ*iscR*/*lcrF*^{ptypeI} mutant is shown. BSA protein was used as a loading control.

These results led us to hypothesize that the amount of holo-IscR present in the cell under standard aerobic, iron replete conditions is sufficient to induce *lcrF* expression in the *lcrF*^{pTypeI} mutant to the same levels of a WT strain. Another possibility could be that, in living cells, apo-IscR is able to drive *lcrF* transcription even in the context of this mutated *lcrF* promoter. To test this possibility, we constructed a *Yersinia* double mutant strain that combined the *lcrF*^{pTypeI} mutation with the apo-locked IscR mutation previously used by our lab (C93A, C98A, C104A; [5]), referred to here as Apo-IscR. Our lab previously showed that an apo-IscR mutation leads to a proton motive force defect and therefore an inability to carry out type III secretion ([5]). Therefore, we analyzed expression of the LcrF target gene YopH as a readout of LcrF activity, using a *pyopH*-mCherry transcriptional reporter plasmid [6]. WT, *lcrF*^{pTypeI},

lcrF^{pNull}, apo-IscR/*lcrF*^{pTypeI}, Δ*lcrF* and Δ*iscR* strains carrying the plasmid pMMB67EH:*pyopH*-mCherry were grown under T3SS-inducing conditions and mCherry fluorescence determined. Similar to what we observed in Fig. 3 above, the *lcrF*^{pTypeI} mutant displayed *yopH* promoter activity similar to that of the WT strain (Fig. 5). However, the apo-IscR/*lcrF*^{pTypeI} mutant displayed mCherry expression to the same level of the *lcrF*^{pNull} mutant, suggesting that apo-IscR cannot drive *lcrF* transcription in the context of the *lcrF*^{pTypeI} mutation. While mCherry expression of both the *lcrF*^{pNull} and the apo-IscR/*lcrF*^{pTypeI} mutant was higher than that of the Δ*iscR* mutant in low calcium media (Fig. 5A), in high calcium media, *yopH* promoter activity in the *lcrF*^{pNull} and the apo-IscR/*lcrF*^{pTypeI} mutants was the same as in the Δ*iscR* mutant (Fig. 5B). This likely reflects stabilization of *lcrF* and LcrF target gene mRNA upon secretion of the regulator YopD out of the cell [7]. Taken together, these results suggest that holo-IscR cannot drive transcription from the *lcrF*^{ptypeI} promoter, and that the amount of holo-IscR present under standard aerobic conditions is sufficient to drive T3SS expression to the same levels as WT.

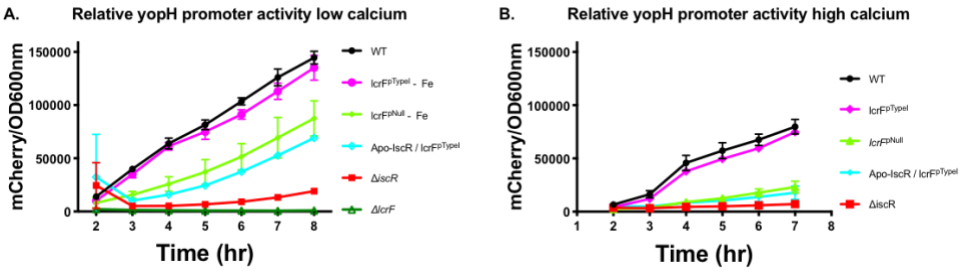

Fig. 5. Apo-IscR cannot drive T3SS expression in a *lcrF*^{pTypeI} mutant. *Y. pseudotuberculosis* p*yopH*-mCherry reporter strains were used to assess *yopH* expression under aerobic iron replete conditions. mCherry fluorescence intensity normalized to OD_{600} is shown. Data shown represent the average of three independent experiments.

In agreement with the data above, preliminary Yop translocation assays following growth of bacteria under standard aerobic T3SS-inducing conditions in 2xYT media, suggest that the *lcrF*^{pTypeI} mutant translocates the YopM-Bla reporter effector protein into CHO cells at the

same level as the WT strain (data not shown). This translocation was at a level that is much higher than the Δ*iscR* and *lcrF*^{pNull} mutants, which do not translocate detectable YopM-Bla. Taken together, these results suggest that, under standard T3SS-inducing conditions, either holo- or apo-IscR is necessary for *Yersinia* to express its T3SS and deliver T3SS effector protein into host cells.

***The lcrF*^{pTypeI} mutant displays a secretion defect after iron starvation under both aerobic and anaerobic conditions.** To assess if iron availability could affect how holo-IscR regulates the type I binding site upstream of *lcrF* in the *lcrF*^{pTypeI} mutant, we starved *Yersinia* of iron and incubated them under either aerobic or anaerobic conditions and examined T3SS expression. In Chapter 3, we showed that *iscR* gene expression does not change under aerobic conditions in response to iron in the WT strains, and this was the case in the *lcrF*^{pTypeI} mutant as well (Fig. 6A). Additionally, *lcrF* and *yopE* gene expression was unchanged between the *lcrF*^{pTypeI} mutant and WT. However, the *lcrF*^{pTypeI} mutant displayed a secretion defect following iron depletion in the presence of oxygen, even after the media was supplemented with iron (Fig. 6B).

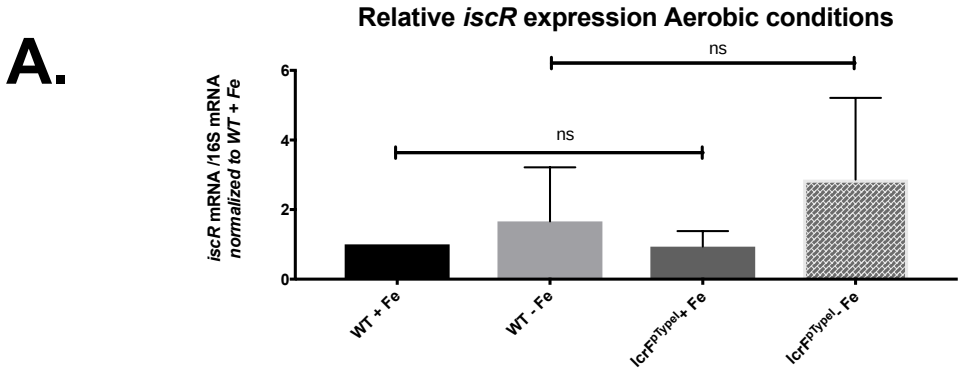

B.

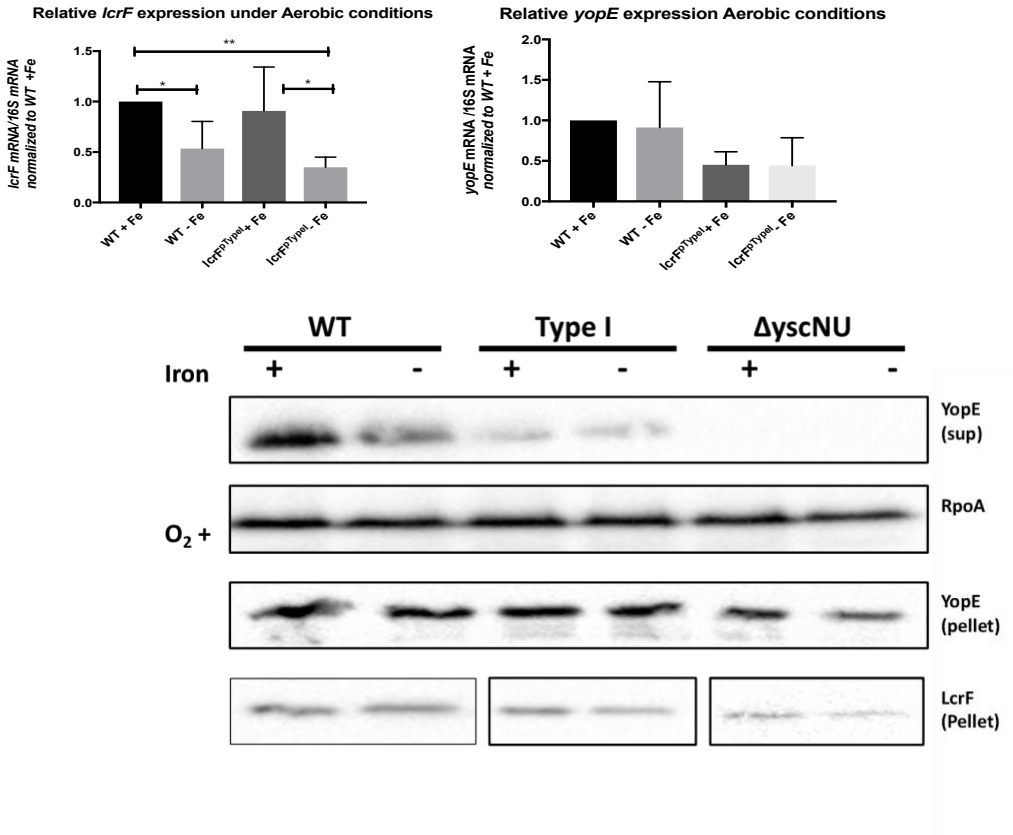

Fig. 6. The *lcrF*^{pTypeI} mutation does not affect LcrF, YopH, or YopE expression following iron starvation, but does lead to a decrease in YopE secretion. Iron starved *Y. pseudotuberculosis* was shifted to growing in iron replete (+Fe) or iron limited (-Fe) conditions at 37°C. After 4 hrs, (A) RNA was isolated and qPCR used to

determine relative expression of *iscR, yopE,* and *lcrF* by normalizing to 16S rRNA levels. Data shown represent the average of four independent experiments. ***p≤0.001 (One-Way ANOVA with Tukey post-test). (B) T3SS cargo proteins secreted into culture supernatant and precipitated with TCA were probed with antibodies for YopE. Cell lysates were probed with antibodies for RpoA, YopE, and LcrF. The Δ*yscNU* negative control strain does not express a functional T3SS. All samples in Figure 6 are from the same experiment but were run on separate gels. LcrF and YopE were probed on separate membranes. RpoA was blotted in each membrane as a loading control. One representative experiment out of four is shown.

Interestingly, under anaerobic conditions, *iscR, lcrF,* and *yopE* mRNA levels in the *lcrF*^{pTypeI} mutant were upregulated by continued iron limitation, similar to the WT strain (Fig. 7A). However, this mutant displayed a secretion defect under anaerobic conditions. Yet, the *lcrF*^{ptypeI} displayed an increase in intracellular YopE protein levels, but not LcrF protein levels (Fig. 7B), although the reason behind this remains unclear. Taken all together, these data suggest that the *lcrF*^{ptypeI} mutant displays a type III secretion defect following iron depletion that does not appear to stem from a decrease in LcrF protein levels.

A.

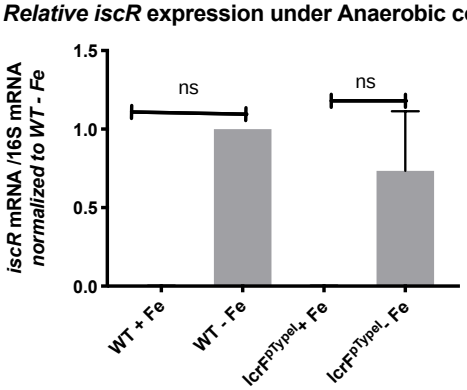

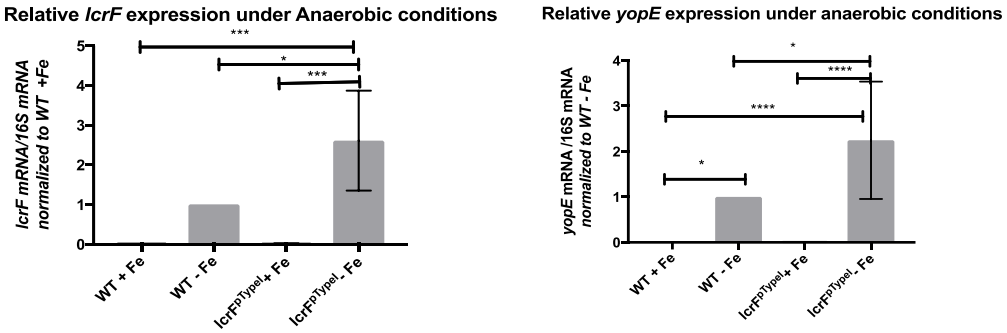

B.

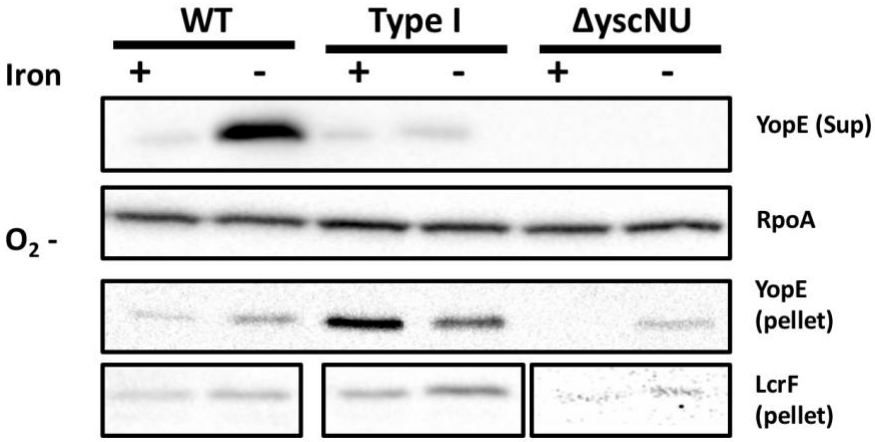

Fig. 7. The *lcrF*^{pTypeI} mutation decreases the ability of *Y. pseudotuberculosis* to secrete YopE under anaerobic conditions regardless of iron supplementation . Iron starved *Y. pseudotuberculosis* was shifted to growing in iron replete (+Fe) or iron limited (-Fe) conditions for 12 hrs, then shifted to 37°C for 4 hrs. (A) RNA was isolated and qPCR used to determine relative expression of *iscR, yopE,* and *lcrF* by

normalizing to 16S rRNA levels. Data shown represent the average of four independent experiments. ***p≤0.001 (One-Way ANOVA with Tukey post-test). (B) T3SS cargo proteins secreted into culture supernatant and precipitated with TCA were probed with antibodies for YopE. Cell lysates were probed with antibodies for RpoA, YopE, and LcrF. All samples in Figure 7 are from the same experiment but were run on separate gels. LcrF and YopE were probed on separate membranes. RpoA was blotted in each membrane as a loading control. One representative experiment out of four is shown.

YopH-mCherry reporters were also used to determine if iron or oxygen affected promoter activity of *yopH.* However, we could not detect sufficient mCherry signal in the absence of oxygen (Fig. 8). Under aerobic conditions, iron had no effect on mCherry fluorescence in any of the strains tested. Taken together, these results suggest that iron does not affect *yopH* expression under aerobic conditions. However, there was a significant difference between the WT strain and the *lcrF*^{pTypeI} strain under the same iron conditions at all time points. This is in contrast to the qPCR data presented in Figure 6 for *yopE* expression. The reason behind this discrepancy remains unclear.

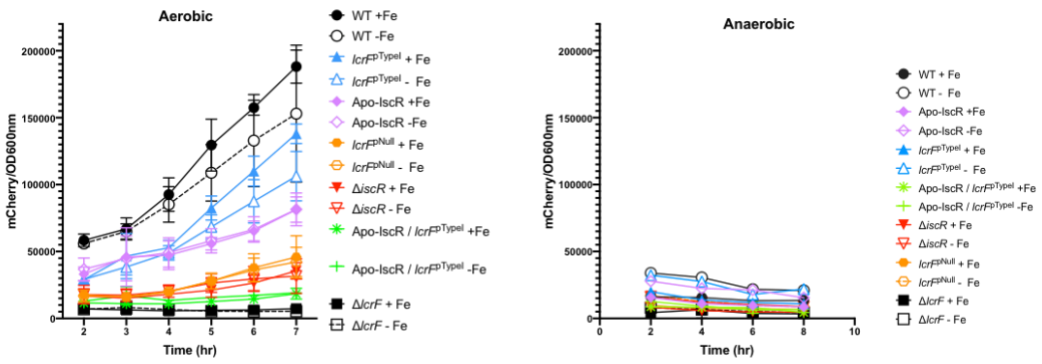

Fig. 8. Iron starvation does not affect YopH-mCherry expression under aerobic conditions, but mCherry fluorescence is too low to measure in the absence of oxygen. *Y. pseudotuberculosis* p*yopH*-mCherry was used to assess *yopH* expression under aerobic and anaerobic, iron replete or iron limited conditions. mCherry fluorescence intensity normalized to OD_{600} is shown. Data shown represent the average of three independent experiments.

Proper regulation of the T3SS by IscR is necessary for colonization. To examine the impact that the *lcrF*^{pTypeI} mutation has on infection, we performed oral inoculation of mice using a bread feeding model. Interestingly, the *lcrF*^{ptypeI} mutant displayed a colonization defect in the small intestine by 1000-fold. This is in contrast to a lack of small intestine colonization defect of the *lcrF*^{pNull} mutant (Fig. 9 and Chapter 3). Similarly, the *lcrF*^{pTypeI} mutant showed a 1000-fold decrease in Peyer's patch colonization, and a 100-fold decrease in mesenteric lymph nodes, when compared to the WT strain. In contrast, the *lcrF*^{pNull} mutant did not display a significant decrease in colonization of the mesenteric lymph nodes. Furthermore, the *lcrF*^{pTypeI} mutant was deficient in colonization of the liver and spleen by 1000-fold. (Fig. 9). These results suggest that proper regulation of LcrF and subsequently the T3SS by both holo- and apo-IscR, in response to environmental signals that drive the holo-/apo-IscR ratio, is critical for *Yersinia* virulence and colonization of every organ in the mouse model of infection.

As the T3SS is recognized by the innate immune system [8, 9] we hypothesized that the *lcrF*^{ptypeI} mutant, which expresses excess YopE under anaerobic iron replete conditions (Fig. 7) such as those found in the small intestine, might cause increased inflammation. To test this hypothesis, we conducted a preliminary experiment where mice were infected with either the WT stain or the *lcrF*^{ptypeI} mutant strain. Five days post-inoculation, the small intestine was isolated and fixed for histology analysis by a board-certified pathologist. Additionally, CFU

were calculated from fecal pellets, MLN, spleen, and liver were analyzed. A caveat to this experiments is that one WT-inoculated mouse and one *lcrF*^{ptypeI} -inoculated mouse was not colonized by *Yersinia* in any tissue (Table 1). Nevertheless, the *lcrF*^{ptypeI} mutant strain overall colonized at a lower level than WT, as expected. Tissue histology analysis, by E&H stain, of the intestinal tissue suggest that both the WT and the *lcrF*^{ptypeI} mutant caused some inflammation and intestinal lumen dysbiosis (Table 1). This preliminary result is interesting given that the *lcrF*^{ptypeI} -infected mice have fewer CFUs than WT-infected mice, and therefore may have a higher inflammation relative to colonization ratio. However, this experiment should be repeated with more mice per group to test this hypothesis.

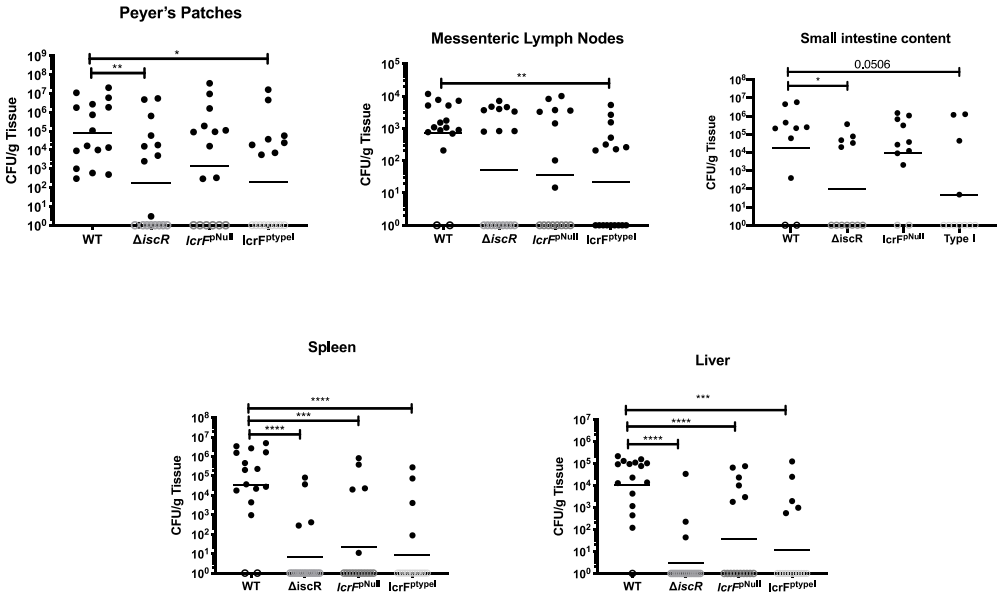

Fig. 9. Proper regulation of the T3SS in response to the appropriate iron and oxygen signal by IscR is essential for virulence in the mouse model of infection. Mice were infected with ~2x10^8 *Y. pseudotuberculosis* using a bread feeding model, and organs and intestinal contents were harvested 5 days post-inoculation. CFUs were normalized to the weight of the organ in grams. Each symbol represents one animal. Unfilled symbols indicate that CFU were below the limit of detection. These data represent 5 independent experiments.

**p<0.01, *** p<0.001, ****p <0.0001 was determined by an unpaired Mann-Whitney rank sum test. Dashes represent geometric mean.

Comparative Pathology Laboratory http://cpl.ucdavis.edu/ (530) 752-2832

			Histologic findings					
CPL acc#	**Cassette#**	**Study ID#**	Small intestine	PP	Cecum	Colon	Luminal contents	**colonization**
0739-19E	6	TI1	Mild mucosal hyperplasia	NE	Mild non-suppurative typhlitis	NSF	Mild dysbiosis	MLN, L
	7	TI2	Neutrophilic enteritis with mucosal hyperplasia and focal PP ulceration (cocci)	LFH	Focal chronic non-suppurative typhlitis	NSF	NSF	MLN, L
	8	TI3	NSF	Y	NSF	NSF	NSF	----------
	4	UN1	NSF	Y	NSF	NSF	NSF	----------
	5	UN2	NSF	LFH	NSF	NSF	NSF	----------
	1	WT1	Neutrophilic enteritis with segmental mucosal hyperplasia and focal PP ulceration	LFH	Focal neutrophilic typhlitis with mucosal hyperplasia and submucosal edema	Focal ulcerative colitis	Dysbiosis	MLN,SP, L
	2	WT2	Mild mucosal hyperplasia	Y	NSF	NSF	NSF	MLN, L
	3	WT3	NSF	LFH	NSF	NSF	NSF	----------

Histological findings:
NSF = No significant histologic changes were observed.
NE = Not examined, not present in section examined.
PP = Peyer's patch
Y = present in section.
LFH = Lymphofollicular hyperplasia

Summary:
The pattern of inflammation (necrosis and ulceration targeting the Peyer's patches) in mice WT1 and TI2 is consistent with the expected pathogenesis of *Yersinia pseudotuberculosis*. Similar changes may be present in mouse TI1 but due to sample bias, the target of inflammation (PP) is not present in section. Mild inflammation is also present in the cecum and colon. Dysbiosis and lymphofollicular hyperplasia are non-specific reactive changes that occur when the intestinal homeostasis is perturbed.

There are positive mice (mice exhibiting inflammation that would be consistent with enteric yersiniosis) in both the TI and WT groups. There are no positive mice in the UN groups. Unfortunately, the numbers are not sufficient for statistical significance.

Denise M. Imai-Leonard, DVM, PhD, DACVP
Pathologist and Assistant Health Sciences Clinical Professor

Table 2. Histological analysis of the mouse small intestine following infection with the *Y. pseudotuberculosis* WT and *lcrF*^{ptypeI} mutant five days post-inoculation. Mice were infected with ~2x10^8 *Y. pseudotuberculosis* using a bread feeding model, and entire intestines harvested five days post-inoculation. Entire intestines were analyzed as a Swiss roll, stained with H&E, and analyzed by the UC Davis pathology lab.

Discussion

In this chapter, we showed that mutating the *Y. pseudotuberculosis lcrF* promoter to prevent apo-IscR, but not holo-IscR, binding leads to a defect in type III secretion, specifically after iron starvation. While the mechanism behind this remains to be tested, this mutation is

associated with a colonization defect in all mouse tissues tested following oral infection. These data suggest that changes in iron-sulfur cluster homeostasis, which is sensed by IscR and affects the holo-/apo-IscR ratio, is an important environmental cue *Yersinia* uses to control its major virulence factor *in vivo*.

This *lcrF*^{ptypeI} mutation enables only holo-IscR, rather than both holo- and apo-IscR, to bind to the *lcrF* promoter. Indeed, we observed that expression of an apo-locked IscR allele in the *lcrF*^{ptypeI} mutant blocked T3SS expression, as measured by *yopH*-mCherry signal. Furthermore, the *yopH*-mCherry expression in this double mutant was as low as in the Δ*iscR* mutant and the *lcrF*^{pNullI} mutant, in which IscR binding to the *lcrF* promoter was completely ablated, suggesting that apo-IscR cannot bind to the *lcrF* promoter region of the *lcrF*^{ptypeI} mutant. Additionally, EMSA assays demonstrated that *E. coli* apo-IscR cannot bind to the *lcrF* promoter region of the *lcrF*^{ptypeI} mutant. Nevertheless, further DNA-binding analysis needs to be performed to determine if holo-IscR can bind to this promoter region. Together these results indicate that the T3SS expression observed in the *lcrF*^{ptypeI} mutant is induced by the holo-IscR present in the cell.

As holo-IscR alone can induce LcrF expression in the *lcrF*^{ptypeI} mutant, we speculated that LcrF and T3SS expression in this mutant should reflect holo-IscR levels. Holo-IscR, which should be more plentiful relative to apo-IscR in anaerobic and iron replete conditions, represses *isc* expression and in turn decreases overall IscR levels. Therefore, the conditions in which the holo-/apo-IscR ratio may be highest are the conditions where overall IscR levels are lowest (i.e.-anaerobic, iron replete). We observed similar levels of IscR, LcrF, and YopE expression in both the WT and *lcrF*^{ptypeI} mutant under aerobic iron replete and iron limited conditions. However, the *lcrF*^{ptypeI} mutant had higher LcrF and YopE expression than the WT in the absence of oxygen. Yet, the *lcrF*^{ptypeI} mutant did not secrete YopE under anaerobic iron limited conditions while the WT did. The mechanism behind this lack of secretion despite

expression of LcrF and YopE is unclear. One possible explanation is that the *yscW* pilotin gene, which encodes a protein that enables the YscC secretin T3SS basal body compoment to insert into the outer membrane, is encoded in the same operon as *lcrF*, just upstream of *lcrF*. It is possible that the *lcrF*^{ptypeI} mutation alters YscW expression in such a way as to block secretion without affecting expression of other T3SS genes. This hypothesis should be tested. One other discrepancy is that we observed a decrease in the amount of secreted YopE protein without a change in *lcrF* or *yopE* mRNA levels. These data suggest that post-transcriptional regulation of *yopE* may occur in the *lcrF*^{ptypeI} mutant in addition to a block in type III secretion.

One major conclusion from our combined *in vitro* and *in vivo* experiments with the *lcrF*^{ptypeI} mutant is that standard aerobic iron replete laboratory conditions do not completely mimic the environmental conditions under which *Y. pseudotuberculosis* needs to express the T3SS during infection, as the *lcrF*^{ptypeI} mutant displays normal type III secretion under standard conditions. As apo-IscR is unable to drive LcrF expression in the *lcrF*^{ptypeI} mutant, and the *lcrF*^{ptypeI} mutant is attenuated for virulence in all mouse tissues tested, we conclude that apo-IscR control of the *yscW-lcrF* operon is critical for *Yersinia* virulence. However, a deeper understanding of the *lcrF*^{ptypeI} mutation is needed to interpret the virulence data. This will include assessment of whether the *lcrF*^{ptypeI} mutation affects binding of protein and/or RNA factors other than IscR to the *lcrF* promoter. In addition, T3SS assembly in the *lcrF*^{ptypeI} mutant under anaerobic conditions should be examined to test if the T3SS basal body is affected in this mutant. This could be done by immunohistochemistry looking at YscF needles. Additionally, more *in vivo* studies need to be performed to determine if indeed the *lcrF*^{ptypeI} mutant causes more inflammation in the intestines. Furthermore, intraperitoneal infections should also be conducted to establish if this mutation also affects colonization and dissemination through this route of infection, which would bypass passage through the intestines. Lastly, *in vivo* gene expression should be assessed to determine where during

infection iron and oxygen conditions vary, and examined if those changes correlate with IscR and T3SS expression in both the WT and the *lcrF*^{ptypeI} mutant. Investigating how IscR regulates T3SS *in vivo* would allow us to have a better understanding of the different environments that *Y. pseudotuberculosis* encounters during infection, and how they affect how virulence is regulated.

References

1. Nesbit AD, Giel JL, Rose JC, Kiley PJ. Sequence-Specific Binding to a Subset of IscR-Regulated Promoters Does Not Require IscR Fe–S Cluster Ligation. Journal of Molecular Biology. 2009;387(1):28-41. doi: 10.1016/j.jmb.2009.01.055.

2. Giel JL, Rodionov D, Liu M, Blattner FR, Kiley PJ. IscR-dependent gene expression links iron-sulphur cluster assembly to the control of O2-regulated genes in Escherichia coli. Molecular Microbiology. 2006;60(4):1058-75. doi: 10.1111/j.1365-2958.2006.05160.x.

3. Cheng LW, Anderson DM, Schneewind O. Two independent type III secretion mechanisms for YopE in Yersinia enterocolitica. Molecular microbiology. 1997;24(4):757-65. PubMed PMID: 9194703.

4. Schwiesow L, Mettert E, Wei Y, Miller HK, Herrera NG, Balderas D, et al. Control of hmu Heme Uptake Genes in Yersinia pseudotuberculosis in Response to Iron Sources. Front Cell Infect Microbiol. 2018;8:47. Epub 2018/03/10. doi: 10.3389/fcimb.2018.00047. PubMed PMID: 29520342; PubMed Central PMCID: PMCPMC5827684.

5. Miller HK, Kwuan L, Schwiesow L, Bernick DL, Mettert E, Ramirez HA, et al. IscR Is Essential for Yersinia pseudotuberculosis Type III Secretion and Virulence. PLoS Pathogens. 2014;10(6). doi: 10.1371/journal.ppat.1004194.

6. Morgan JM, Lam HN, Delgado J, Luu J, Mohammadi S, Isberg RR, et al. An Experimental Pipeline for Initial Characterization of Bacterial Type III Secretion System Inhibitor Mode of Action Using Enteropathogenic Yersinia. Frontiers in Cellular and Infection Microbiology. 2018;8:404. doi: 10.3389/fcimb.2018.00404.

7. Kusmierek M, Hoßmann J, Witte R, Opitz W, Vollmer I, Volk M, et al. A bacterial secreted translocator hijacks riboregulators to control type III secretion in response to host cell contact. PLOS Pathogens. 2019;15(6). doi: 10.1371/journal.ppat.1007813.

8. Zhou P, She Y, Dong N, Li P, He H, Borio A, et al. Alpha-kinase 1 is a cytosolic innate immune receptor for bacterial ADP-heptose. Nature. 2018. doi: 10.1038/s41586-018-0433-3.

9. Philip NH, Zwack EE, and Bacterial B-IE. Activation and Evasion of Inflammasomes by Yersinia. Inflammasome Signaling and Bacterial 2016.